ABSTRACT

STUDY OF MECHANISMS OF PHYTOTOXICITY OF ALUMINA NANOPARTICLES

by
Anthony Elijius

Plant growth inhibitory effect of alumina nanoparticles has recently been reported (Ling Y, Watts D, 2004) but the mechanisms of such an effect are yet to be established. The phytotoxicity of aluminum and some of its compounds is well known, but the rapid expansion of nanotechnology resulting in the introduction of new sets of materials in the nanometer range has led to the development of new approaches, experimental methods and modes of investigation.

In this study, the observed phytotoxic effects of alumina nanoparticles suspension on five plant species (*Zea mays, Cucumis sativus, Daucus carota, Brassica oleracea, Lactuca sativa*) were investigated. Factors that were examined, which are thought to potentially contribute to the observed inhibitory root growth effect included; presence of hydrogen peroxide in Alumina nanoparticles suspension, mechanical contacts between root cell walls and particles, surface characteristics, the presence of residual aluminum in alumina nanoparticles, and movement of very small particles directly through the cell wall. The study of the latter possibility was made possible by the use of ultra-filtration techniques utilizing both 0.025µm and 0.05µm pore size membranes from Millipore®, in addition to the use of both Alumina nanoparticles and fumed Silica nanoparticles. Significant differences exist between the two pore sizes at the highest concentration of

20mg/ml of Alumina nanoparticles permeate for all the plant species used in this investigation, except *L.sativa*.

To investigate the surface characteristics, nanoparticle supernatants of different concentrations were obtained through centrifugation and used to treat plant species seedlings.

The presence (*or absence*) of Aluminum in alumina nanoparticles was established through the help of Spectrophotometric technique using Morin as a florescence agent, and the phytotoxicity of dilutions of Aluminum standard solution was compared to that of Alumina supernatants of varying concentrations. A trace of Aluminum was found in the Alumina nanoparticles supernatants from the highest concentration of 20mg/ml of Alumina nanoparticles suspension, with an absorbance of 0.2 AU compared to 4 AU from Aluminum standard solution. There was no statistical difference between the phytotoxicity from the 20mg/ml Alumina nanoparticles supernatants and that from the undiluted, 0.0371 M Aluminum standard solution, with p values for *D.carota, L.sativa, B.oleracea* and *C.sativus* being; 0.7, 0.64, 0.05 and 0.32, respectively, while the p value for *Z.mays* was < 0.0001, as a result of Aluminum resistance from this plant species, suggesting a common source of phytotoxicity.

This investigation answers questions raised by the previous researchers by using the same source of Alumina and Silica nanoparticles, similar experimental methods, data analysis but different approaches.

STUDY OF MECHANISMS OF PHYTOTOXICITY OF ALUMINA NANOPARTICLES

by
Anthony Elijius

A Dissertation
Submitted to the Faculty of
New Jersey Institute of Technology
in Partial Fulfillment of the Requirements for the Degree of
Doctor of Philosophy in Materials Science and Engineering

Interdisciplinary Program in Materials Science and Engineering

January 2011

APPROVAL PAGE

STUDY OF MECHANISMS OF PHYTOTOXICITY OF ALUMINA NANOPARTICLES

Anthony Elijius

Dr. Daniel J. Watts, Dissertation Advisor Panasonic Endowed Chair in Sustainability, NJIT	Date
Dr. Somenath Mitra, Dissertation Co-advisor Professor of Chemistry and Environmental Science, NJIT	Date
Dr. Kwabena Narh, Committee Member Professor of Mechanical Engineering, NJIT	Date
Dr. Reginald Farrow, Committee Member Research Professor, Department of Physics, NJIT	Date
Dr. Gordon Thomas, Committee Member Professor of Physics, NJIT	Date

BIOGRAPHICAL SKETCH

Author: Anthony Iheanyichukwu Elijius

Degree: Doctor of Philosophy

Date: January 2011

Undergraduate and Graduate Education:

- Doctor of Philosophy in Materials Science and Engineering
  New Jersey Institute of Technology, Newark, New Jersey, 2011
- Master of Technology in Mechanical Engineering,
  Rivers State University of Science and Technology, Port Harcourt, Nigeria, 1997
- Bachelor of Engineering in Materials and Metallurgical Engineering,
  Federal University of Technology, Owerri, Nigeria, 1992

Major: Materials Science and Engineering

Presentations and Publications:

Anthony Elijius and Daniel J. Watts, "The Phytotoxic Effect of Ultra Filtered Alumina and Silica Nanoparticles on Five Plant Species," to be submitted to *Toxicology Letters.*

Anthony Elijius and Daniel J. Watts, "Study of mechanisms for the phytotoxicity of Alumina nanoparticles" 2010 Conference in Science and Engineering, AGEP Alliance, City University of New York, New York, March 12th 2010.

Anthony Elijius and Daniel J. Watts, "Study of mechanisms for the phytotoxicity of Alumina nanoparticles" 12th Annual Conference in Science and Engineering, AGEP Alliance, City University of New York, New York, January 23rd, 2009.

Anthony Elijius and Daniel J. Watts, "Study of mechanisms for the phytotoxicity of Alumina nanoparticles" 11th Annual Conference in Science and Engineering, AGEP Alliance, City University of New York, New York, January 13th, 2008.

To the memory of my father, mother and sister Felicia

ACKNOWLEDGMENT

First and foremost, I want to extend my thanks, appreciation and gratitude to my advisor, Dr. Daniel J. Watts, who provided me with resources, advice, support, guidance and in most cases patience throughout this work.

My appreciation also goes to my co-advisor, Dr. Somenath Mitra, for his encouragement and advice. In addition, I also want to thank other distinguished members of the dissertation committee: Dr. Kwabena Narh, Dr. Reginald Farrow, and Dr. Gordon Thomas, for their kind suggestions and comments that helped improve the quality and content of this dissertation.

My special thanks goes to Dr. Ronald Kane, Dean of Graduate Studies, Ms. Clarisa Gonzalez, Associate Director, Graduate Studies, and Ms. Lynnette Randall of the financial aid department for their much needed financial assistance and support through the NSF/AGEP alliance, in addition to their encouragement, guidance, insight and immense kindness.

I wish to thank Dr. Rose Ann Dios, Professor of Mathematics, NJIT, for her very useful advice and assistance in the computation and data processing aspect of this dissertation.

I want to extend my sincere gratitude to Dr. Trevor A. Tyson, Professor of Physics and past Academic Director of Materials Science and Engineering for his encouragement and financial assistance. I also want to thank the current Academic Director of Materials Science and Engineering, Dr. Nuggehalli M Ravindra, for his kindness and assistance.

I want to thank Dr. Larisa G Krishtopa, and Dr. Xueyan Zhang, for providing me with materials, and technical assistance needed to complete this dissertation.

And finally, I want to send my utmost thanks to my brother Lemmy, who instilled in me, the desire to learn, laid the foundation for my academic success, taught and fine tuned my study skills. I also want to thank my sister Beauty, and my friend Ngozi, both of whom consistently encouraged me to complete this dissertation, my late father and mother who put me through my prior academic pursuit.

Most importantly, I want to thank Almighty God for his protection, guidance and strength that enabled me to persevere.

TABLE OF CONTENTS

TABLE OF CONTENTS
(Continued)

Chapter **Page**

TABLE OF CONTENTS
(Continued)

TABLE OF CONTENTS
(Continued)

TABLE OF CONTENTS
(Continued)

LIST OF TABLES

LIST OF TABLES
(Continued)

LIST OF TABLES
(Continued)

LIST OF TABLES
(Continued)

LIST OF TABLES
(Continued)

LIST OF FIGURES

LIST OF FIGURES
(Continued)

LIST OF FIGURES
(Continued)

LIST OF FIGURES
(Continued)

LIST OF FIGURES
(Continued)

Figure **Page**

LIST OF FIGURES
(Continued)

CHAPTER 1

INTRODUCTION

1.1 Objective

The set of materials called "Nanomaterials" as a result of their nanometer size range is believed to be "the next big thing" (http://www.weforum.org/pdf/TechPioneers/apax04.pdf), to lead the globe into an era of technological advancements and achievements. But the development, production, usage and subsequent release of these materials into the environment has led to worries of potential toxic effects. In a recent study (Ling Y, Watts D, 2004), five plant species; *Zea mays, Cucumis sativus, Daucus carota, Brassica oleracea, and Lactuca sativa* were exposed to three Nanomaterials; particles of Alumina, Silica and Titania within the nano-size range. According to these investigations, Alumina has an inhibitory effect on plant root growth compared to Silica and Titania. In fact, Silica promoted plant root growth, while Titania had no effect.

The primary objective of this investigation is to identify the mechanism(s) of this inhibitory growth effect. Factors that were previously postulated as possible contributors to the phytotoxicity of Alumina nanoparticles are; (1) the presence of hydrogen peroxide in suspensions of the particles (2) the mechanical/physical effect of the contact of alumina nanoparticles with root cell walls (3) the surface characteristics of Alumina nanoparticles (4) the possible presence and effect of residual Aluminum in Alumina nanoparticles (5) the size effect of Alumina nanoparticles, facilitating transport

into the interior of the plant cells and impacting cell growth. In this research, efforts were made to answer critical questions as a way of shedding more light on this phenomenon. These questions are; 1. Why were Alumina nanoparticles found to be phytotoxic? 2. What was the source(s) of this phytotoxicity? 3. Could size be a factor in the aforementioned phytotoxicity? 4. Since Aluminum is a well known phytotoxic agent, could it be present in the Alumina nanoparticles, if so, could it have contributed to the observed phytotoxicity? To answer these questions, standard experiments were carried out, based, in part, on observations from previous investigators as well as current hypothese.

1.2 Background Information

The prefix *nano* comes from the ancient Greek *νᾶνος*, through the Latin, *nanus* meaning literally *dwarf* and, by extension, *very small*. Within the convention of the International System of Units (SI) it is used to indicate a reduction factor of 10^9 times. So, the nanosized world is typically measured in nanometers (1 nm corresponding to 10^{-9} m) and it encompasses systems whose size is above molecular dimensions and below macroscopic ones (generally > 1 nm and < 100 nm (Psaro M, et al, 2004).

Quantum-size effects, where in the case of metals, typical "metallic" properties, like conductivity, decreases when the size is reduced and when the number of constituent atoms in the sample is significantly diminished, arise in nanosized objects because their global dimensions are comparable to the characteristic wavelength for fundamental excitations in materials. These excitations (including the wavelength of electrons, photons and so on) carry the quanta of energy through materials and therefore govern the dynamics of their propagation and conversion from one form to another.

However, if the size of the structures falls in the same order of magnitude of these characteristic wave functions, the propagation and the behavior of quanta are noticeably perturbed and thus quantum mechanical selection rules, which are not usually evident at larger scale, appear. Indeed, the electronic conduction band of a metal gradually evolves from continuous levels of a bulk infinite material into discrete states as a function of size reduction, resulting in an increase in the band-gap energy (Figure 1.1).

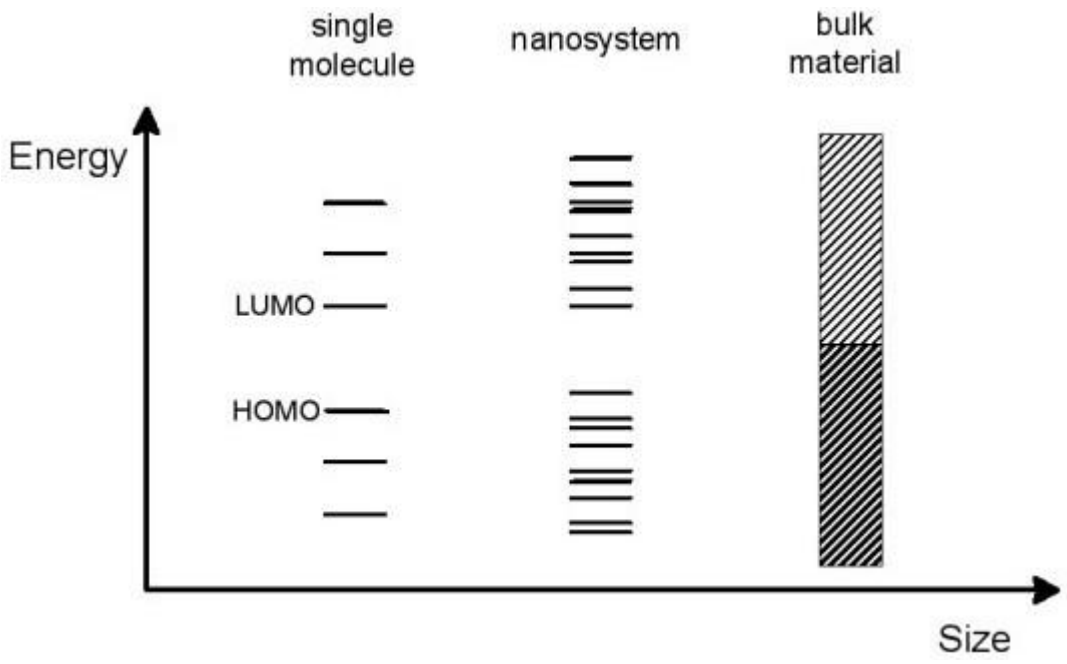

Source: (Psaro, M et al, 2004).

Figure 1.1 Comparisons between Energy Gaps from Single Molecules to Bulk Materials.

Advances in engineering nanostructures with exquisite size and shape control, elucidation of their unique properties, and demonstration of their broad applications have made nanotechnology an exciting research area (Medintz I L et al, 2005; Caruthers S D et al, 2007; Kumar C, 2007). Engineered nanostructures are used as probes for ultrasensitive molecular sensing and diagnostic imaging, agents for photodynamic therapy (PDT) and

actuators for drug delivery, triggers for photo thermal treatment, and precursors for building solar cells, electronics and light emitting diodes (Medintz I L et al, 2005; Caruthers S D et al, 2007; Kumar C, 2007; Akeman M E et al, 2002; Gao X et al, 2004).

Currently, a complete understanding of the size, shape, composition and aggregation-dependent interactions of nanostructures with biological systems is lacking (UK Department for Environment, 2005), and thus it is unclear whether the exposure of humans, animals, insects and plants to engineered nanostructures could produce harmful biological responses (Colvin V L, 2003).

Furthermore, there is a common assumption (Nel A et al, 2006; Oberdorster G et al, 2005, Colvin V L, 2003) that the small sizes of nanostructures allows them to easily enter tissues, cells, organelles, and functional biomolecular structures (DNA, ribosome) since the actual physical size of an engineered nanostructure is similar to many biological molecules (e.g. antibodies, proteins) and structures (e.g. viruses).

A corollary is that the entry of the nanostructures into vital biological systems could cause damage, which could subsequently cause harm to human health or to the well being of other organisms. However, a number of recent studies have demonstrated that despite the size of the nanostructures they do not freely go into all biological systems. Instead they are governed by the functional molecules added to their surfaces. For example, citrate-stabilized gold nanostructures entered mammalian cells but were not able to enter the cytoplasm or nucleus (Chithrani B D, Ghazani A A, Chan W C W, 2006); whereas one can engineer the nanostructure's surface chemistry for access to the nucleus or mitochondria (Chen F, Gerion D, 2004).

The first ever insight into the toxic effects of nanoparticles in plants came after a recent study (Ling Y, Watts D, 2004). In this study, the authors exposed five plant species (*Zea mays, Cucumis sativus, Daucus carota, Brassica oleracea, Lactuca sativa*) to three different nanoparticles; silica, titania and alumina nanoparticles and demonstrated that alumina has an inhibitory root growth effect, while the other two do not.

CHAPTER 2
LITERATURE REVIEW

2.1 Nanotoxicity

"Nanotoxicity" is the term used by scientists to describe the toxic effect of Nanomaterials on humans, animals and the environment (Oberdoster G et al, 2005).

Engineered Nanomaterials include particles of all sizes and shapes that exist at a scale of 100 nm or less, or have at least one dimension that affects their functional behavior at this scale (Oberdoster G et al, 2005). Engineered Nanomaterials are deliberately manufactured and can be distinguished from nanoparticles that exist in nature (an example of the latter is ash, which results from volcanoes or forest fires) or are by-products of other human activities (examples are high energy industrial processes such as welding or grinding) (Georgia M, 2006), that produce fine metallic or ceramic powders.

Nanotechnology is a powerful new technological approach for taking apart and reconstructing natural materials at the atomic and molecular level using the method of *self assembly*, one atom at a time. Nanotechnology and nanoscience encompasses the study of phenomena, materials and systems at the atomic, molecular and macromolecular scales, where properties differ significantly from those at larger scales.

In 2004, the world's oldest scientific organization, the Royal Society, warned that the risks of Nanotoxicity were significantly serious as to warrant Nanomaterials being assessed as new chemicals (The Royal Society and The Royal Academy of Engineering, UK, 2004). It warned that the toxicity of nanoparticles cannot be predicted from the

known properties of larger sized particles of the same substance. The fundamental properties of matter change at the nano-scale. The properties of atoms and molecules are not governed by the same physical laws as larger objects or even larger particles, but by "quantum mechanics". The physical and chemical properties of nanosized particles can therefore be quite different from those of larger particles of the same substance. Altered properties can include but are not limited to color, solubility, material strength, electrical conductivity, magnetic behavior, "mobility (within the environment and within the human body), chemical reactivity and biological activity" (Oberdorster G, Oberdorster E, and Oberdorster J, 2005).

There is a general relationship between particle size and toxicity; the smaller a particle is, the greater its surface area to volume ratio, and the more likely it is to prove toxic (Institute of Occupational Medicine for the Health and Safety Executive, 2004). Toxicity is partly a result of the increased chemical reactivity that accompanies a greater surface area to volume ratio (The Royal Society and The Royal Academy of Engineering, UK, 2004).

The small size, greater surface area and greater chemical reactivity of nanoparticles result in increased production of reactive oxygen species (ROS), including free radicals (Nel A, Xia T, Li N, 2006). ROS production has been found in a diverse range of Nanomaterials including carbon fullerenes, carbon nanotubes and nanoparticles sized metal oxides (Oberdorster G, Oberdorster E, and Oberdorster J, 2005). ROS and free radical production is one of the primary mechanisms of nanoparticle toxicity; it may result in oxidative stress, inflammation, and consequent damage to proteins, membranes and DNA (Nel, A. Xia T, Li N, 2006).

Size is therefore a key factor in determining the potential toxicity of a particle. Other factors influencing toxicity include shape, chemical composition, surface structure, surface charge, aggregation and solubility (Nel A, Xia T, Li N, 2006).

Because of their size, nanoparticles often are more readily taken up by the human body than larger sized particles and are able to cross biological membranes and access cells, tissues and organs that larger sized particles normally cannot (Holsapple M et al, 2005). Nanomaterials can gain access to the blood stream following inhalation or ingestion, and possibly also via skin absorption, especially if the skin is damaged (Oberdorster G, Oberdorster E, and Oberdorster J, 2005). Once in the blood stream, Nanomaterials can be transported around the body and are taken up by organs and tissues including the brain, heart, liver, kidneys, spleen, bone marrow and nervous system. While in the blood stream, the major distribution sites for nanoparticles appear to be the liver, followed by the spleen (Oberdorster G, Oberdorster E, and Oberdorster J, 2005). The length of time that nanoparticles may remain in the vital organs and what dose may cause a harmful effect remains unknown (Tran C et al, 2005).

Diseases of the liver suggest that the accumulation of even normally harmless foreign matter may impair its function and result in harm (Swiss Re, 2004). Carbon nanotubes (nano-scale cylinders made of carbon atoms) have been shown to cause the death of kidney cells and to inhibit further cell growth (Oberdorster G et al, 2005).

Many types of nanoparticles have proven to be toxic to human tissue and cell cultures, due to increased oxidative stress, inflammatory cytokine production, DNA mutation and even cell death (Oberdorster G et al, 2005). Unlike larger particles, nanoparticles may be

transported within cells and be taken up by cell mitochondria (Li N et al, 2003), and the cell nucleus (Geiser M et al, 2005) where they can cause major damage.

Copper nanoparticles have been found to be toxic to animal cells at a relatively high dose of 200mg/kg/d (Lei R et al, 2008). These investigators exposed rats to 50, 100 and 200mg/kg/d for 5 days and observed induced overt hepatoxicity and nephrotoxicity in addition to increased amount of citrate, succinate trim ethylamine-N-oxide, glucose and amino acids, while there was a decrease in creatinine levels. While another group of researchers (Chen Z et al, 2008) has discovered that old rats subjected to physiologically inhaled air containing an aerosol of manufactured Silica nanoparticles (24.1mg/m^3; 40min/day) for four weeks developed pulmonary alterations compared to adult or young rats.

Zinc oxide (ZnO) nanoparticles have also been found to be phytotoxic to *Lolium perenne* (ryegrass) (Xing B and Lin D, 2008). Treating *L.perenne* with both Zn^{2+} ions and Zinc oxide nanoparticles in a hydroponic culture system resulted in a significant reduction in biomass, shrinking of both root tips and shoots, in addition to the high vacuolation or collapse of root, epidermal and cortical cells at a dose of 1000mg/L of Zinc oxide nanoparticles or Zn^{2+} ions. Though toxicity begins at 10mg/L for the shoots and 50mg/L for the roots for Zinc oxide nanoparticles and 20mg/L for Zn^{2+} ions, the Zinc oxide uptake remained lower compared to that of the Zn^{2+} ions.

A recent study has shown the toxic effects of Silver nanoparticles on *Caenorhabditis elegans*, a nematode (Roh J et al, 2009). Using survival, growth and reproduction as the ecotoxicological endpoints, the research group found that Silver nanoparticles exerted considerable toxicity on *C.elegans* in the form of decreased

reproduction potential when using 0.1 and 0.5mg/L of Silver nanoparticles, and based the mechanism on oxidative stress.

The body distribution of particles is strongly dependent on their surface characteristics. For example, coating poly (methyl methacrylate) nanoparticles with different types and concentrations of surfactants significantly changes their body distribution (Araujo L, Lobenberg R and Kreuter J, 1999). Coating these nanoparticles with 1 % poloxamine 908 reduces their liver concentration significantly (from 75 to 13 % of total amount of particles administrated) 30 min after intravenous injection. Another surfactant, polysorbate 80, was effective above 0.5%. A different report (Labhasetwar V et al, 1998) shows that modification of the nanoparticle's surface with a cationic compound, didodecyldimethylammonium bromide (DMAB), facilitates the arterial uptake 7-10-fold. The authors noted that the DMAB surface modified nanoparticles had a zeta potential of +22.1 +/- 3.2 mV (mean +/- sem, n = 5) which is significantly different from the original nanoparticles which had a zeta potential of -27.8 +/- 0.5 mV (mean +/- sem, n = 5). The mechanism for the altered biological behavior is rather unclear, but surface modifications have potential applications for intra-arterial drug delivery.

2.2 Aluminum Toxicity

Aluminum is among the list of substances listed as toxic by the Environmental Protection Agency (EPA) under the National Priorities List (NPL) (Draft Toxicological Profile for Aluminum, 2006).

Aluminum is a naturally occurring substance and constitutes 8.8% of the earth's crust. It is a highly reactive metal, therefore, in nature it is found in combination with other non-metallic elements forming compounds. Examples are alumina, which is as a result of aluminum combining with oxygen, or aluminum hydroxide, which occurs by a combination with hydroxyl groups. These chemical compounds are commonly found in soil, minerals (example, sapphires, rubies, turquoise), rocks (especially igneous rocks), and clays. Aluminum as a metal is obtained from aluminum-containing minerals, primarily bauxite. Small amounts of aluminum are even found dissolved as ions in water. Organic acids have been found to be important weathering agents for dissolving and transporting aluminum in an alpine soil environment (Litaor M I, 1987).

Aluminum compounds are used in many diverse and important industrial applications such as alum (aluminum sulfate) in water-treatment and alumina in abrasives and furnace linings. They are found in consumer products such as antacids, astringents, buffered aspirin, food additives, and antiperspirants. Furthermore, because of its high reactivity with oxygen, powdered aluminum is used in explosives and fireworks.

Though aluminum can be found naturally in air, water and soil, higher levels of aluminum in the environment are as a result of mining and processing of aluminum ores, the metal and its compounds, and from coal-fired power plants.

Toxicity of aluminum to living cells and the environment is well reported, for example; dose and time-dependent killing of cultured rat hepatocytes was produced by aluminum maltolate (AIM), a neutral, water-soluble complex technically called aluminum 3-hydroxy-2-methyl-4H-pyran-4-one. Treatment with 10Mm for 1 hr killed 50 percent or more of the cells within 3 hrs (Snyder J W, et al 1995). Mostly, toxicity of

aluminum and its compounds is based on the dose and duration of exposure, and not on the form of existence, that is, on the nature of the compound (or element).

Respiratory effects of aluminum dust particles as a result of inhalation have been reported, these respiratory effects include increases in alveolar macrophages, granulomatous lesions in the lungs and peribronchial lymph nodes, and increases in lung weight (Drew R T et al, 1974; Klosterkotter W 1960; Pigott G H et al, 1981; Steinhagen W H et al, 1978; Stone C J et al, 1979). The lung effects observed in humans and animals are suggestive of dust overload, meaning; higher presence of dust particles in the lungs, signified mainly by an increase in lung weight. Some neurological effects have been observed in workers chronically exposed to aluminum dust or fumes. These effects include impaired performance on neurobehavioral tests (Akila R et al, 1999; Bast-Pettersen R et al, 2000; Buchta M et al, 2003; Hanninen M et al, 1994).

There is also evidence that gestational and/ or lactational exposure can cause other developmental effects. Gestation and/ or lactation exposure at a concentration of 160mg/kg/d for 90 days can result in significant decrease in pup body weight gain in rats and mice, (Golub M S and Germann S L 2001; Golub M S et al, 1992). The decreases in pup body weight are often associated with decreases in maternal body weight during the lactation phase of the study; however, decreases in body weight have also been observed in a cross-fostering study when gestation-exposed pups were nursed by control mice (Golub M S et al, 1992). Ingestion of over 100mg/L aluminum is known to cause musculoskeletal effects in humans. Joint pains were common symptoms reported in people in England who, for 5 days or more, consumed elevated levels (over 45mg/L) of aluminum sulfate in drinking water which also contained elevated levels (20mg/L and

15mg/L, respectively) of copper and lead (Ward N, 1989). Osteomalacia, which is the softening of the bones due to defective bone mineralization (http:/www.nlm.nih.gov/medlineplus/ency/article/000376.htm), has been observed in healthy individuals following long-term use of aluminum-containing antacids and in individuals with kidney disease. Hepatic dysfunction was reported in 1 of 15 people acutely exposed to an unspecified amount of aluminum phosphide (Khosla S N et al, 1988), though this is thought to be due to the formation of highly toxic phosphine gas instead of aluminum.

2.3 Phytotoxicity of Aluminum

The toxic effect of aluminum on plants is well known but the mechanism of toxicity is still being debated. Aluminum phytotoxicity is usually restricted to acid mineral soils where low pH favors the presence of the highly toxic Al^{+3} ions in soil suspension (Kidd P S et al, 2001). In many experimental situations, phytotoxicity is measured in terms of Relative Root Growth, which compares the length of root growth of plant seedlings that are exposed to the agent in question with the growth of unexposed controls. The inhibition of such growth by aluminum at a concentration of 840μM for 2 hours has been attributed to extensive membrane damage, peroxidation of membrane lipids, and loss of cell compartmentation (Barceló J and Poschenrieder C, 1999). Selective supply of aluminum at a dose of 25mg/L to different parts of the root system clearly shows that root tips are the primary sites of Al-induced injury (Ryan P R et al, 1993). The distal part of the transition zone has been identified as the target site in maize (Sivaguru M and Horst

W J, 1998). It has been shown by an earlier work (Clarkson D T, 1965) that mitosis in plants can be inhibited by aluminum ($10^{-3}/10^{-4}$M) binding to the nucleic acid in roots. This has further been proved with improvements in the methods used for aluminum detection inside cells, which indicates that aluminum can enter the symplasm within a few minutes. Other researchers believe that the cross-linking of peptic substances in cell walls is a mechanism of aluminum-induced inhibition of root cell extension (Klimashevsky E and Dedov C, 1975). More recently, cell pressure probe measurement has revealed aluminum-induced cell wall stiffening in root cells of aluminum sensitive maize using an aluminum concentration of 50μM (Gunse B et al, 1997). Aluminum can cause abnormal cell division planes by interfering with the cortical actin filaments that are thought to play an early role in fixing the site of the preprophase band that is involved in the direction of the cell plate to the correct position (Verma D P S, 2001).

Plants can resist phytotoxicity of aluminum by either extracellular precipitation or detoxification of Al^{3+} by complexation with chelating root exudates or binding to mucilage as may be implied with the term for this protective mechanism exclusion (Barceló J and Poschenrieder C, 2002). Chelation of this aluminum ion by organic ligands in the rhizosphere and root apoplast is a major mechanism that prevents toxicity by excluding toxic aluminum species from the sensitive root tips (Barceló J, Poschenrieder C, and Tolver P R, 2005). Aluminum-induced exudation of flavonoid-type phenolics seems to be implied in silicon-mediated amelioration of aluminum toxicity in maize (Kidd P S et al, 2001).

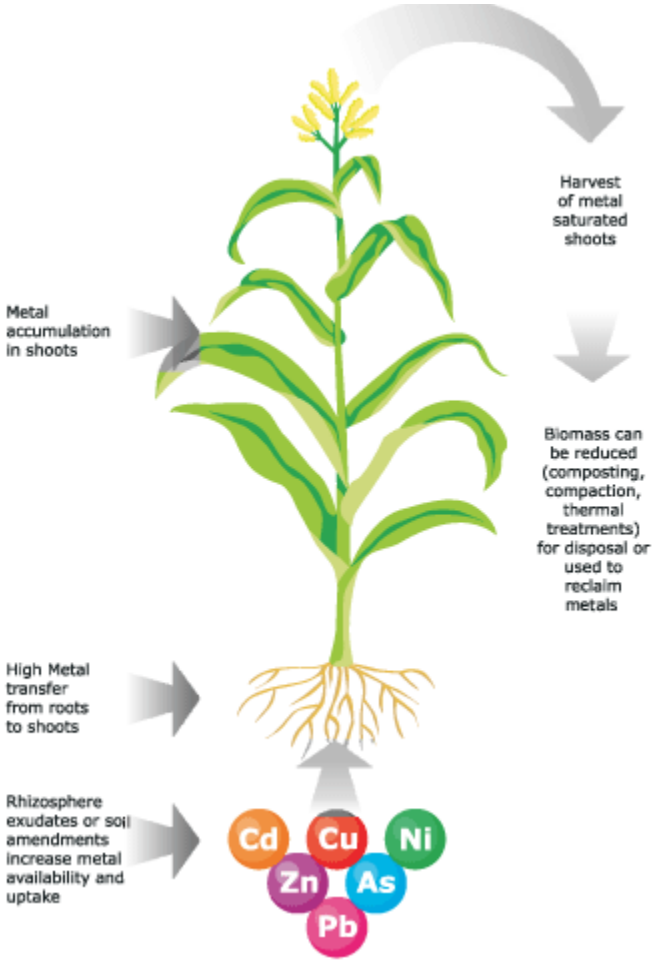

Figure 2.1 Absorption and uptake of metal by plants with the aid of the Rhizosphere.

Source: www.scielo.br/img/revistas/sa/v63n3/29836f1.gif

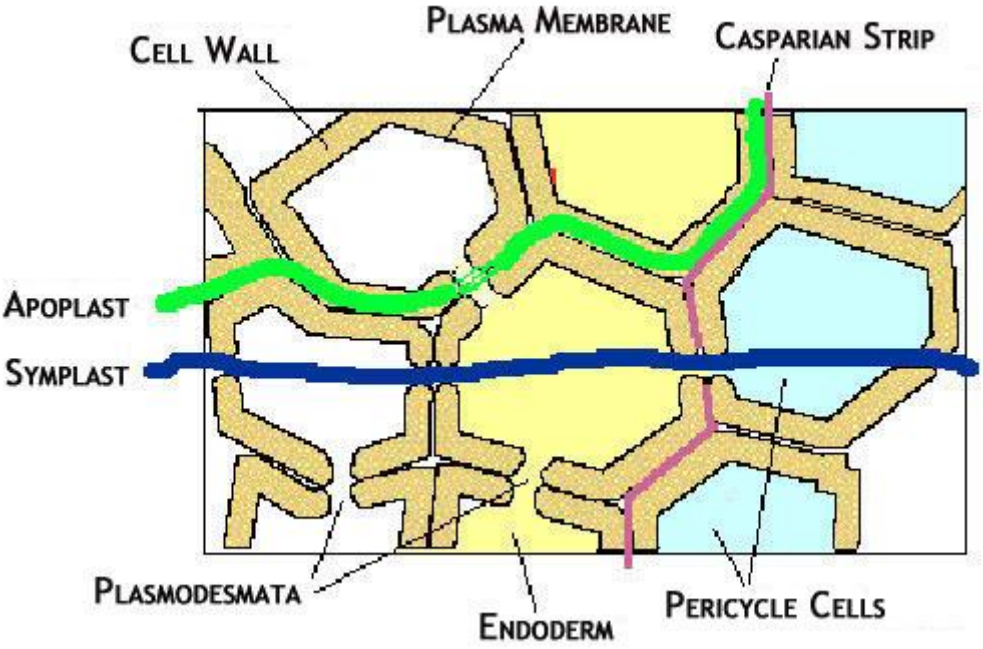

Figure 2.2 Diagram of the cell structure showing the Apoplast.

Source: www.sparknotes.com/.../section2.rhtml

2.4 Synthesis of Alumina Nanoparticles

Alumina is an oxide of Aluminum, and it is a white powder frequently produced from Bauxite ores (iron alumino silicates) by the Bayer process. This involves digesting Bauxite at high temperatures with caustic soda which dissolves the alumina as sodium aluminate, leaving iron oxide and silicates as waste products (red mud). On controlled cooling, alumina hydrate is precipitated which is calcined (heated) at 900 to 1000˚C to alumina. Caustic soda is lost mainly with the clay and iron oxide particles,

(www.chemlink.com.au/alumina.htm). The most common naturally occurring crystalline form of alumina is Corundum, with its gem derivatives of ruby and sapphire (Edwards J D, Tosterud M, 1993). Industrially, alumina is used as an insulator, refractories, abrasive and as an ingredient in cutting tools.

For oxide nanoparticles, the production routes most often used are the sol-gel and free jet expansion methods in order to provide the desired small particle sizes.

2.4.1 Sol-gel Method

This is a Nanomaterials production route that involves the combination of suspension of reactants (sol); such as Oligomers of about 0.5-1 nm and a Gel, which is mainly a structure providing micro pores, of about 2-5 nm diameter.

The concept is that the sol-gel process through a combination of chemical reactions turns a homogeneous suspension of precursors and reactants into an infinite-molecular-weight oxide polymer. This polymer is a three-dimensional skeleton surrounding interconnected pores (Edelstein A S and Cammarata R C, 2002).

For Nanomaterials synthesis, the sol-gel process involves initially a homogeneous suspension of one or more selected alkoxides (Mukherjee S P, 1980). Alkoxides are the organometallic precursors for alumina, silica, titania and zirconia, among others (Bradley D C, Mehrotra R C and Gaur D P, 1978). A catalyst is used to start the reaction and control the pH. The reactions are, first, hydrolysis, to make the suspension active, followed by condensation polymerization along with further hydrolysis. These reactions increase the molecular weight of the oxide polymer.

For alumina, the production through sol-gel is a four stage process. First starting from the precursor, aluminum-sec-butoxide (ASB), the reactions are as follows:

$Al(OC_4H_9)_3 + H_2O \rightarrow Al(OC_4H_9)_2(OH) + C_4H_9OH$

$Al(OC_4H_9)_2 (OH) + H_2O \rightarrow Al(OC_4H_9)(OH)_2 + C_4H_9OH$

$2Al (OC_4H_9)(OH)_2 \rightarrow 2AlO(OH) + 2C_4H_9OH$

$2Al(OC_4H_9)(OH)_2 + 2H_2O \rightarrow 2Al(OH) + 2C_4H_9OH + H_2$

$2AlOOH \rightarrow Al_2O_3 + H_2O$

or $2Al(OH)_3 \rightarrow Al_2O_3 + 3H_2O$.

Either the monohydroxide AlOOH (Boehmite) or the trihydroxide $Al (OH)_3$ (Bayerite) can be transformed to gamma alumina (Yoldas B E, 1975); which is composed of minute colorless cubic crystals with specific gravity of 3.6, that are transformed at high temperatures to the alpha form, which has a hexagonal crystal structure.

2.4. 2 Free Jet Expansion Method

In this synthetic route, aluminum metal is first vaporized and then mixed with an inert carrier gas (usually He or Ar), at a total pressure P_0 and a temperature $T_{0.}$ Then it is adiabatically expanded through a nozzle or orifice of diameter d into an ambient background containing oxygen at a pressure $P_{1.}$ The gas mixture starts from a negligibly

small velocity defined by the stagnation state ($P_{0,}$ T_0) and, due to the pressure difference ($P_0 - P_1$); accelerates toward the source exit (Edelstein A S and Cammarata R C, 2002). The vapor initially expands isentropically from the nozzle where it is continuum flow or collision dominated, to a region downstream where the flow becomes free molecular or collisionless and is no longer isentropic. The vapor cools during the expansion, crosses the gas/liquid coexistence line and becomes supersaturated. The density of clusters formed depends on the degree of supersaturation.

In comparing the two routes of production, the free jet expansion method is more expensive than the sol-gel method, and produces nanoparticles with a wider size range; 1-100nm. The sol-gel route produces particles with closer size ranges; 2-5nm but needs further drying after production and is the most widely used method for the production of oxide nanoparticles. Standard characterization techniques are employed for both methods and these are; TEM, SEM and XRD.

2.5 Alumina Toxicity

Rat tissue responses to alumina powder administered at low doses (10μg/ml and 8μg/ml), have been investigated (Di-Silvestre M et al, 1991), it was found that powdered alumina implantation in the subcutis, the muscle and the peritoneum of the rat produced the same intense acute inflammatory reaction in all implantation sites after 2 weeks. However, after 8 weeks the inflammatory reaction had regressed and there was a thin layer of connective tissue around the implanted material, completely isolating it from the surrounding tissues.

Other investigators (Nkamgueu E M et al, 2000) found that alumina microparticles ingested by human blood monocytes that had been forced to differentiate into macrophages over a 7-day period decreased the macrophages' intracellular K/Na ratio (a measure of cell vitality), decreased their phagocytic ability by 27%, and reduced their oxidative metabolism by a factor of 5.

The responses of a few other cell types to alumina ceramic powders have also been investigated. For example, cultured human fibroblasts exposed to 1-500 μg/cm^3 alumina powder showed no cytotoxic effects with cell viability at different exposure times measured by colony formation efficiency, neutral red uptake and colorimetric tetrazolium reduction (Li J et al, 1993). No cytotoxic or antiproliferative effects were induced in fibroblast-like mesenchymal cell monolayer populations cultured in vitro on powdery alumina ceramic (Neupert G, Ziller R, Glien W, 1984). Alumina powders generally induce no cytotoxicity in cell cultures (Dion I, Bordenave L, Lefebre F et al, 1994) of human gingival fibroblasts or osteoblast like cells (Lang H, Mertens T H, 1990). It has been found (Nishio K et al, 2001) that the delta-crystal phase of alumina powder promoted greater differentiation in osteoblasts than the alpha-crystal phase when present in a complex composite ceramic. Alumina ceramics are obtained by combining powdered alumina with silica and feldspar in addition to other binding materials, with alumina being the major component. As mentioned before, the difference between gamma alumina and alpha alumina lies in their individual crystal structures; gamma alumina is cubic and transforms into the hexagonal crystal structure of alpha alumina at high temperatures.

Alumina refinery workers exposed to >100 mg/m^3-year of gamma alumina for >20 years had a 3- to 4-fold excess of individuals with an abnormal forced expiratory volume at 1 second, with abnormal being defined as <80% of the predicted figure, though smoking had a far more deleterious effect on ventilatory capacity (Townsend M C, Enterline P E et al, 1985). Alpha-alumina 100-700 nm particles have only minimal (Stacy B D et al, 1959) or no (Meiklejohn A, 1963) fibrogenic reactivity, and only at doses instilled intratracheally that are massive compared to the amount which could reasonably be inhaled in any one breath. Such massive doses of gamma-alumina in the 20-40 nm size range did produce a fatal fibrosis of the lungs in rats (King E J, Harrison C V, Mohanty G P, Nagelschmidt G, 1955), but it is not known if other materials of similar sizes will produce the same or similar toxic result.

From a recent size related toxicity study of alumina nanoparticles (Stanley K J et al, 2010), nano-sized alumina particles were found to be more phytotoxic to *Hyalella azteca* (an amphipod crustacean) than micro-sized alumina particles, when treated with 55.1±0.6g/kg micro-sized particles and 66.2 ± 0.6g/kg nano-sized particles. The authors studied the toxicity of alumina nanoparticles on a variety of sediment non-plant organisms; *Tubifex tubifex, Hyalella azteca, Lumbriculus variegates*, and *Corbicula fluminea* and found that *H.azteca* was most affected, especially at high concentration, based on their survival and growth profile. The period of exposure was 14 days, after which a comparison was made of the effect of both micro-sized and nanometer sized alumina particles.

2.6 Root Exudates

Many plant species do posses the ability to defend themselves against toxic agents by exuding defensive substances from their roots, these exudates will then react with these toxic materials, thereby neutralizing most, if not all, of their effect.

Root exudation can be broadly divided into two active processes. The first, root excretion, involves gradient-dependent output of waste materials with unknown functions, whereas the second, secretion, involves exudation of compounds with known functions, such as lubrication and defense (Bais H P et al, 2004; Uren N C, 2000). Roots release compounds via at least two potential mechanisms. Root exudates are transported across the cellular membrane and secreted into the surrounding rhizosphere. Plant products are also released from root border cells and root border-like cells, which separate from roots as they grow (Hawes M C et al, 2000; Vicre M et al, 2005). Different phytotoxins in root exudates affect metabolite production, photosynthesis, respiration, membrane transport, germination, root growth, shoot growth, and cell mortality in susceptible plants (Einhellig F A, 1995; Weir T L, 2004). These effects on plant physiology, growth, and survival may in turn influence plant and soil community composition and dynamics (Harsh P et al, 2006).

The ecological relevance of phytotoxic root exudates also depends on the susceptibility of the plants with which the allelopathic (a situation whereby an organism produces one or more biochemicals that influences the growth, survival and reproduction of other organisms) plants coexist. For example, (±)-Catechin and 8-hydroxyquinoline inhibit the growth of native North American plants in communities invaded by *Centaurea*

maculosa, the Spotted Knapsweed, (Bais H P et al, 2003; Weir T L, Bais H P, Vivanco J M, 2003 and Vivanco J M et al, 2004).

Many plants also produce secondary metabolites that inhibit the growth of nonspecific plants of the same species, also known as autotoxicity. Autotoxicity has been widely observed in agricultural crops and weeds, as well as in some plants that inhibit natural systems (Singh H P, Batish D R and Kohl R K, 1999). Some plants may avoid effects of phytotoxins by sequesting the toxins in vacuoles or specialized tissues, or by secreting the phytotoxins as they are taken up (Williamson G B, 1990).

Other plants avoid inhibition from phytotoxins by altering the chemical structure of the toxins. Root exudates also play an integral role in Striga haustorial formation. Striga is an African plant without a developed root system that lives by tapping into the roots of other plants for nutrients. Haustoria are specialized root structures in plant parasites that allow the parasites to infect host vascular tissue. Haustoria often penetrate the host cell membrane. On penetration, the fungus increases the surface area in contact with host plasma membrane, releasing enzymes that break down the cell wall enabling greater potential movement of organic carbon from host to fungus (http://science.yourdictionary.com/haustorium). The most recent evidence suggests that the chemical cross talk between Striga seedlings and host roots that results in haustorial formation begins with the constitutive release of hydrogen peroxide from Striga seedling root tips into the rhizosphere (Kim D J et al, 1998). Hydrogen peroxide activates host, and perhaps parasite, peroxidases that degrade host cell wall pectins, oxidatively releasing benzoquinones into the rhizosphere (Keyes W J et al, 1998). Some root exudates that act as metal chelators in the rhizosphere can increase the availability of

metallic soil micronutrients, including iron, manganese, copper and zinc (Dakora F D, Phillips D A, 2002). Metal chelators form complexes with soil metals, thus releasing metals that are bound to soil particles and increasing metal solubility and mobility.

As mentioned earlier, reactive oxygen species (ROS) can have wide-ranging damaging effects on biology through directly modifying cellular components. One such action that may be highly relevant to allelochemical-induced toxicity is ROS-related effects on the lipid bilayer, such as lipid peroxidation (Harsh P et al, 2006). Lipid peroxidation leads to the destruction of the polyunsaturated fatty acids that are integral to membrane integrity and transport activities across the plasma membrane. Increase in lipid peroxidation accompanies addition of aqueous allelochemicals in tomato and cucumber roots (Cruz-Ortega R, Ayala-Cordero G, Anaya A L, 2002; Politycka I, 1996).

2.7 Ultra Filtration (Membrane Filtration)

In this investigation, an ultra-filtration technique was utilized to effect particle size separation in order to determine any possible particle size –inhibitory growth effect on plant root by alumina and silica nanoparticles.

The membrane separation process is based on the use of semi permeable membranes. The principle is quite simple: the membrane acts as a very specific filter that will let water flow through, while it retains suspended solids and other substances based on a specific size cut-off that is a function of the particular membrane. There are various methods to facilitate the rate of transfer across such a membrane. Examples of these methods are the applications of high pressure, the maintenance of a concentration gradient on both sides of the membrane and the introduction of an electric potential.

Certain substances can pass through the membrane, while other substances are retained. Membrane filtration can be used as an alternative for flocculation, sediment purification techniques, adsorption (sand filters and active carbon filters, ion exchangers).

Membrane filtration can be divided between micro and ultra filtration on the one hand and nano filtration and Reverse Osmosis (RO or hyper filtration) on the other hand. When membrane filtration is used for the removal of larger particles, micro filtration and ultra filtration are applied. Nano filtration and RO membranes do not work according to the principle of pores; separation takes place by diffusion through the membrane. The pressure that is required to perform nano filtration and Reverse Osmosis is much higher than the pressure required for micro and ultra filtration, while productivity is much lower. (http://www.lenntech.com/membrane-technology, accessed May, 2009)

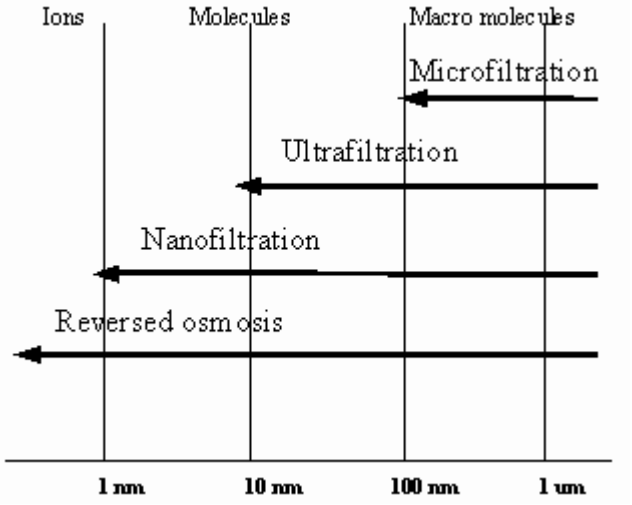

Figure 2.3 Filtration methods in relation to particle size.

Source: (http://www.lenntech.com/membrane-technology,)

The physical and chemical nature of the membrane (for example; pore size and pore distribution) affects the separation of the liquid and its components. Hydrostatic force is the key driving force in achieving separation, (Singh RP and Heldman DR, 1993). The smaller the pore size, the smaller the size of the particles that can pass through the membrane. As the pores get smaller, the system is more costly to operate. Larger pores have fewer membrane elements and lower operating pressure, (http://www.gewater.com accessed May, 2009).

Ultra Filtration involves the pressure-driven separation of materials from water using a membrane pore size of approximately 0.002 to 0.1 microns, an MWCO of approximately 10,000 to 100,000 Daltons, and an operating pressure of approximately 200 to 700 kPa (30 to 100 psi), (http://www.ndwc.wvu.edu, accessed May, 2009).

Ultra Filtration is a process by which colloids, particulates, and high molecular mass soluble species are retained by a process of size exclusion, and, as such, provides means for concentrating, separating into parts, or filtering dissolved or suspended species. Ultra Filtration allows most ionic inorganic species to pass through the membrane and retains discrete particulate matter and nonionic and ionic organic species. It is a single process that removes many water-soluble organic materials, as well as microbiological contaminants. Since all Ultra Filtration membranes are capable of effectively straining protozoa, bacteria, and most viruses from water, the process offers a disinfected filtered product with little load on any post-treatment sterilization method, such as UV radiation, ozone treatment or even chlorination (http://www.ndwc.wvu.edu, accessed May, 2009).

Though Ultra Filtration is a promising method for particle size separation, the limiting conditions are membrane fouling and permeate flux decline. Fouling problems are a result of concentration polarization while flux decline is caused by (i) osmotic pressure increase near the membrane-solution/suspension interface (ii) growth of a gel-layer and (iii) solute adsorption and pore blocking. The initial flux decline in most Ultra Filtration processes is osmotic pressure controlled until gel formation starts. Once the gel layer is formed, the flux decline is controlled by the gel-layer growth (Bhattacharjee S and Bhattacharya P K, 1992).

CHAPTER 3

RESEARCH SUMMARY AND METHODOLOGY

As stated earlier, the objective of this research is to determine the mechanism(s) responsible for the phytotoxic effects of alumina nano-particles as observed by previous researchers, and confirmed during this work.

In order to do this, certain relevant hypotheses were investigated. In this study, five plant species were used as was the case with the previous investigators in order to maintain consistency. They were: 1. *Zea mays* (corn), 2. *Cucumis sativus* (cucumber), 3. *Daucus carota* (carrot), 4. *Brassica oleracea* (cabbage) and 5. *Lactuca sativa* (lettuce). These plants were germinated into seedlings and exposed to a suspension of 13nm alumina particles at concentrations similar to those used by the previous investigators, which were mainly; 20mg/ml, 2mg/ml, 200µg/ml and 20µg/ml. It was important to use similar concentrations, plant species and experimental conditions so as to ascertain the mechanism(s) responsible for the observed inhibitory growth of plants when exposed to Alumina nano-particles, as well as Silica nanoparticles to a more limited extent.

3.1 Research Summary

Previous researchers (Ling. Y, D. Watts, 2004), subjected five plants species (*Zea mays, Cucumis sativus, Daucus carota, Brassica oleracea, Lactuca savita*) to three types of nanoparticles; alumina, titania and silica, at four concentrations; 20mg/ml, 2mg/ml,

200µg/ml and 20µg/ml, and demonstrated that alumina nanoparticles are more inhibitory to plant root growth than the other two.

The major objective of this investigation is to find out why alumina nanoparticles are phytotoxic to plant roots by determining the mechanism(s) of this effect. As a first approach to this determination, the hypothesis put forth by the initial investigators was investigated; they suggested that the inhibitory growth effect of alumina nanoparticles on plants roots might be due to the presence of peroxides in the alumina nanoparticles suspension.

As reported in the previous chapter, peroxides are known to hinder and inhibit the growth of at least some plant roots. So, the question of whether ; peroxides are present in the alumina nanoparticles suspension used by these investigators was considered by preparing samples of alumina nanoparticles of the same concentrations as used by the previous investigators and prepared as they did. A standard test for the presence of peroxide was carried out using potassium iodide (KI). Another hypothesis that these researchers put forth, was that, there could have been a mechanical contact between the root cell wall/ boundaries of the seedlings and the particles in suspension. A plan to investigate this hypothesis included the preparation of alumina nanoparticle paste and germination of plant seedlings using the same techniques employed by the previous researchers with, the application of this substance on only one side of the roots.

A resulting curved growth of the root after 72 hours would support the hypothesis, because only the side of the roots without paste would be expected to grow unhindered, while the side with the paste would experience inhibited growth. During the course of past investigations, the investigators coated the particles with Phenanthrene. Based on their results that showed no inhibitory effect on root growth they proposed that surface characteristics might play a role in the phytotoxic effect of alumina nanoparticles on plant roots. This assertion was investigated by obtaining the supernatants of alumina nanoparticles suspensions and loading the seedlings with these. Additional work was carried out based on the literature, to investigate the hypothesis that there could have been the presence of residual aluminum in the alumina nanoparticles. Aluminum is a well known toxic agent, for plants and could be the cause of the phytotoxic effect observed by the previous researchers. This research involved the use of Morin, which is a fluorescent agent for aluminum and uv/vis spectrophotometry. The process was verified by using a standard aluminum solution, at 420 nm, wavelength, followed by the testing of the specimen of alumina nanoparticles supernatants for aluminum content. The aluminum standard solution, together with several different dilutions was used to load plant seedlings and the effects were compared to that of different concentrations of alumina nanoparticles supernatants.

Last, it was hypothesized that agglomeration may have occurred before or after the coating of particles with Phenanthrene by the previous investigators that may have resulted in the formation of large particles that could not interfere with plant root cells division and growth, thereby exhibiting the observed non-inhibitory effect of alumina under these circumstances. This is in addition to the fact that the obtained alumina

nanoparticles exist in a range of sizes (size aggregates), thereby the need arose to determine the effect of specific sizes of these particles. This led to the use of membranes with 0.025µm and 0.05µm pore sizes to filter the suspensions using ultra-filtration. The obtained permeate were then used to load onto plant seedlings in order to determine their effect. Additionally, silica nanoparticles were ultra filtered and the resulting permeate used for comparison purposes.

3.1.1 RE / RRG

According to EPA standard procedures for root elongation tests, the test results are reported as 1. Relative Elongation (RE) and 2. Relative Root Growth (RRG), also in line with the previous investigation, statistical tools such as the Student's t-Test and one-way ANOVA were used to analyze and present results.

Root elongation (RE) during the exposure period was calculated using equation (3.1) below. A unified method of data analysis must be used for comparative purposes, because the root elongations of seedlings are not constant among different test batches and different plant species. A Relative Root Growth (RRG) was calculated for this purpose, based on what was proposed by Schildknecht (Schildknecht P H P A and Vidal D B, 2002), using equation (3.2):

$$RE\ (mm) = L_{after}\ (mm) - L_{before}\ (mm) \tag{3.1}$$

$$RRG = RE_{sample} / RE_{control} \tag{3.2}$$

Where L_{after} and L_{before} refer to the measured root lengths after and before exposure, respectively.

3.1.2 Statistical Analysis

Results in this research are displayed as mean ± standard deviation (SD), along with 95% confidence interval. The statistical tools are *Student's t-test* and *one-way* ANOVA *procedure.*

3.1.2.1 Student's t-Test

Statistically significant difference is reported when the probability of the result assuming the null hypothesis (p) is less than 0.05. At this point, the calculated *t* value is larger than the upper critical *t* value in the *Student's t distribution table* with the same degree of freedom and significance level of $\alpha = 0.05$. The student's t-test program is available many places including on the website (physics.csbsju.edu, 2009).

3.1.2.2 *One-way ANOVA*

The Analysis of variance (ANOVA) is an important tool used universally to test the hypothesis that the means among two or more groups are equal. As with the previous study, concentration remains the only experimental variable factor in this investigation, except in chapter six, where size was also considered, in that case, analysis was done one factor at a time. That led to the use of the *one-way* ANOVA *procedure.* The null hypothesis of *one-way* ANOVA in this study is that there is no difference in the

population means of the root growth measurements after treatment with different levels of the concentration factor of the nanoparticles. The objective of the process is to divide the total variation in the data into a portion due to randomness and portions due to changes in the values of the independent variable(s). The variance of total measurement in the data can be given as:

$$s^2 = \frac{\sum_{i=1}^{n}(y_i - \bar{y})^2}{n-1} \tag{3.3}$$

Where $\bar{y}$ is the mean of the total measurements, *n* is the number of measurements, and *y* is the value of each measurement. The numerator is termed the *sum of squares* of deviations from the mean (Total SS), under one-way ANOVA, there are two components; *sum of squares of treatments*, SST, and *sum of squares of error*, SSE:

$$SST = \sum_{i=1}^{k} n_i(\bar{y}_i - \bar{y})^2 \tag{3.4}$$

$$SSE = \sum_{i=1}^{k}\sum_{j=1}^{n_i}(y_{ij} - \bar{y}_i)^2 \tag{3.5}$$

In the above equations, *k* is the number of groups, n_i is the number of values in the group, $\bar{y}_i$ is the mean value of the group, $\bar{y}$ is the mean value of the total measurements, and y_{ij} is the value of the j^{th} measurement in the i^{th} group.

The mean square for treatment, MST, and mean square for error, MSE, can be gotten by dividing the SST and SSE by DFT, degree of freedom for treatment and DFE, degree of freedom for error respectively, as expressed by the equations below:

$$MST = SST / DFT \tag{3.6}$$

$$MSE = SSE / DFE \tag{3.7}$$

Where, $DFT = k - 1$, k is the number of groups of treatments, and $DFE = N - k$, where N is the total number of measurements in all groups.

The test statistic, used in testing the equality of treatment means is:

$$F = MST / MSE \tag{3.8}$$

The critical value is the tabulated value of the F distribution, based on the chosen α level and the degrees of freedom, DFT and DFE. The probability of the result assuming the null hypothesis (p) was calculated from the F, DFT, and DFE, using an online program (Graphpad.com, 2009).

And lastly, the coefficient of determination, R^2, is given by;

$$R^2 = 1 - SS_{total} / SS_{error} \tag{3.9}$$

Where SS_{error} is the error sum of square while SS_{total} is the total sum of square.

3.1.3 Materials

Particles used in this study were Alumina (Al_2O_3) nanoparticles generously given to us by another research group on campus, and fumed hydrophilic Silica (SiO_2) nanoparticles, Cab-O-Sil® M5 purchased from Cabot. Both materials were the exact materials used by the previous investigators and their aggregate sizes plus/minus standard deviation are 201.0 ± 74.7 nm for Alumina and 215.7 ± 56.3 nm for Silica (Yang L, Watts D, 2004). Manufacturers average particle size specifications were 13nm for Alumina and 14nm for Silica.

Seeds of five plant species used in this research were; *Zea mays (corn), Daucus carota* (carrot), *Lactuca sativa* (lettuce), *Brassica oleracea* (cabbage), *Cucumis sativus* (cucumber). These seeds were purchased from Territorial Seed Company (Oregon, USA), and were among the ten plant species recommended by the US EPA (EPA, 1996) to determine ecological effects of pesticides and toxic substances.

3.2 Research Methodology

3.2.1 Determination of Hydrogen Peroxide in Test Suspension

This procedure was carried out as described by recent users of the technique (Catron D H, Schlatter L K and Thornton G L, 1998).

3.2.1.1 Preparation of Starch Indicator

Starch indicator was prepared by dissolving 3.2grams of corn starch in 0.2 Liters of Milli-Q water, thereby, resulting in a concentration of 16g/L.

3.2.1.2 Preparation of Potassium Iodide Suspension

This was done by dissolving 14.2grams of Potassium Iodide (KI) crystals in 10 ml of Milli Q, water giving a concentration of 1.42 g/ml of KI.

3.2.1.3 Preparation of Alumina Nanoparticles Suspension

400 ± 0.15mg of 13nm alumina particles was weighed using the Ohaus electronic weighing machine from Precision Plus and mixed with 20 ml of Milli Q water in a volumetric flask. It was then sonicated using a Branson 5210 Sonicator for 3 hours thereby giving a concentration of 20 mg/ml.

3.2.1.4 Test for Hydrogen Peroxide

At the end of 3 hours of sonication, 10 ml of the Alumina nano-particles suspension was measured out into a test tube; 2 ml of the prepared KI suspension was then gradually added into the test tube. Finally, 1 ml of the starch indicator was added into the same test tube. The mixture was shaken and left to stand for 30 minutes.

A positive confirmation will result in the color of the suspension turning into purple as the KI is reduced to Iodine. But after 30 minutes, the color of the suspension changed from milky white to light brown, indicating the absence of hydrogen peroxide in the alumina nano-particle suspension.

The effectiveness of the reagents was then verified by measuring out 5mls of 35% pure hydrogen peroxide, from Fluka Chemika, into a test tube followed by the addition of 0.5 ml of corn starch indicator, this mixture was shaken gently. 1ml of the prepared Potassium Iodide solution was then gently added, there was an instant exothermic chemical reaction that was accompanied by color change from almost colorless to purple.

3.2.2 Determination of the Effect of Mechanical Contact on Root Growth

3.2.2.1 Preparation of Seeds for Germination

30 seeds of *Zea mays (corn)* were soaked in 10% Sodium Hypochlorite suspension for cleansing and disinfection for 10 minutes, then rinsed 3 times with Milli Q water. The seeds were then submerged in 80ml of Milli Q water and placed in an incubator at $25 \pm 1^{\circ}$ C for 24 hours. At the end of the 24 hours, the seeds were removed from the incubator

and transferred to 3 Petri dishes, of size 100 ×15 mm, with 10 seeds per dish. 5 ml of Milli Q water was then added to each Petri dish; the dishes were taken back to the incubator and placed in the dark at 25 ± 1°C. The water in the Petri dish was changed every day with fresh Milli Q water in order to maintain freshness and avoid the growth of unwanted micro-organisms.

It normally took up to 3 days (72 hours) for *Zea mays* to fully germinate. So, on the third day, the seeds were removed from the incubator and inspected. About 10 seeds, either did not germinate up to 5mm or did not germinate at all, those were discarded. The remaining 20 seedlings had their roots measured and recorded and then labeled for identification. They were placed in four Petri dishes, the first two with 5 seedlings per dish, constituted the Blank (control) while the other two were subjected to alumina nano-particle treatment.

3.2.2.2 Preparation of Alumina Nanoparticles Paste

400 ± 0.15mg of 13nm Alumina nanoparticles was weighed into a beaker and 10ml of Milli Q water was then added to the particles and the suspension was stirred with a glass rod until a thick paste resulted, thereby giving a concentration of 40mg/ml, the pH was measured and recorded (pH 4.11) with the aid of pH strips.

3.2.2.3 Application of Alumina Paste

The aim of this experiment was to determine if close contact with the particles could have affected the growth rate of plant roots as observed by previous investigators.

If the paste is applied on one side of the root and the interaction between the root and particles is inhibitory in nature, then it will result in greater growth being achieved on the side without the paste, hence producing a curved growth, which can visually be ascertained.

In order to apply the paste, a little brush with tiny bristles was obtained and used to carefully apply the paste. In this way, the paste was applied to one side only of each of the 10 seedlings of the *Zea mays*. *Zea mays* was chosen for this experiment because the roots are a bit bigger than the rest of the plant species used in this research, and hence it is easier to apply the paste. After the paste application, 3ml of Milli Q was added to the Petri dish to moisten the filter paper. 5ml of Milli Q water was also added to the Petri dish containing the blank seedlings. Both the blank and exposed samples were placed in the dark in an incubator at $25 \pm 1^{\circ}C$ and allowed to grow for 72 hours.

On the third day, the samples were removed and inspected; the samples with the paste did not show any evidence of curved growth, the samples were then measured for growth. As a result of the lack of effect of alumina paste on *Zea mays*, that is, the alumina paste did not obstruct root growth or cell division on the side the paste was applied, which could have resulted in curved growth, other plant species were then exposed to the same paste using the procedure as described above in this section (3.2.2.3) and preparation of the seeds for germination is as described in 3.2.2.1. The additional plant species investigated were *Daucus carota* (carrot), *Lactuca sativa* (lettuce), *Brassica oleracea* (cabbage), *Cucumis sativus* (cucumber). After 72 hours of exposure, they were brought out from the incubator and inspected, results of the growth pattern were similar

to those of *Zea mays*, that is; there was no curving of the roots during growth. Root lengths of the samples and Blanks were measured and recorded.

3.3 Preparation of 20mg/ml of Alumina Nanoparticles Suspension

10 ± 0.15 grams of alumina nanoparticles were weighed and poured into a glass flask containing 500 ml of Milli Q water and sonicated for three hours, after covering the flask with a transparent plastic.

3.4 Application of 20mg/ml Alumina Nanoparticles Suspension

The preparation of all seeds used in this investigation for germination and exposure to nanoparticles suspension was as described in 3.2.2.1. After germinating seeds into seedlings, they were carefully rinsed with Milli Q water and placed 1cm apart on fresh filter papers in petri dishes, five per petri dish, and labeled. Then 5 ml of alumina nanoparticles suspension was carefully poured into the dishes so as not to move or change the position of the seedlings. A different batch was prepared as blanks by applying 5 ml of Milli Q water to each petri dish instead of alumina nanoparticle suspension. A volume of 5 ml of suspension was chosen because it was sufficient to partially submerge the seedlings without ‘drowning’ them. After this treatment, both batches were placed in the dark in the incubator for 72 hours, at 25 ± 1ºC.

At the end of the 72 hours, the samples were inspected, measured and recorded.

3.5 Preparation of Alumina Nanoparticles Suspension and Supernatants

Four volumetric flasks were filled to the 400 ml mark with Milli Q water, and then 8 ± 0.15g, 0.8 ± 0.05g, 0.08 ± 0.005g and 0.008 ± 0.001g of aluminum nanoparticles were measured out into the four flasks to give the concentrations of 20mg/ml, 2mg/ml, 200µg/ml and 20µg/ml respectfully. These concentrations were determined and used by earlier investigators who discovered that such concentration do cause inhibitory growth in plants. So, it was essential to maintain similar concentrations as to properly determine the mechanism(s) of toxicity.

The suspensions were then sonicated for 3 hours and poured into already labeled centrifuge bottles and centrifuged for 5 hours at a speed of 27000 RPM and a temperature of 21°C, using a Sorvall R_C 28 S centrifuge machine from DuPont. At the end of 5 hours of centrifuging, 40 ml of the supernatant was carefully pipetted out from each concentration, the pH was measured and recorded with the aid of a Dual channel pH/Ion meter model AR25 Accumet Research from Fisher Scientific and stored in test tubes with lids.

3.6 Application of Supernatants

Aliquots of 5 ml of supernatants of each concentration were carefully pipetted into Petri dishes containing the seedlings to be treated, while 5 ml of Milli Q water was applied on the Blank samples. After this treatment, both batches were placed in the dark in the incubator for 72 hours, at 25 ± 1°C.

3.7 Particle Count Analysis

In order to determine if the supernatants from centrifuging contained particles that could be phytotoxic to the seedlings, 10 ml of the supernatants were carefully pipetted from each concentration into the sample container of a Beckman-Coulter N4 Plus particle counting machine, after rinsing the container several times with Milli Q water. This machine was chosen because of its ability to detect particles that are ultrafine, that is, less than 1µm. Three angles were chosen as the critical angles after a preliminary investigation, specifically; 23°, 62.6° and 90°. All tests were run at 25 ± 1ºC under a unimodal mode.

3.8 Determination of Aluminum using Morin

3.8.1 Reagents and Solutions

All the chemicals used in this experiment were of analytical grade of the highest purity available. Glass vessels were cleaned by soaking in acidified solutions of $KMnO_4$ followed by washing with concentrated HNO_3, and rinsed several times with high-purity deionized water (Milli Q water).

3.8.2. Morin Solution

A portion of 40.27mg of Morin, purchased from BDH Chemicals, was dissolved in 100 ml of triply-distilled ethanol. This solution was diluted further as required (Ahmed M J, Hossan J, 1995).

3.8.3. Aluminum Standard Solution

100 ml stock solution of Al (0.0371 M) was prepared by dissolving 1.7582g of $AlK(SO_4)_2.12H_2O$, of analytical grade, from Merck Laboratories, in Milli Q water. Working standard solutions were prepared after suitable dilutions of the stock solution.

3.8.4. EDTA Solution

100 ml stock solution of EDTA (0.01%) was prepared by dissolving 10 mg of A.C.S grade (≥ 99%) ethylenediaminetetraacetic acid, disodium salt dehydrate in (100 ml) Milli Q water.

3.8.5. Tartrate Solutions

A stock solution (100 ml) of tartrate (0.01%) was prepared by dissolving 10 mg of A.C.S grade (99%) potassium sodium tartrate tetrahydrate in 100 ml of Milli Q water.

3.8.6. Dilute Ammonium Hydroxide Solution

A 100 ml solution of dilute ammonium hydroxide was prepared by diluting 10 ml conc. NH_4OH (28-30%, A.C.S grade) to 100 ml with Milli Q water.

3.8.7. Alumina Supernatants

Four concentrations of alumina suspension (20 mg/ml, 2 mg/ml, 200µg/ml and 20µg/ml) were prepared and their supernatants obtained as described in 3.5.

3.8.8. Procedure

Samples (supernatants from each concentration) of 50 ml each were filtered, one concentration at a time, using a Whatman No. 40 filter papers into four volumetric flasks and were then heated with a mixture of 1 ml conc. H_2SO_4 and 2.5 ml conc. HNO_3 in each until sulphur trioxide fumes appeared. After cooling, addition of 2.5 ml conc. HNO_3 and heating was repeated until dense white fumes were observed. The solutions were then cooled and neutralized (pH 6) with dilute NH_4OH in the presence of 2 ml of both 0.01% (w/v) EDTA and tartrate solution. They were transferred into four 50 ml volumetric flasks and diluted up to the mark with Milli Q water. An aliquot of 1 ml of the final solution from each concentration was pipetted into a 10 ml calibrated flask to which was added, 2 ml of 1.33×10^{-3} M of the morine reagent solution, followed by the addition of 0.2 ml of 0.025 M sulfuric acid. The solution was mixed well and allowed to stand for 1 minute, after which 5 ml of ethanol was added. The mixture was diluted up to the required volume with deionized water. The absorbance was measured at 421 nm against a corresponding reagent blank using an Agilent (Model 8453) double beam uv/visible recording spectrophotometer. The same procedure was utilized for the aluminum standard solution and its dilutions.

3.9 Ultra Filtration

In order to determine any possible particle size effect of both alumina and silica nanoparticles on plant growth, two different pore sizes (0.025μm and 0.05μm) of

hydrophilic membranes were obtained from Millipore Inc. in order to prepare filtrates of the nanoparticle suspensions with a known upper limit size range.

3.9.1 Sample Preparation

Eight volumetric flasks, one for each concentration and sample (for both alumina and silica), were filled to the 400 ml mark with Milli Q water, and then 8000 ± 0.15mg, 800 ± 0.15mg, 80 ± 0.15mg and 8 ± 0.05mg of alumina or hydrophilic-silica nanoparticles respectively were measured out into the eight flasks to give the concentrations of 20mg/ml, 2mg/ml, 200µg/ml and 2µg/ml per sample respectively. The solutions were each sonicated for 3 hours. They were then individually poured into the upper chamber of the filtration system with a particular pore size membrane, one concentration at a time, while using a fresh membrane for each run. Filtration was carried out at a suction pressure of 75 kPa for each sample. After each filtration, both the lower and upper chambers were washed and rinsed four times with Milli Q water in order to avoid contamination.

3.9.2 Germination of Seedlings

The preparation and germination of seedlings for these experiments was as described in section 3.2.2.1. Because of the inclusion of hydrophilic-silica in the experiment, twice the regular number of seeds were utilized in addition to extra seeds to accommodate for damaged seeds during germination.

3.9.3 Application of Samples

The application of both the alumina and silica samples (permeates) to the seedlings was as described in section 3.6. Except in this case, permeates were used instead of supernatants.

3.9.4 Particle Count Analysis

The particle count analysis for this experiment was conducted in accordance with the procedure described in section 3.7.

CHAPTER 4

SUPERNATANTS EFFECT ON ROOT GROWTH

The purpose of this phase of the investigation was to determine if surface characteristics of alumina nanoparticles, including and not limited to ions, contaminants and other chemical species were responsible for the observed root growth inhibition. In their study, (Ling Y, Watts D, 2004), nanoparticles were coated with phenanthrene, which resulted in decrease of phytotoxicity, especially with Alumina nanoparticles, thereby giving rise to the hypothesis that surface characteristics of some nature could have been responsible for the observed phenomenon, and hence the motivation to further investigate this effect.

In order to extract any possible adhering surface toxic substances, supernatants from four concentrations; 20mg/ml, 2mg/ml, 200µg/ml and 20µg/ml of alumina nanoparticles suspensions were prepared by centrifugation according to section 3.5. This was followed by carefully pippeting their supernatants onto already germinated seedlings of the plant species used in this investigation, after particle count analysis of the supernatants as described in section 3.7. Seed preparation and germination, in addition to the application of the supernatants were as described in sections 3.2.2.1 and 3.6 respectively.

4.1 Investigation of Inhibition of Plant Root Growth using Alumina Nanoparticles Supernatants

As mentioned earlier, this study was carried out in order to remove significant portions of the particles from the standard suspensions and to utilize the residual very small particles as well as any phytotoxic substances that might be on the surfaces of alumina nanoparticles. Because the plant seedlings showed the effects of the phytotoxicity in an aqueous medium, it was assumed that aqueous treatment of the particles should be sufficient to extract any such materials. Aqueous treatment followed by centrifugation should allow any phytotoxic material to be contained in the supernatants. Plant seedlings were then exposed to these supernatants in order to ascertain any phytotoxicity. To this end, root growth was measured before and after exposure to supernatants and reported as R.E. The same was done with seedlings exposed to Milli-Q water instead of the supernatants, these were the blanks and the average of the R.Es of the blank was used to calculate the R.R.G of the samples exposed to supernatants. Statistical analysis techniques were then used to analyze and compare the difference in the R.E of the treated samples and the blank.

From root elongation measurements shown in Table 4.1, and the bar chart in Figure 4.1, in addition to diminished differences between R.E from different concentrations, it is apparent that *Z.mays* was not noticeably affected by the treatment with supernatants. The rest of the plant species; *D.carota, L.sativa* and *B.oleracea*, and *C.sativus* were impacted by the phytotoxic nature of the supernatants. This immunity shown by *Z.mays* to the supernatants, especially at the high concentration of 20mg/ml, is comparable to that from the suspension as shown in Figure 4.3.

TABLE 4.1 Root Elongation (RE) and Relative Root Growth (RRG) of Plant Seedlings Exposed to Different Concentrations of Alumina Nanoparticles Supernatants for 72 hrs in the Dark at 25 ± 1ºC

The results are reported as mean ± S.D. and 95% confidence interval. And range given as min~max. R.E values are presented in mm.

Conc.	*Z.mays*	*D.carota*	*L.sativa*	*B.oleracea*	*C.sativus*
R.E					
	33.5±1.6	17.0±2.3	66.8±6.6	71.8±2.0	50.2±2.7
Blank	30.7~35.8	12.7~20.3	57.6~76.1	68.7~75.1	46.7~55.7
	27.4±1.3	10.2±1.5	48.0±5.3	56.0±3.8	42.2±2.3
20µg/ml	25.4~29.1	8.0~12.4	39.7~56.2	50.8~62.3	38.7~45.9
	27.1±0.9	7.2±1.0	45.5±4.8	49.0±2.7	35.4±3.7
200µg/ml	25.8~28.4	5.3~8.6	38.9~52.3	45.2~53.2	28.4~40.1
	26.3±0.9	5.2±0.9	38.4±4.4	37.1±3.5	29.0±2.4
2mg/ml	24.1~27.4	3.8~6.8	30.8~45.2	30.7~41.7	24.8~31.8
	24.9±1.1	4.3±0.7	34.5±4.1	30.4±3.2	24.9±2.2
20mg/ml	23.5~26.7	3.2~5.8	29.7~41.2	25.1~35.7	20.8~27.3
R.R.G					
	0.817±0.04	0.597±0.09	0.719±0.07	0.779±0.05	0.58±0.05
20µg/ml	0.758~0.87	0.471~0.73	0.594~0.84	0.71~0.86	0.49~0.63
	0.81±0.03	0.423±0.06	0.675±0.07	0.682±0.04	0.70±0.07
200µg/ml	0.77~0.85	0.312~0.51	0.58~0.78	0.63~0.74	0.56~0.80
	0.787±0.03	0.31±0.06	0.575±0.06	0.517±0.05	0.57±0.04
2mg/ml	0.72~0.82	0.224~0.4	0.46~0.68	0.428~0.58	0.49~0.63
	0.745±0.03	0.251±0.04	0.517±0.06	0.424±0.04	0.50±0.04
20mg/ml	0.70~0.79	0.188~0.34	0.44~0.62	0.35~0.5	0.41~0.54

An explanation to this could be that, at higher concentration there was the possibility of *Z.mays* producing aluminum-activated root exudates, which resisted phytotoxicity.

Though, the R.E of the Blank was 33.5 mm, with a relative standard deviation of 4.78% but reduced to 27.4 mm and a relative deviation of 4.72% when treated with the least concentration of 20µg/ml of the supernatants, which further decreased to 24.9 mm and a relative standard deviation of 4.42%, when the highest concentration of 20 mg/ml was used, but the degree of inhibitory growth did not match other plant species as displayed in Figure 4.1(please note, in this dissertation the bars denote error bars only). This is analogous to the resistance to the growth inhibition effect shown by *Z.mays* to aluminum (Ma J F et al, 2001; Ma J F, 2000; Ryan et al, 2001; Kochian et al, 2004).

Other plants species were noticeably affected by the treatment with alumina nanoparticles supernatants. The most affected being *B.oleracea*, which decreased from 71.8 mm with a relative standard deviation or percentage error of 2.79%, of the Blank to 30.4 mm and a relative standard deviation of 10.53%, when the highest concentration of 20mg/ml was utilized. The R.R.G also decreased from 0.779 to 0.424 when the concentration was increased from 20µg/ml to 20mg/ml. Plant species have different natural growth potentials, but the way they respond to toxic substances which affect their growth could be seen by comparing the effect of different amount of substances and the Blanks. For example, *D.carota* which has the least growth potential out of the five plant species used could also be observed to have been affected by the application of the supernatants, with the highest inhibition occurring with the highest concentration of 20mg/ml. The percentage error or relative standard deviation for *Z.mays* in this study ranged from 3.32% from the 200µg/ml concentration to 4.78% from the Blank. A low percentage error denotes closeness to measured Relative Elongation mean and less variation. Therefore, it could be stated that the 200µg/ml concentration yielded results

that have lesser variation and were closer to the mean when compared to the Blank or the rest of the concentration.

As mentioned earlier, statistical analysis were carried to establish if there was any statistical difference between the treated and untreated samples, in other words; if there was an effect of the application of supernatants to plants species. The results of this analysis are displayed in Table 4.2, from these results it could be seen that at the least concentration of 20µg/ml, the probability, p, of the plant species, were greater than 0.05. A discussion of the phytotoxic difference between alumina nanoparticles suspension and supernatants will be done in section 4.2.

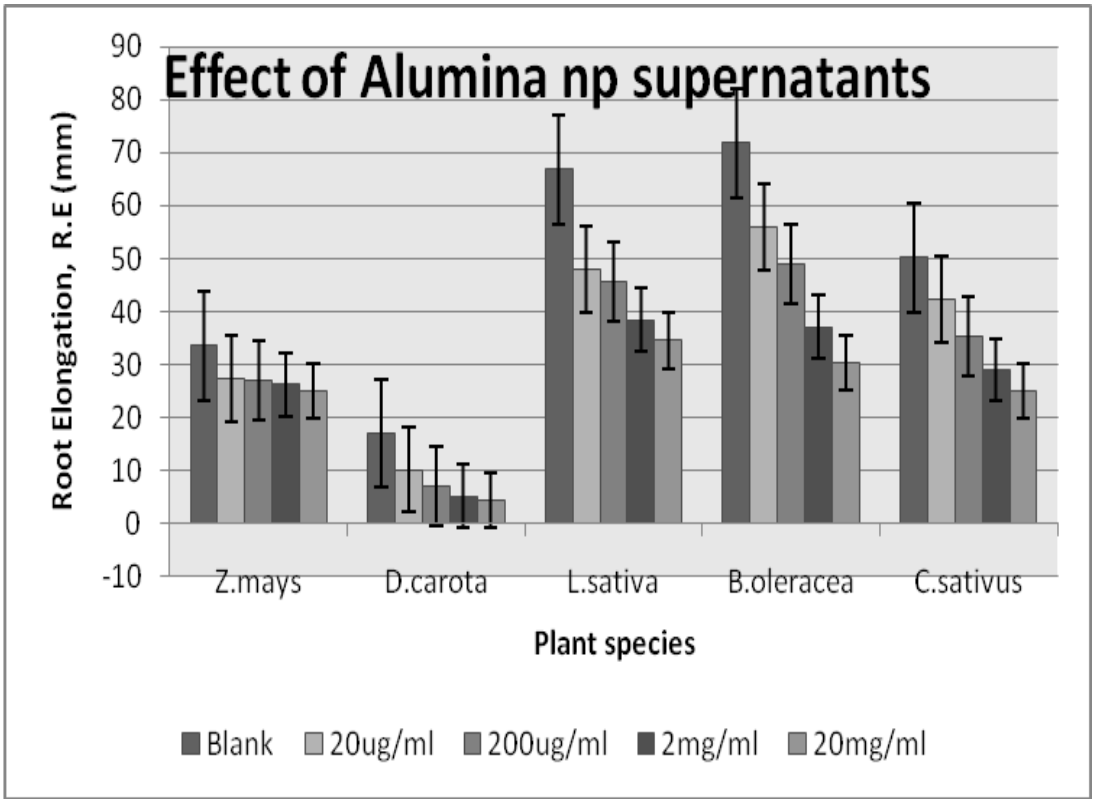

Figure 4.1 Effect of different concentrations of alumina nanoparticle supernatants on plant species.

Table 4.2 Statistical Analysis Results of the Root Elongation (RE) of Plant Seedlings Exposed to Different Concentrations of Alumina Nanoparticles Supernatants for 72 hrs in the Dark at 25 ± 1ºC

Results from the *one-way ANOVA* procedure are reported as the value of *f*, *p*, and the coefficient of determination (R^2). Statistical difference is reported as *p* smaller than 0.05.

Conc.	*Z.mays*	*D.carota*	*L.sativa*	*B.oleracea*	*C.sativus*
20µg/ml	*p*=0.08 R^2= 0.908 *f*=2.096	p= 0.09 R^2= *0.86* *f*= 2.023	p= 0.145 R^2= 0.842 *f*= 1.723	p= 0.1 R^2= 0.817 *f*= 2.517	p=0.053 R^2= 0.718 *f*=2.35
200µg/ml	*p*= 0.04 R^2=0.849 *f*=2.523	p= 0.04 R^2= 0.72 *f*= 2.523	p=0.02 R^2= 0.802 *f*= 2.949	p= 0.035 R^2=0.719 *f*=2.605	p= 0.009 R^2= 0.615 *f*=3.442
2mg/ml	*p*=0.01 R^2= 0.809 *f*=3.377	p= 0.01 R^2= 0.39 *f*= 3.377	p= 0.008 R^2= 0.798 *f*= 3.515	p= 0.018 R^2= 0.582 *f*=3.014	p= 0.000 R^2= 0.467 *f*=6.385
20mg/ml	*p*= 0.006 R^2= 0.793 *f*=3.695	p= 0.002 R^2= 0.12 *f*= 4.389	p= 0.000 R^2= 0.593 *f*= 6.385	p= 0.01 R^2=0.361 *f*=3.377	p= 0.000 R^2= 0.351 *f*= 6.385

It could be stated that for *D.carota*, *Z.mays*, *C.sativus*, *L.sativa*, and *B.oleracea*, there was no statistical difference between the treated group at the lowest concentration and the Blank, as could be seen in Table 4.2. The coefficient of determination, R^2, for the five plant species approached unity with the least concentration of 20µg/ml. The R^2 for *Z.mays*, *D.carota*, *L.sativa*, *B.oleracea* and *C.sativus* are; 0.908, 0.86, 0.842, 0.817 and 0.718 respectively, denoting a close correlation between the R.E of treated and untreated samples. As the concentration of alumina nanoparticles

supernatants was increased to 200μg/ml, remarkable statistical differences began to emerge between the treated seedlings and the Blank (control).

For all the plant species from the 200μg/ml concentration, p values were less than 0.05, suggesting a statistical difference between the two groups. A similar result was obtained when higher concentrations of 2mg/ml and 20mg/ml were used, as the p values with 2mg/ml were; 0.01, 0.01, 0.008, 0.018 and 0.000, for *Z.mays, D.carota, L.sativa*, *B.oleracea* and *C.sativus* respectively and for 20mg/ml, the p values were; 0.006, 0.002, 0.000, 0.01 and 0.000 for the same order of plant species of *Z.mays, D.carota, L.sativa*, *B.oleracea* and *C.sativus.*

With an increase in concentration came a departure of the coefficient of determination, R^2, from unity. For *C.sativus,* R^2 decreased from 0.718 to 0.615 when the concentration was increased from 20μg/ml to 200μg/ml, higher concentrations saw remarkable reductions in the R^2 for all plant species, except for *Z.mays,* with 0.809 and 0.793, when exposed to 2mg/ml and 20mg/ml of alumina nanoparticles supernatants respectively. For the rest of the plants species, when exposed to the 2mg/ml concentration, the R^2, were; 0.39, 0.798, 0.582 and 0.467 for *D.carota, L.sativa*, *B.oleracea* and *C.sativus* respectively, while those from the exposure to 20mg/ml were; 0.12, 0.593, 0.361 and 0.351 for the same order of plant species of *D.carota, L.sativa*, *B.oleracea* and *C.sativus*. The lower R^2 values with higher concentrations means there was greater inhibition to root growth at these concentrations when compared to the Blank. This assertion is further backed by the decrease in the R.E values at these concentrations as discussed earlier. Furthermore, the p values have been shown to be lower than 0.05, thereby depicting statistical difference between the exposed seedlings

and the Blank. Again, discussion on the statistical difference between plant seedlings exposed to alumina nanoparticles supernatants and those exposed to supernatants of alumina nanoparticles will be presented in section 4.2.

The foregoing suggests that the supernatants obtained from higher concentrations of nanoparticle suspensions lead to reduced plant root growth. There seem to be two possible explanations for this phenomenon. The first is that some nanoparticles, probably very small ones, were not spun down by centrifugation under the conditions used. Alternatively, another explanation could be that higher concentration of suspended particles means higher levels of toxic substances eluted from the surface of the alumina nanoparticles. As mentioned before, the essence of this particular study was to determine if exposure to the particles themselves was necessary for growth inhibition to be observed or whether some factor was extractable into the water that could cause the inhibitory effect. Removal of the suspended particles by centrifugation and subsequent evaluation of the supernatant liquids was considered to be a viable approach to make this comparison. To determine the possible presence of particles remaining in the supernatant, particle counting analysis was carried out as described in section 3.7; results are displayed in Appendix B. For particles dispersed in fluid, particle size distribution is a list of values that defines the relative amounts of particles present, sorted according to size. Particle counting was done using the Coulter counting technique which uses electro resistance. This measures the momentary changes in the conductivity of a liquid passing through an orifice that take place when individual non-conducting particles pass through. The particle count is obtained by counting pulses, and the size is dependent on the size of each pulse (http://www.beckmancoulter.com/coultercounter/product multisizer.jsp).

Considering the particle size count result in Figures B.1 to B.4 and Tables B.1 to B. 4, there was an indication that larger particle mean diameter and high polydispersity index were obtained with the highest concentration levels and that these measurements decreased as the concentrations of alumina nanoparticles supernatants were decreased. Polydispersity indices that were less than 0.1 suggest particles that are monodispersed in suspension, if a higher value is obtained, aggregates or other larger molecular weight structures are considered to have been formed as a result of agglomeration or a related mechanism (Bodmeier R et al, 1998). Based on the foregoing, the starting 20mg/ml suspension produced an average run, particle mean diameter of 4334.1nm with an average polydispersity index of 1.110, while 2mg/ml, 200µg/ml, and 20µg/ml had an average run particle mean diameters of 362nm, 334.7nm and 357.9nm with associated polydispersion indices of 0.738, 0.543 and 0.417. These observations support the idea that at the highest concentration of 20m/ml alumina nanoparticles suspension, sufficient numbers of particles remain in the supernatant liquid to lead to the formation of stable comparatively large agglomerates, in contrast to the observations from the lower concentrations.

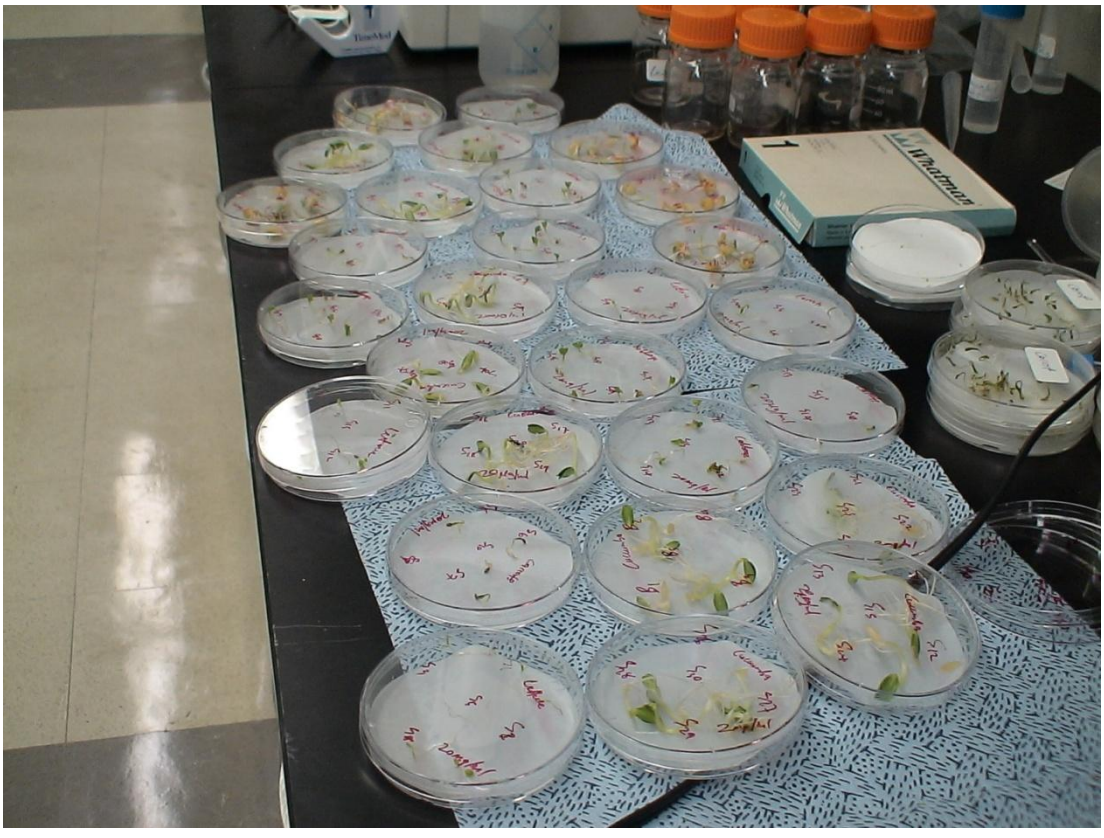

Figure 4.2 Plants seedlings exposed to alumina nanoparticles supernatants.

Z.mays R.E at higher concentrations did not deviate much from those at lower concentrations or from the control. The same can be said for its R^2 values, as can be seen in Figure 4.1, Table 4.1 and Table 4.2. This was probably a result of phytotoxic resistance and therefore less sensitivity by *Z.mays* as explained before.

Conclusion

From the results of the investigation of phytotoxicity using alumina nanoparticles supernatants, it is apparent that the supernatants contained materials that were toxic to the plant species used in this investigation, especially as seen with the supernatants prepared from higher concentrations of suspension. All the plant species were affected, at

concentrations other than the least concentration of 20μg/ml. The inhibitory growth effect of the supernatants on *Z.mays* was less pronounced probably as a result of phytotoxic resistance associated with the species perhaps due to the production of root exudates.

4.2 Investigation of the Effect of Alumina Nanoparticles Suspension on Inhibition of Plant Root Growth

The phytotoxicity of alumina nanoparticles suspension has been well investigated and reported by the previous investigators, so no attempt was made to duplicate or repeat the process other than to use the experimental approach as a basis for further mechanistic studies, but it became important to compare the phytotoxicity of alumina nanoparticles supernatants to that of its suspension at the same concentration, preferably at the highest concentration of 20mg/ml. This was important in order to determine whether or not some materials in the aqueous supernatant derived from the nanoparticles were actually responsible for the phytotoxic characteristics rather than the presence of the entire nanoparticle suspensions themselves.

To this end, the 20mg/ml alumina nanoparticles suspension was prepared as detailed in section 3.5 without the centrifugation and applied to seedlings as described in section 3.4.

Table 4.3 Root Elongation (RE) and Relative Root Growth (RRG) of Plant Seedlings Exposed to 20mg/ml of Alumina Suspension for 72 hrs in the Dark at 25 ± 1ºC

The results are reported as mean ± S.D. and 95% confidence interval. And range given as min~max. R.E values are presented in mm.

Conc.	*Z.mays*	*D.carota*	*L.sativa*	*B.oleracea*	*C.sativus*
Blank	33.5±1.6	17.0±2.3	66.8±6.6	71.8±2.0	50.2±2.7
R.E	30.7~35.8	12.7~20.3	57.6~76.1	68.7~75.1	46.7~55.7
20mg/ml	22.1±1.98	3.96±0.73	28.2±3.75	25.5±2.83	20.6±3.35
R.E	19.2~25.7	3.1~5.3	22.9~33.4	20.8~29.1	18.6~24.1
20mg/ml	0.659±0.06	0.233±0.04	0.423±0.06	0.355±0.04	0.411±0.1
R.R.G	0.57~0.77	0.182~0.31	0.343~0.5	0.29~0.41	0.28~0.51

Table 4.3 contains the results of root elongation measurements on five plant species obtained before and after exposure to 20 mg/ml alumina nanoparticles suspension and expressed as R.E and R.R.G. As mentioned earlier in this dissertation, the R.R.G is the ratio of the R.E of the treated samples to the mean R.E of the untreated ones (Blank), hence, what is displayed in Table 4.3 are the mean values of both the R.E and R.R.G plus or minus their standard deviation. Therefore, samples with R.R.G of unity or close to unity, suggests a close match between the treated samples and the Blank, in other words, the treated samples would have been less affected by the exposure to the suspension. Based on the foregoing, it can be seen in Table 4.3 that all the plant species were affected by the nanoparticle suspension, with the most affected being *D.carota* with an average

R.R.G of 0.233, and an R.E of 3.96, thereby denoting considerable sufficient detrimental effect to the toxic alumina nanoparticles.

Similarly, from Table 4.3, *Z.mays* was the least affected judging from its average R.R.G of 0.659 and an average R.E of 22.1. Since the R.R.G was more than 0.5, it could safely be said that toxic effect on *Z.mays* was less pronounced as compared to that experienced by other species in the group; this once again is consistent with the phytotoxic resistance mechanism of *Z.mays*.

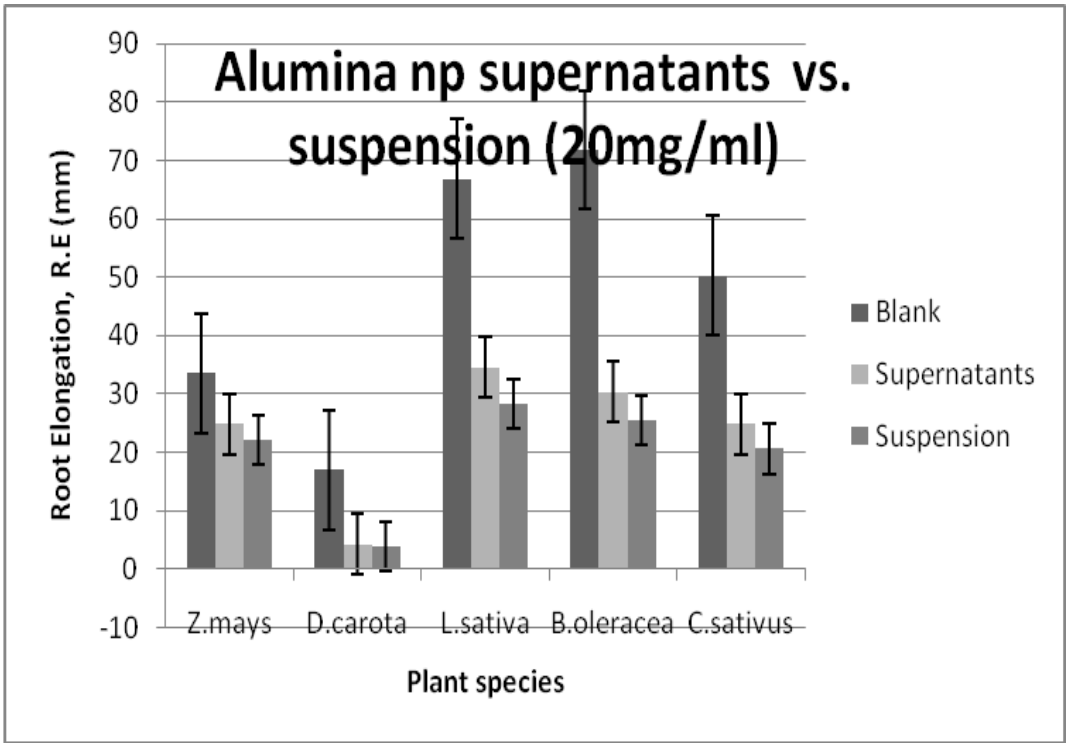

Figure 4.3 Effect of the exposure of plant species to 20mg/ml alumina nanoparticles supernatants and suspension, (effect compared to that from the Blank).

Figure 4.3 compares the effects of both alumina nanoparticle supernatants and suspensions of the same starting concentration of 20mg/ml to the root elongation shown, and the Blanks. Based on the results shown in Figure 4.3, (please refer to Tables 4.1 and

4.3 for the data) alumina nanoparticles suspension had more effect on the root growth of plant species used in this investigation than did the supernatant liquid from centrifugation of analogous suspensions, except in the case of D.carota, where no significant difference could be seen between the two treated groups. All the plant species showed differences between the R.E of the treated sample and those exposed only to the Milli-Q water-Blank. This implies that at same concentration, the suspension contained more substances that impeded root growth than did the supernatants; this supports the hypothesis that phytotoxicity could be attributed to factors other than surface characteristics alone.

Table 4.4. Statistical Analysis of Results of the Root Elongation (RE) of Plant Seedlings Exposed to Different Concentrations of Alumina Nanoparticle Supernatants and 20mg/ml Alumina Nanoparticles Suspension for 72 hrs in the Dark at 25 ± 1ºC (Student t test of **Supernatants** vs. **20mg/ml** of Alumina Nanoparticles **Suspension**)

Results from the *Student's t*-test are reported as the value of *t* and the value of probability of the result assuming the null hypothesis (*p*). Statistical significance is reported when p is less than 0.05.

Conc.	*Z.mays*	*D.carota*	*L.sativa*	*B.oleracea*	*C.sativus*
20µg/ml	*t=6.99* p< 0.001	t= 11.18 p<0.0001	t= 9.68 P= 0.000	t= 20.3 p<0.0001	t= 16.8 P= 0.000
200µg/ml	*t=7.27* p<0.0001	t= 8.25 P=0.000	t= 8.74 p<0.0001	t= 19.0 p <0.0001	t= 9.29 p<0.0001
2mg/ml	*t= 6.03* p<0.0001	t= 3.26 p= 0.004	t= 5.56 P= 0.000	t= 8.14 p<0.0001	t= 6.45 P= 0.000
20mg/ml	*t=4.02* p= 0.001	t= 3.94 p= 0.001	t= 3.59 p= 0.002	t= 3.65 p=0.0018	t= 3.35 p= 0.004

Table 4.4 contains the result of statistical analysis done on the R.Es of both the suspension of 20mg/ml concentration and supernatants of varying concentrations, using

the student's t method. The idea was to see if there was any difference between plant seedlings exposed to alumina nanoparticles suspension of the highest concentration of 20mg/ml and those exposed to supernatants prepared from varying concentrations of nanoparticle suspension. The highest concentration of 20mg/ml for the suspension was chosen because, it was the concentration that in previous studies had shown the strongest inhibitory growth effect, and hence would be most likely to show a difference when compared to the supernatants.

In this analysis, the student's t test that results in values higher than the critical t value of 1.734, in addition to the p value being less than the level of significance of 0.05, were deemed to be statistically significant and hence the rejection of the null hypothesis. On the other hand, t values that were less than the critical t value and p values higher than the level of significance, were not statistically significant and hence led to the acceptance of the null hypothesis, that there was no difference between the two groups of samples; those treated with alumina supernatants and those treated with 20 mg/ml alumina suspension.

Table 4.5 Statistical Analysis of Results of the Root Elongation (RE) of Plant Seedlings Exposed to 20mg/ml of Alumina Suspension for 72 hrs in the Dark at 25 ± 1ºC, Effect Compared to the Blank.

Results from the *one-way ANOVA* procedure are reported as the value of *f*, *p*, and the coefficient of determination (R^2). Statistical difference is reported as *p* smaller than 0.05.

Conc.	*Z.mays*	*D.carota*	*L.sativa*	*B.oleracea*	*C.sativus*
20mg/ml	*p= 0.001* R^2= 0.76 *f=4.836*	p= 0.03 R^2= 0.62 *f= 2.7*	p= 0.01 R^2= 0.81 *f= 3.377*	p= 0.000 *R^2=0.519* *f=6.385*	p= 0.035 *R^2= 0.619* *f= 2.605*

Based on the above discussion and from Table 4.4, all the plant species and concentrations showed remarkable statistical differences between those treated with 20mg/ml alumina suspension and those treated with varying concentrations of alumina nanoparticles supernatants, except for *D.carota* at the supernatant concentration of 20mg/ml. Thereby suggesting for *D.carota* that at the concentration of 20mg/ml, there was no difference between the effect observed when either alumina nanoparticles suspension or alumina nanoparticle supernatants was used, for this plant species. In short, they both have the same effect at 20 mg/ml. This is further displayed in Figure 4.3, with both groups having comparable R.E values that were different from that of the Blank.

Table 4.5 displays the result of the phytotoxicity study done on the five plant species used in this investigation, by exposing them to the 20mg/ml alumina nanoparticles suspension. The results are expressed as p, f and R^2, and the basis of discussion followed the pattern established above. From these results, all the species were inhibited by their exposure to the suspension as portrayed by the p values being less than 0.05, furthermore, the coefficient of determination, R^2, being greater than half, but less

than unity indicates a strong effect. These suggest that the plant species experienced inhibitory root growth, because there was a statistical difference between the treated samples and the Blank, resulting from the poor correlation of the R.Es of both the treated samples and Blank.

Conclusion

Results from this investigation re-affirm the conclusion reached by past investigators on the toxicity of alumina nanoparticles suspension on plant species; that alumina nanoparticles suspension is phytotoxic to plant species. A comparison between alumina nanoparticles suspension and alumina nanoparticles supernatants led to the conclusion that both produce statistically different results at same starting concentrations, although both still inhibit root growth. The exception to this observation is the case of *D.carota* where both the 20mg/ml suspension and the supernatant from the same concentration suspension appear to have similar phytotoxicity, as depicted in Figure 4.3.

CHAPTER 5

SPECTROPHOTOMETRIC DETERMINATION OF ALUMINUM BY MORIN

A direct spectrophotometric method for the determination of aluminum has been developed (Ahmed M J, Hossan J, 1995); this technique will help distinguish aluminum from alumina in aqueous media. Morin reacts in slightly acidic 50% ethanolic media (0.0001-0.0015M H_2SO_4) with aluminum to give a deep-yellow chelate which has an absorption maximum at 421 nm. The average molar absorptivity and Sandell's sensitivity were found to be 5.3 x 10^3 l $mol^{-1}cm^{-1}$ and 5 ng of Al cm^{-2}, respectively. The reaction was instantaneous and absorbance remained stable for 48 hours. According to these researchers, the color system obeyed Beer's law from 10 ng ml^{-1} to 5.0 µg ml^{-1} of Al; the stoichiometric composition of the chelate was 2:3 (Al: Morin).

Morin is a phenolic compound derived from hydroxyl substitutions on the flavone chromophore. It complexes with metal cations to form stable products which in several cases are highly fluorescent, a property which has been exploited in analytical methods of metal and ligand identification(Markham K R, Guilbault G G, 1973; Wolfbeis O S et al, 1983; Ahmed M J, Hossan J, 1995; Robards K, Antolovich M, 1997; Hollman P C H et al, 1996; Porter L J, Markham J, 1970; Pusz J, Kopacz M, 1992; Pusz J, Nitka B, 1997; Deng H, Van Bekel G J, 1998). The enhancement of the fluorescence signal upon chelation of flavones with a nonparamagnetic metal is related to the inhibition of the excited state intramolecular proton transfer (ESPT) processes (Sengupta P K, Kasha M, 1979; McMorrow D Kasha M, 1984; Strandjord A J G, Barbara P F, 1985; Wolfbeis

O S, Knierzinger A and Schipfer R, 1983; Sarkar M, Guharay J and Sengupta P K, 1996; Guharay J et al, 1997; Guharay J ,Sengupta P K, 1997; Smith G J, Markham K R, 1998) between hydroxyl and 4-keto groups of the cromone ring. The ESPT mechanism, which occurs in several hydroxyl substituted flavones, gives rise to a fast excited state equilibrium between the normal and tautomeric forms, and therefore to dual fluorescence usually with low emission quantum yields at room temperature.

5.1 Spectrophotometric Determination of Aluminum in Aluminum Standard Solution and its Dilutions

The objective of this study was to investigate the hypothesis that soluble non-oxide aluminum was present in the alumina nanoparticles matrix, which contributed to the observed phytotoxic effect on root growth. The procedure and reagents utilized in this work was described in section 3.8. The first step was to confirm this process by producing Aluminum: Morin chelate using the aluminum standard solution, and with the aid of the uv/vis recording spectrophotometry, the spectrum in Figure 5.1 was obtained. As can be seen, the chelate peaked at 421 nm as expected with absorbance of 4 AU, an indication of the presence of aluminum. Subsequently, dilutions of the aluminum standard solution were made using Milli Q water, their chelates were made and subjected to the same analysis as the standard solution and results displayed in Figures 5.2, 5.3 and 5.4. As the dilution was increased with 10 ml to 1000 ml of Milli Q water, the recorded absorbance decreased from 4 AU to 0 AU.

To this end, a hypothesis was advanced that suggested the presence of un-oxidized aluminum within or on the surfaces of alumina nanoparticles, as a result of incomplete oxidation during production and that such aluminum was responsible for the observed phytotoxic effects. In order to explore this hypothesis, investigations using uv/vis spectrophotometer with the aid of Morin, which is a fluorescence agent for aluminum, was carried out with alumina nanoparticles supernatants, followed by a comparison of the two sets of spectra from the dilutions of the 1.0mg/ml Aluminum standard solution and that from alumina nanoparticles supernatants. This was subsequently followed by the loading of plant seedlings with 1.0mg/ml aluminum standard solution and its dilutions, and again, a comparison made between the Relative Elongation measurements obtained and that obtained with alumina nanoparticles supernatants.

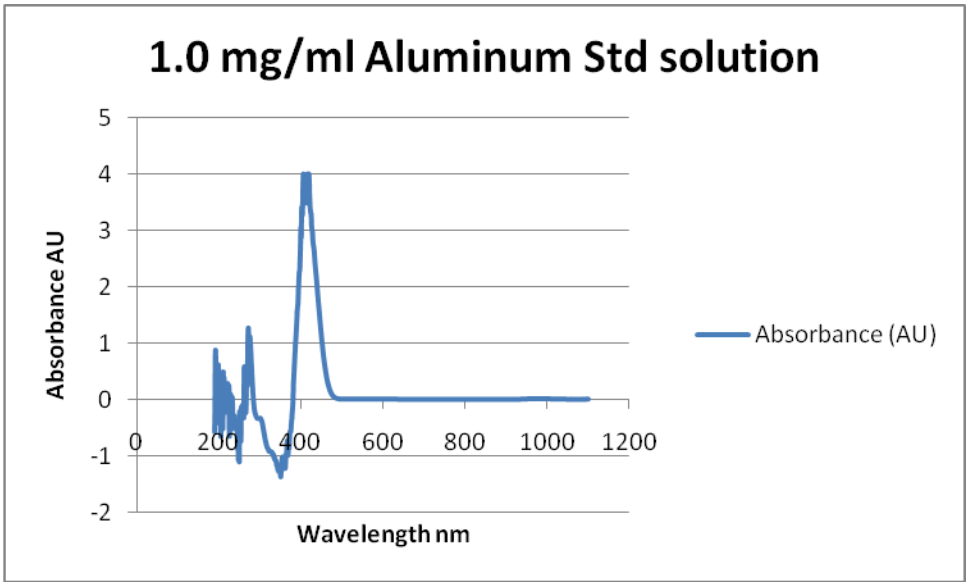

Figure 5.1 Spectrum of 1.0mg/ml aluminum standard solution, peaked at a wavelength of 420 nm and absorbance of 4 AU.

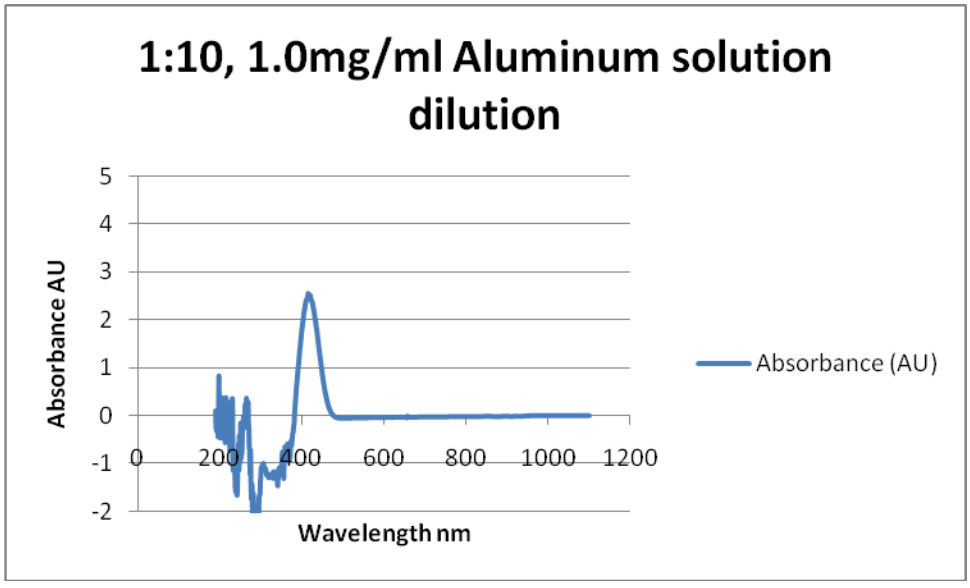

Figure 5.2 Spectrum of 1.0mg/ml aluminum standard dilution of 1:10 (0.10 mg/ml aluminum solution), peaked at a wavelength of 420 nm and an absorbance of 2.5 AU.

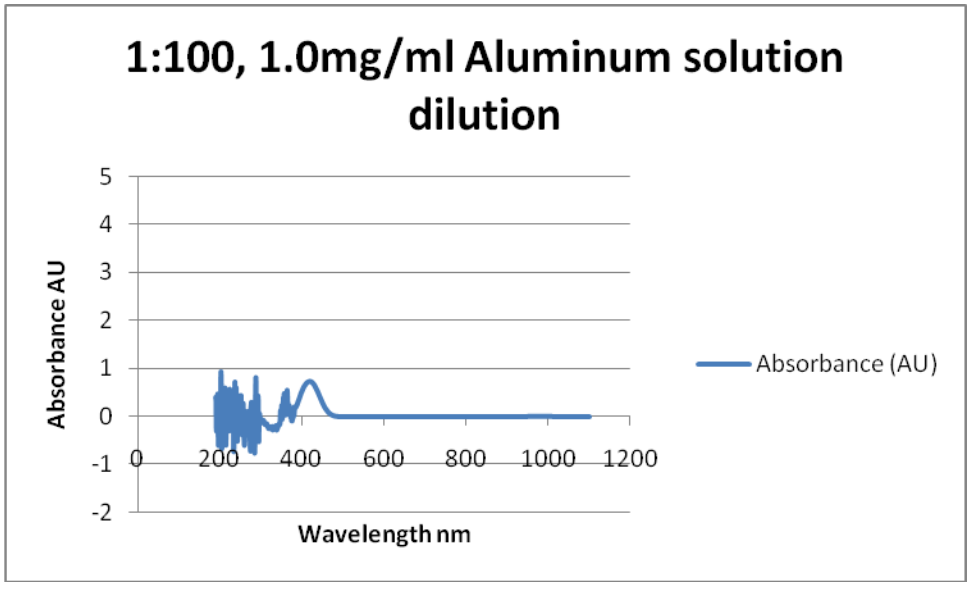

Figure 5.3 Spectrum of 1.0mg/ml aluminum standard dilution of 1:100, (0.010 mg/ml aluminum solution) peaked at 419 nm and at an absorbance of 0.75 AU.

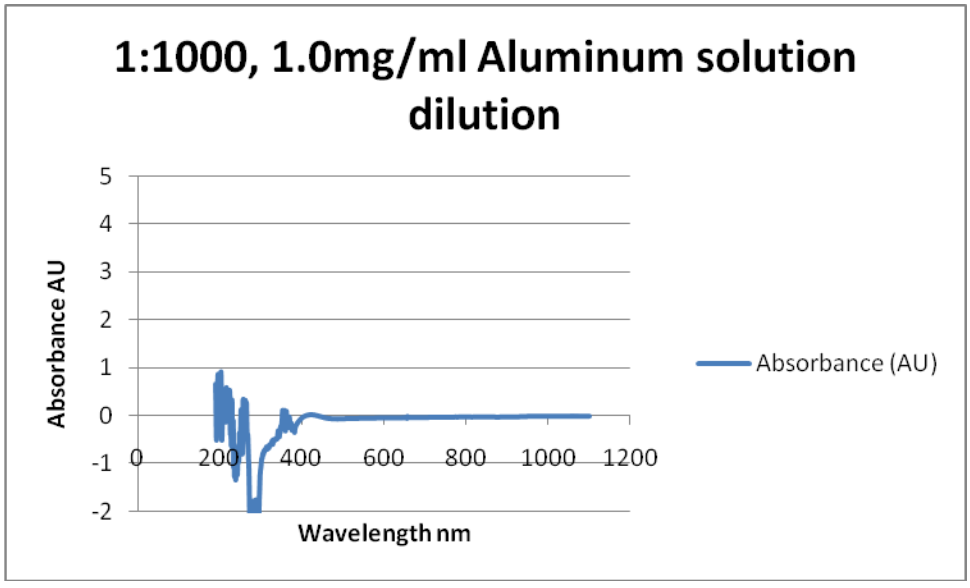

Figure 5.4 Spectrum of 1.0mg/ml Aluminum standard dilution of 1:1000, (0.0010 mg/ml aluminum solution) reaching zero absorbance at a wave length of 425 nm.

Conclusion

The experiment went as predicted, since the known Aluminum standard solution produced a sufficient peak of 4 AU to suggest a strong presence of Aluminum, as stated in the literature. Furthermore, as this standard solution was diluted, the concentrations of Aluminum were reduced, leading to a decrease in recorded absorbance. This section of the experiment was designed in order to validate the use of spectrophotometric procedure using Morin in determining the presence of un-oxidized Aluminum in Alumina nanoparticles.

5.2 Spectrophotometric Determination of Aluminum in Alumina Nanoparticles Supernatants

All the four concentrations of alumina nanoparticles supernatants used in this research; 20mg/ml, 2mg/ml, 200µg/ml and 20µg/ml, were subjected to the same procedure as with the 1.0mg/ml aluminum standard solution (except diluting with Milli Q water) and as described in Section 3.8. The spectral results for 20mg/ml, 2mg/ml and 20µg/ml are displayed in Figures 5.5 to 5.7. The absorbance obtained from the 20mg/ml concentration was 0.2 AU indicating a small presence of aluminum in the suspension when compared to the 1.0mg/ml aluminum standard solution, the other three concentrations had zero AU, suggesting insignificant or no amount of aluminum in the alumina nanoparticles supernatants for these concentrations. Hence, result of 1: 1000 dilution of the standard solution is comparable to those of 2mg/ml, 20µg/ml and 200µg/ml concentrations or they were below the level of detection.

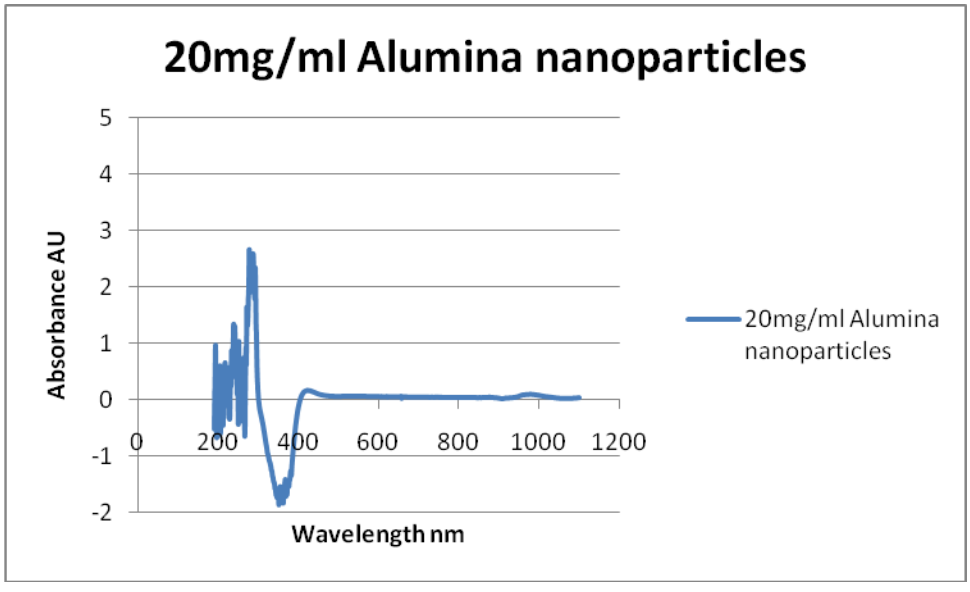

Figure 5.5 Spectrum of 20mg/ml of alumina nanoparticles supernatants treated with morin peaked at 422 nm and an absorbance of 0.2 AU.

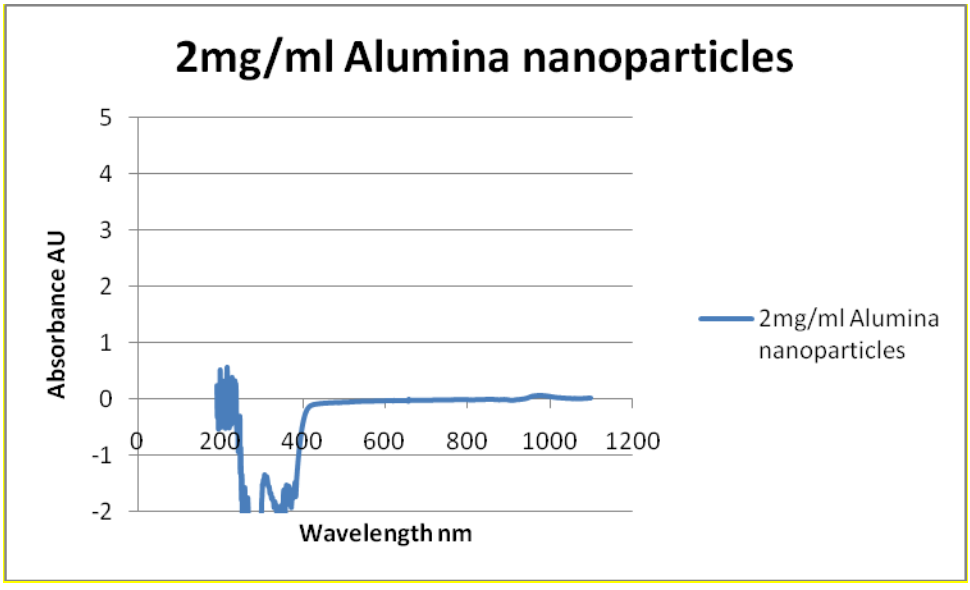

Figure 5.6 Spectrum of 2mg/ml alumina nanoparticles supernatants treated with morin reached zero absorbance at a wavelength of 430 nm.

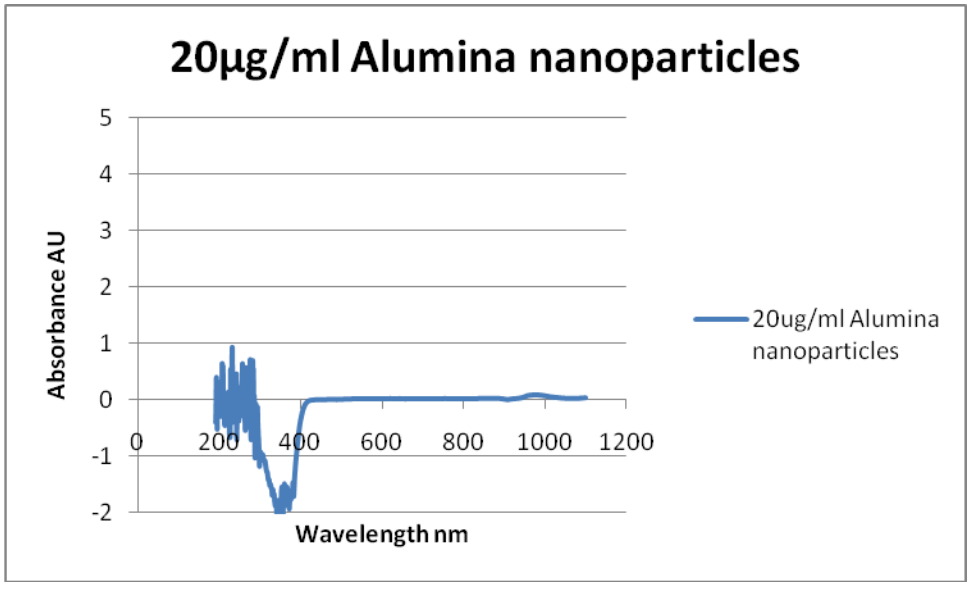

Figure 5.7 Spectrum of 20µg/ml of alumina nanoparticles supernatants treated with morin reached zero absorbance at a wavelength of 434 nm.

Conclusion

The results of the spectrophotometric analysis of alumina nanoparticles supernatants indicates that the presence of morin-complexable Aluminum in the alumina nanoparticles supernatants becomes detectable at a concentration of 20mg/ml of alumina in the original suspension that was centrifuged to provide the supernatant. Suspensions with lower concentrations investigated, did not yield detectable levels of complexable aluminum. It could then be concluded that the alumina nanoparticles used contain traces of complexable Aluminum that remained in the supernatant liquid after centrifugation. Furthermore, from Figures 5.1 and 5.5, and using the Beer-Lambert equation (www.chemguide.co.uk) the calculated concentration of Aluminum in the 20mg/ml Alumina suspension is 0.05mg/ml. Based on these results, the possibility of aluminum being partly responsible for the observed phytotoxic effect became apparent.

5.3 Effects of Plants Root Exposure to 1.0mg/ml Aluminum Standard Solution

In addition to the spectrophotometric analysis, the five plant species used in this study; *Z.mays, D.carota, L.sativa, C.sativus* and *B.oleracea* were treated with 1.0mg/ml aluminum standard solution and several dilutions, in order to ascertain the effect aluminum might have on them. Results were also compared with those obtained earlier using the 20mg/ml concentration of alumina nanoparticles supernatants and 20mg/ml concentration of alumina nanoparticles suspension and as usual with their Blanks.

The Root elongation and Relative root growth results are displayed in Table 5.1,

From this Table, it is apparent that all the species were affected by the exposure to aluminum, except in the case of *Z.mays* that showed less growth inhibition. The mechanism for this resistance to aluminum is well accepted in the literature to be due to Aluminum–activated exudation of the organic acids, malate, citrate, or oxalate, depending on the plant species(Ma J F et al, 2001; Ma J F, 2000; Ryan et al, 2001; Kochian et al, 2004).

It is also important to note that the presence of aluminum in the 20mg/ml concentration of alumina nanoparticles suspension and 20mg/ml concentration of alumina nanoparticles supernatants is likely responsible for the phytotoxic resistance by *Z.mays*. With Aluminum standard solution and supernatants from Alumina nanoparticles showing more resistance, because they both contain higher amounts of elemental Aluminum as seen in Figure 5.8. This suggests that, an increased presence of Aluminum in the test samples amounted to an increased amount of root exudates produced by *Z.mays* and hence increased resistance to toxicity. Furthermore, this also suggests that for alumina nanoparticles, soluble aluminum species existed on the surfaces of particles and therefore were able to be sufficiently retained in the supernatants during centrifugation to impact the root cells.

All other species were affected by the application of 1.0mg/ml Aluminum standard solution, Alumina nanoparticles supernatants and suspension. For *L.sativa* and *C.sativus,* the toxic effect from the 1.0mg/ml Aluminum standard solution and 20mg/ml Alumina nanoparticles suspension was more than that obtained from the supernatants. *D.carota* seemed to be more affected by the 1.0mg/ml Aluminum standard solution than by either Alumina nanoparticles supernatants or the 20mg/ml Alumina suspension.

B.oleracea, from Figure 5.8, was more affected by the exposure to Aluminum standard solution than by the 20mg/ml Alumina nanoparticles suspension, while the 20 mg/ml Alumina nanoparticles supernatants has the least effect on the plant species.

From Table 5.1, it could be observed that *Z.mays* exhibited limited phytotoxic effect when treated with undiluted 1.0mg/ml Aluminum standard solution, as well as other dilutions of it, when compared to the Blank. The R.E of *Z.mays* when treated with Milli Q water (Blank) was 29.1 mm, while with undiluted Aluminum(1.0 mg/ml) it was 27.5 mm, thereby denoting phytotoxic resistance by *Z.mays* as explained earlier in this dissertation. With dilutions using Milli Q water, reported R.Es were; 26.2, 27.4 and 27.8 (mm), for dilutions of; 1:10, 1:100 and 1:1000 respectively. Other plant species, that did not display this resistance, were evenly affected by the toxicity of Aluminum; *D.carota*, when treated with the Blank had an R.E of 14.1 mm, with undiluted 1.0mg/ml Aluminum standard solution, it was 3.87 mm and when exposed to the highest dilution of 1:1000, its R.E rose to 13.3 mm.

With *L.sativa*, exposure to the Blank gave an R.E of 65.4 mm, with the undiluted 1.0mg/ml Aluminum standard solution, it was 27.4 mm, and 51.9 mm when the highest dilution of 1:1000 (0.0010mg/ml) was used.

For the R.R.G, *Z.mays* had a ratio of 0.945 when the undiluted 1.0mg/ml Aluminum standard solution was used; it then dropped to 0.90 with a dilution of 1:10, and a final decrease to 0.712 with the highest dilution of 1:1000. In contrast to *Z.mays*, the rest of the plant species had their R.R.Gs increasing as their dilution increases, denoting that the R.Es of the samples were increasing as the dilution was increased with respect to the Blank.

For *B.oleracea*, the R.R.G increased from 0.331 with undiluted 1.0mg/ml Aluminum standard solution to 0.397 and 0.777 when dilution was increased to 1:10 and 1:1000 respectively.

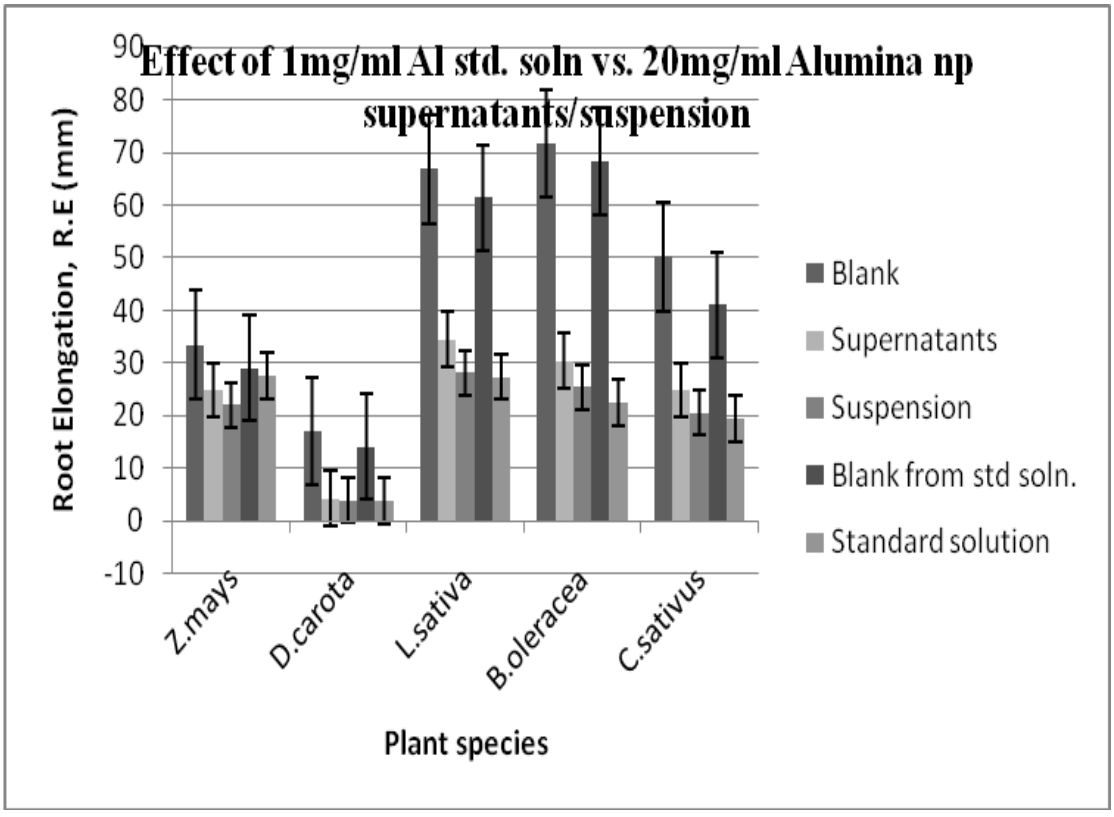

Figure 5.8 Comparison of the effect of exposure of plant species to 1.0mg/ml Aluminum standard solution, 20mg/ml Alumina nanoparticles suspension and 20mg/ml Alumina nanoparticles supernatants.

The data for the above figure can be found in tables 4.1, 4.3 and 5.1.

Table 5.1 Root Elongation (RE) and Relative Root Growth (RRG) of Plant Seedlings Exposed to Different Aluminum Dilutions for 72 hrs in the Dark at 25 ± 1ºC

The results are reported as mean ± S.D. and 95% confidence interval. And range given as min~max. R.E values are presented in mm.

	Dilution	*Z.mays*	*C.sativus*	*B.oleracea*	*D.carota*	*L.sativa*
RE	Blank	29.1±2.62 25.3~32.6	41.0±3.48 35.7~47.5	68.3±7.31 58.2~82.7	14.1±2.01 10.0~16.3	61.5±11.9 49.7~88.1
	100%Al	27.5±2.71 24.1~32.7	19.4±1.8 17.3~21.6	22.6±3.29 16.4~26.7	3.87±0.73 3.1~5.1	27.4±3.71 21.7~32.8
	1|10	26.2±0.67 24.9~27.0	24.0±1.22 22.7~26.1	27.1±3.32 21.8~31.6	3.66±0.59 2.9~4.9	40.0±3.07 35.2~43.8
	1|100	27.4±2.86 23.7~31.6	28.6±2.58 25.6~32.5	33.8±2.75 29.9~37.1	4.36±0.62 3.4~5.3	41.4±3.7 34.6~46.3
	1|1000	28.1±0.87 26.4~29.0	36.2±1.81 33.8~39.1	53.1±4.28 48.5~61.8	13.3±1.57 10.8~15.6	50.6±4.73 44.9~62.1
RRG						
	100%Al	0.945±0.09 0.828~1.12	0.473±0.04 0.422~0.52	0.331±0.04 0.24~0.391	0.274±0.05 0.22~0.362	0.42±0.05 0.33~0.50
	1|10	0.90±0.023 0.856~0.92	0.587±0.02 0.554~0.63	0.397±0.04 0.319~0.46	0.2590±.04 0.206~0.34	0.61±0.04 0.53~0.67
	1|100	0.927±0.03 0.846~0.96	0.699±0.06 0.624~0.79	0.495±0.04 0.438~0.54	0.381±0.06 0.255~0.48	0.62±0.06 0.52~0.70
	1|1000	0.966±0.02 0.675~0.74	0.883±0.04 0.824~0.95	0.777±0.06 0.71~0.905	0.946±0.11 0.766~1.11	0.79±0.07 0.68~0.95

Table 5.2 Statistical Analysis for Results of the Root Elongation (RE) of Plant Seedlings Exposed to Dilutions of Aluminum Standard Solution for 72 hrs in the Dark at 25 ± 1ºC

Results from the *one-way ANOVA* procedure are reported as the value of *f*, *p*, and the coefficient of determination (R^2). Statistical difference is reported as *p* smaller than 0.05.

Dilution	*Z.mays*	*C.sativus*	*B.oleracea*	*D.carota*	*L.sativa*
100%	*p*=0.001 *f*=4.836 R^2=0.3066	*P*=0.001 *f*=4.836 R^2=0.1029	*p*=0.002 *f*=4.389 R^2=0.1066	*p*=0.001 *f*=4.836 R^2=0.1031	*P*=0.01 *f*=3.377 R^2=0.1728
1|10	*P*=0.012 *f*=3.264 R^2=0.7693	*P*=0.001 *f*=4.836 R^2=0.1244	*p*=0.000 *f*=6.385 R^2=0.1127	*p*=0.001 *f*=4.836 R^2=0.100	*p*=0.000 *f*=6.385 R^2=0.301
1|100	*p*=0.05 *f*=3.36 R^2=0.8209	*p*=0.001 *f*=4.836 R^2=0.2828	*p*=0.003 *f*=4.131 R^2=0.1672	*p*=0.000 *f*=6.385 R^2=0.1031	*p*=0.006 *f*=3.695 R^2=0.3599
1|1000	*p*=0.04 *f*=3.63 R^2=0.8538	*p*=0.000 *f*=6.385 R^2=0.6399	*p*=0.000 *f*=6.385 R^2=0.4649	*p*=0.005 *f*=3.809 R^2=0.559	*p*=0.000 *f*=6.279 R^2=0.4186

For *Z.mays* (from Table 5.1), the relative standard deviation or the percentage errors are 9%, 9.9%, 2.56%, 10.44% and 3.13% from Blank, 1.0mg/ml, 1:10, 1:100 and 1:1000 respectively. Based on these results and previous discussion, the lowest percentage error of 2.56% from 1:10 dilution suggests closeness to the mean of the Relative Elongation measurements and least variation of data as opposed to other dilutions and /or concentration. The same can be said of measurements obtained while using *D.*carota; the Blank, 1.0mg/ml and 1:1000 dilution resulted in percentage errors of 14.26%, 18.86% and 11.8% respectively, thereby denoting increased variations.

Results of the statistical analysis of R.E measurements of root growth of plant species are contained in Table 5.2, and shows that all the plant species were affected by the 1.0mg/ml Aluminum standard solution and its dilutions.

Table 5.3: Statistical Analysis for Results of the Root Elongation (RE) of Plant Seedlings Exposed to Dilutions of Aluminum Standard Solution for 72 hrs in the Dark at 25 ± 1ºC (RE results are compared with that obtained using 20mg/ml alumina nanoparticles suspension)

Results from the *Student's t*-test are reported as the value of *t* and the value of probability of the result assuming the null hypothesis (*p*). Statistical significance is reported when p is less than 0.05.

Conc.	*Z.mays*	*D.carota*	*L.sativa*	*B.oleracea*	*C.sativus*
100% Al vs. 20mg/ml	*t=5.13* P<0.0001	t= 0.277 p=0.70	t= 0.474 p=0.64	t= 2.1 p=*0.05*	t= 1.02 p= 0.32
1|10 vs. 20mg/ml	t= 6.24 p<0.0001	t= 1.32 p= 0.2	t= 7.71 P= 0.00	t= 1.17 p= 0.26	t= 3.04 p= 0.007
1|100 vs. 20mg/ml	t= 6.88 p<0.0001	t=3.79 P<0.0001	t= 7.88 P<0.0001	t= 6.66 P<0.0001	t= 6.01 P<0.0001
1|1000 vs. 20mg/ml	t= 8.41 p<0.0001	t= 17.2 p<0.0001	t= 12.4 p<0.0001	t= 17.0 p<0.0001	t= 13.0 p<0.0001

This was accompanied by an increase in R^2 values from 0.8209 at the dilution of 1: 100 to 0.8538 at 1: 1000, compared to the value of 0.3066 while using the undiluted 1.0mg/ml Aluminum standard solution. The progressive increase in R^2 for all plant species used in this study when the dilution was increased from the undiluted up to the highest dilution of 1:1000 is an indication of decreasing toxicity with increasing dilution.

It then became important in this study to compare the phytotoxicity of 20 mg/ml of Alumina nanoparticles suspension to that of 1.0mg/ml Aluminum standard solution and its dilutions. To this end, the student's t statistical tool was used to make this comparison and the results are displayed in Table 5.3. The highest concentration of 20 mg/ml was utilized because from section 5.2 and Figure 5.5, it appeared to be the only concentration among the four concentrations used in this study with a measureable trace of non-oxide Aluminum, and from Chapter 4, phytotoxicity is more apparent at this high concentration.

Hence from Table 5.3, t values higher than the critical t value are considered to show significant statistical difference with attending p values lower than the limit of significance; 0.05. With these considerations, *Z.mays* appears to show sufficient statistical difference with all dilutions, including the undiluted 1.0mg/ml Aluminum solution. This is due to the higher resistance posed by *Z.mays* when treated with Aluminum and its dilutions as opposed to that from the suspension. For the four other species; *D.carota, L.sativa, B.oleracea* and *C.sativus,* there was no statistical difference between the two groups of samples. When comparing the 20mg/ml alumina nanoparticles suspension to the undiluted 1.0mg/ml Aluminum standard solution, the p values were; 0.70, 0.64, 0.05 and 0.32 for *D.carota, L.sativa, B.oleracea* and *C.sativus* respectively.
As the dilution was increased, statistical differences between the two groups became obvious as the p values decreased to values less than 0.05, suggesting that the 20mg/ml alumina nanoparticles suspension is more phytotoxic than 1.0mg/ml Aluminum standard solution, especially at higher dilutions.

Conclusion

From the proceeding it could be stated that, traces of soluble Aluminum are present on Alumina nanoparticles or at least associated with them, which becomes noticeable at high concentrations of nanoparticles suspension as was seen in Figure 5.2 and hence could be responsible at least in part, for the reduction in root growth experienced at the concentration of 20 mg/ml Alumina suspension. Application of 1.0mg/ml Aluminum standard solution and its dilutions to the plant species used in this investigation resulted in noticeable phytotoxic effect.

Comparing the phytotoxicity of 1.0mg/ml Aluminum standard solution and its dilutions to that of 20mg/ml Alumina nanoparticles suspension, resulted in no statistical difference from the undiluted 1.0mg/ml Aluminum standard solution, except for *Z.mays*, but demonstrated remarkable statistical difference when higher dilutions were used. Significant statistical difference occurred when the phytotoxic effect of both 20mg/ml Alumina nanoparticles suspension and 1.0mg/ml Aluminum standard solution on *Z.mays* were compared, irrespective of the dilution of the 1.0mg/ml Aluminum standard solution. Though the major source of phytotoxicity at the highest concentration of 20mg/ml was from the aluminum contained in the Alumina nanoparticles of that concentration (0.05mg/ml), but the contribution from particles size cannot be overlooked, thereby necessitating further investigation.

CHAPTER 6

PARTICLE SIZE EFFECT ON PLANT ROOT GROWTH

Alumina and hydrophilic Silica nanoparticles occur as aggregates in solution and when not in solution, exist in size ranges; for the samples used in this study, the aggregate sizes plus/minus standard deviation are 201.0 ± 74.7 nm for Alumina and 215.7 ± 56.3 nm for Silica (Ling Y, Watts D, 2004). Manufacturer's average particle size specifications are 13nm for Alumina and 14nm for Silica. Therefore there was a need to consider possible relationships between specific individual particles' sizes and observed phytotoxicity.

Table 6.1 Physical Properties of 0.025µm and 0.05µm Millipore Membranes

Description	Refractive index	Water flow rate, ml/min x cm^2	Wettability	Thickness, µm	Gravimetric Extractables, %	Air flow Rate, l/min x cm^2	Porosity %
25 mm diameter, mixed cellulose esters, Hydrophili-c white plain membrane	1.5	0.15 (0.025µm) & 0.74 (0.05µm)	Hydrophil-ic	105	1.5	0.15 (0.025µm) & 0.25 (0.05µm)	72

Source: www. Millipore .com

The Silica nanoparticles used in this study were Cab-O-Sil® M5; they were purchased from Cabot, Inc., and were used for comparison purposes.

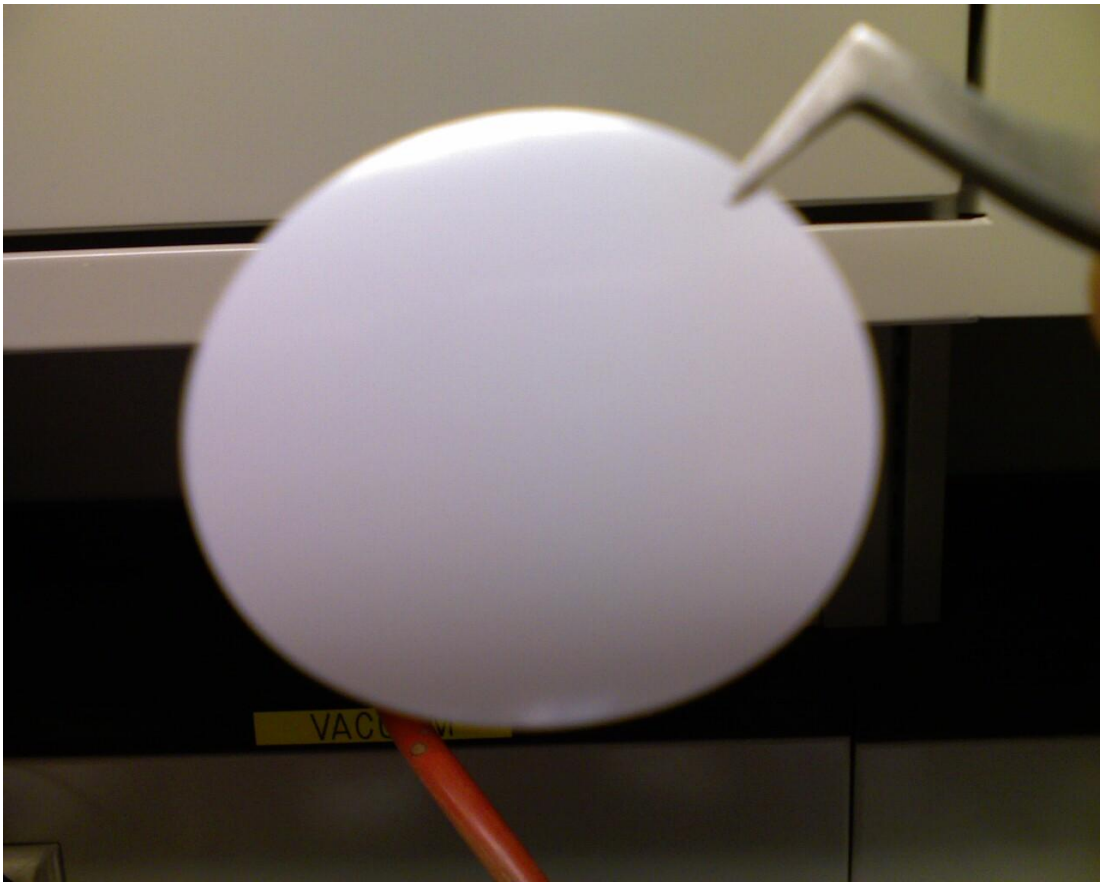

Figure 6.1 25mm diameter, 0.025µm pore sized, white hydrophilic mixed cellulose membrane filter.

In order to achieve this objective, the Ultra Filtration of 13 nm alumina and 14 nm hydrophilic silica nanoparticles suspensions were carried out using 25 mm diameter white hydrophilic mixed cellulose MF-Millipore™ membrane filters. These membranes were purchased from Millipore™ with pore sizes; 0.025 µm and 0.05 µm, these pore sizes were the smallest obtainable in the market. The Ultra Filtration technique was chosen for this study because of the fine pore sizes involved, which falls within the operating size range (approximately 0.002 to 0.1microns) of the technique.

The filtration arrangement consisted of a lower chamber made up of a 1000 ml conical flask and an upper chamber of 200 ml conical glass ware with both ends open and the membrane in-between. The lower chamber was connected to the laboratory vacuum supply with a trans-membrane suction pressure of 75 kPa, with the retentate and/or nanoparticles suspension in the upper chamber. When the vacuum pressure was turned on, the permeate trickled through the enclosed membranes in a drop wise fashion, with flux as depicted in Table 6.2, and finally came to a stop after a period of time depending on the concentration and sample type. It was collected in the 1000 ml conical flask of the lower chamber. The decrease in flux was as a result of membrane fouling which is associated with the Ultra Filtration technique, but there was no need to de-foul membranes in order to increase flux since enough permeate was collected for the study in each case. Fresh membranes were used for each filtration procedure involving different concentrations and nanoparticles in order to avoid contamination; this was in addition to thoroughly rinsing the filtration chambers with Milli Q water.

For either alumina or hydrophilic silica nanoparticles, the preparation and application of samples were as reported in sections 3.9.1 and 3.9.3, while the germination of seedlings and particle count analysis can be found in section 3.9.2 and 3.9.4 respectively.

Before the application of the permeate to the seedlings, the permeate was sonicated for 60 minutes in order to minimize any possible effect of agglomeration. Prior to this, and immediately after filtration, about 10 ml was measured out from each concentration and type of nanoparticles permeate for particle size counting using the N4 Plus Beckman-Coulter particle counting machine, and using the procedure as described in

section 3.7 and 3.9.4. The results of the particle size counting are shown in appendix B. Comparing the average particle mean diameter from the same concentration of 20mg/ml but different pore sizes of 0.05 and 0.025µm, an average particle mean diameter of 230.8nm was obtained using the least pore size of 0.025µm with a polydispersity index of 0.452, while the run average particle mean diameter of 498.6nm, with a polydispersity index of 0.696 was obtained when the larger pore size of 0.05 was used. Larger particle mean diameter was obtained due to the presence of more particles in the permeate with the use of the larger pore size, more particles means a greater possibility for agglomeration to occur. This is in addition to the higher polydispersity index of 0.696, which is much higher than 0.1, thereby denoting poor monodispersity.

Figure 6.2 Ultra filtration apparatus used in the filtration of Alumina nanoparticles.

A timing device was used to establish the start and finish time of each filtration process and the rate of filtration (flux) was calculated using an equation according to EPA/NSF/ETV protocol and expressed in l/hr-m^2, (www.epa.gov/nrmr/std/etv);

$$J_P = Q_P \div S \qquad 6.1$$

Where J_P is the flux in l/hr-m^2, Q_P is the permeate flow in l/hr, and S is the membrane surface area, m^2.

Table 6.2 Fluxes and pH Readings of both Alumina and Silica Nanoparticles Permeate of Different Concentrations from 0.025µm and 0.05µm Pore Size Membrane Respectively

Np	Conc.	0.025µm flux l/hr-m	0.05µm flux l/hr-m	pH
Alumina	20mg/ml	10.4	11.56	4.19
	2mg/ml	32.37	33.53	4.27
	200µg/ml	57.8	86.25	4.73
	20µg/ml	65.68	412.7	5.13
Silica	20mg/ml	20.23	27.75	6.11
	2mg/ml	34.39	86.7	7.43
	200µg/ml	87.57	190.75	7.87
	20µg/ml	93.23	231.21	8.1

Furthermore, the pH of the permeate from each filtration process was determined immediately after filtration with the aid of a dual channel pH/Ion meter, model AR25 Accumet Research from Fisher Scientific , the results are also depicted above in Table 6.2.

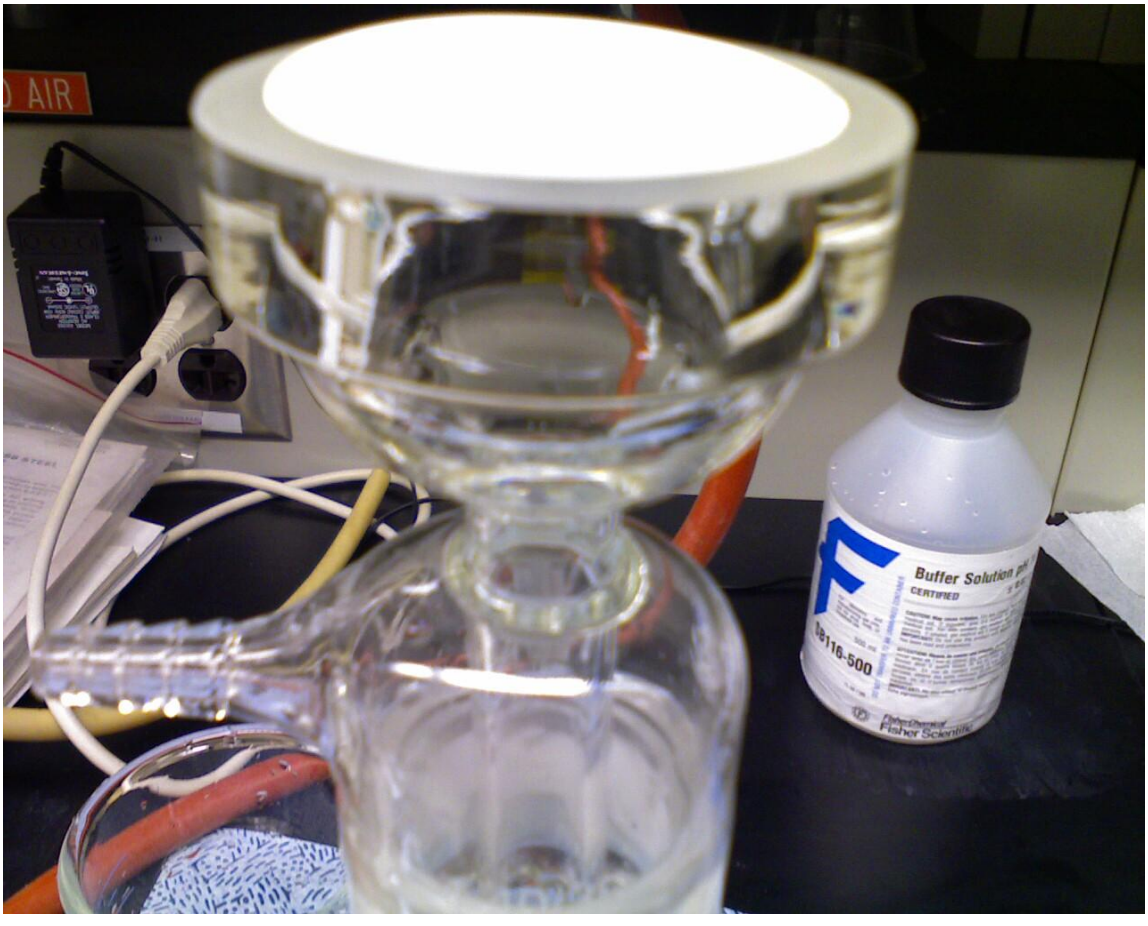

Figure 6.3 Filtration chamber containing a filtration membrane.

6.1 Plant Root Exposure to Ultra Filtered Alumina Nanoparticles Permeate

Five different plant species that had been used for previous studies in this dissertation were used throughout this investigation, together with the four concentrations of both alumina and silica nanoparticles, in order to maintain consistency.

The effect of alumina nanoparticle permeate from 0.025µm membranes using the four different concentrations; 20mg/ml, 2mg/ml, 200µg/ml and 20µg/ml, on the five plant species; *Z.mays*, *D.carota*, *L.sativa*, *B.oleracea*, and *C.sativus* are reported in Table 6.3. The results as tabulated makes a comparison between the Blank(control) and the treated species based on their mean root elongation, R.E and their relative root growth, R.R.G, which as before mentioned, is the ratio of the treated R.E to the Blank R.E.

Table 6.3 Root Elongation R.E of Plant Seedlings Exposed to Alumina Nanoparticles **Suspension** of 20mg/ml Concentration, compared to those obtained by using 20mg/ml Alumina Nanoparticles Permeate from **0.025µm** and **0.05µm** Pore Size Membranes for 72 hrs in the Dark at 25 ± 1ºC.

The results are reported as mean ± S.D. and 95% confidence interval. R.E values are presented in mm.

Conc. R.E	*Z.mays*	*D.carota*	*L.sativa*	*B.oleracea*	*C.sativus*
Blank[a]	33.5±1.6	17.0±2.3	66.8±6.6	71.8±2.0	50.2±2.7
20mg/ml Suspension	22.1±1.98	3.96±0.73	28.2±3.75	25.5±2.83	20.6±3.35
Blank[b]	32.2±4.1	7.5±0.5	35.8±2.7	16.6±1.6	21.1±2.3
0.025µm	24.6±3.2	1.7±0.5	11.0±2.1	8.6±2.1	14.1±2.1
0.05µm	29.0±1.1	3.0±0.2	10.2±1.9	10.5±1.4	16.6±1.8

Blank[a]: obtained during the study of the effect of alumina nanoparticles suspensions on plants.

Blank[b]: obtained during the study of the effect of alumina nanoparticles permeate on plants.

Table 6.4 Root Elongation (RE) and Relative Root Growth (RRG) of Plant Seedlings Exposed to Different Concentrations of Alumina Nanoparticles Permeate using **0.025µm** Membrane for 72 hrs in the Dark at 25 ± 1ºC

The results are reported as mean ± S.D. and 95% confidence interval. And range given as min~max. R.E values are presented in mm.

Conc.	*Z.mays*	*D.carota*	*L.sativa*	*B.oleracea*	*C.sativus*
R.E	32.3 ± 4.1	7.5 ± 0.5	35.8 ± 2.7	16.6 ± 1.6	21.1 ± 2.3
Blank	30.5~38.4	6.8~8.4	32.1~40.7	13.5~19.0	17.0~24.4
	32.3 ± 3.8	6.4 ± 0.6	31.7 ± 2.5	13.5 ± 1.4	18.8 ± 2.0
20µg/ml	25.4~37.6	5.6~7.4	27.5~35.9	11.7~15.8	15.1~22.1
	32.2 ± 2.7	4.5 ± 0.6	20.3 ± 2.3	10.8 ± 1.9	16.5 ± 1.4
200µg/ml	27.6~35.4	3.6~5.5	15.8~23.6	7.6~14.1	14.0~19.6
	30.6 ± 1.8	3.2 ± 0.4	18.3 ± 1.3	9.4 ± 1.5	15.9 ± 1.1
2mg/ml	27.7~33.3	2.6~3.7	16.3~20.6	7.5~12.2	13.9~17.6
	24.6 ± 3.2	1.7 ± 0.5	11.0 ± 2.1	8.6 ± 2.1	14.1 ± 2.1
20mg/ml	19.1~29.0	1.1~2.6	7.6~ 13.3	5.6~12.3	10.7~17.3
R.R.G					
20µg/ml	1.02±0.107	0.851±0.09	0.88±0.062	0.767±0.09	0.88±0.10
	0.805~1.16	0.616~1.00	0.788~0.99	0.67~0.948	0.69~1.10
200µg/ml	0.996±0.09	0.542±0.05	0.553±0.06	0.625±0.14	0.77±0.07
	0.817~1.11	0.469~0.62	0.422~0.65	0.423~0.85	0.64~0.91
2mg/ml	0.931±0.05	0.439±0.04	0.484±0.03	0.55±0.08	0.79±0.05
	0.811~1.00	0.388~0.53	0.422~0.55	0.48~0.767	0.71~0.90
20mg/ml	0.75±0.12	0.213±0.02	0.26±0.06	0.522±0.15	0.65±0.08
	0.526~0.92	0.20~0.254	0.141~0.36	0.35~0.755	0.51~0.79

From Table 6.4 it could be concluded that at low concentrations, alumina nanoparticles permeate obtained by using 0.025µm pore-sized membrane has minimal root growth

inhibitory effect on all the plant species, compared to those from high concentrations using the same pore size of 0.025µm. This is evidenced by the R.E of the species treated with both 20µg/ml and 200µg/ml comparable to the R.E of their Blanks (species treated with Milli-Q water). The low impact on root growth at these concentrations was due to decreased presence of toxic alumina nanoparticles in the permeate as a result of the filtration process from already low concentrations using very fine pore-sized membranes, thus resulting in the retentate being more concentrated than the permeate.

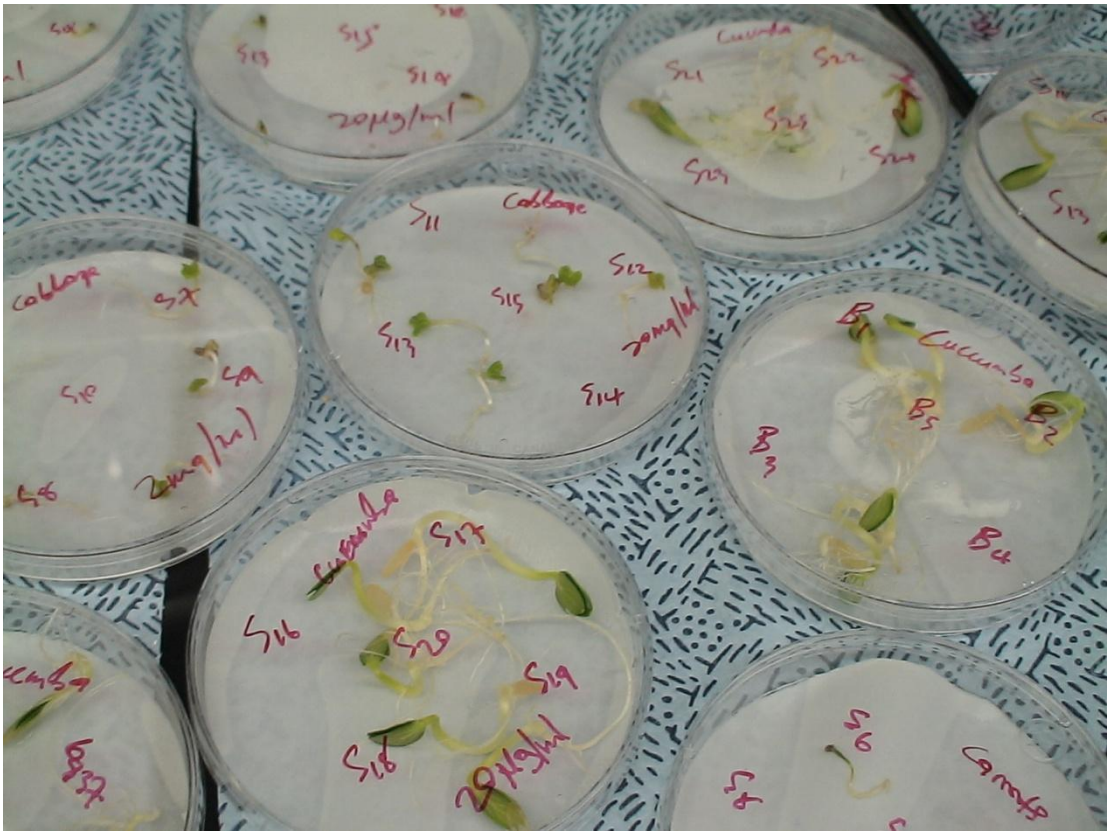

Figure 6.4 Plants seedlings exposed to different concentrations of Alumina nanoparticles permeate from 0.025µm pore sized membrane and the Blank.

Table 6.5 Root Elongation (RE) and Relative Root Growth (RRG) of Plant Seedlings Exposed to Different Concentrations of Alumina Nanoparticles Permeate using **0.05µm** Membrane for 72 hrs in the Dark at 25 ± 1ºC

RE expressed in mm, plus and minus the standard deviation, Range expressed as Min~Max

Conc.	*Z.mays*	*D.carota*	*L.sativa*	*B.oleracea*	*C.sativus*
R.E					
Blank	32.3±4.1	7.5±0.5	35.8±2.7	16.6±1.6	21.1±2.3
	30.5~38.4	6.8~8.4	32.1~40.7	13.5~19.0	17.0~24.4
20µg/ml	30.2±1.8	5.1±0.4	32.7±1.3	12.5±0.4	18.9±1.4
	26.9~32.2	4.3~5.6	30.9~35.1	12.2~13.4	16.7~20.8
200µg/ml	28.8±1.7	4.2±0.3	21.6±0.6	12.1±0.6	17.2±1.9
	26.1~31.2	3.7~4.8	20.7~22.4	11.0~12.9	13.3~19.7
2mg/ml	28.4±1.2	3.3±0.1	17.9±0.8	11.6±0.6	16.2±2.0
	26.6~30.3	3.1~3.5	16.6~19.0	10.4~12.4	12.8~19.6
20mg/ml	29.0±1.1	3.0±0.2	10.2±1.9	10.5±1.4	16.6±1.8
	27.4~30.7	2.6~3.4	7.3~12.9	8.2~12.9	13.2~19.4
R.R.G					
20µg/ml	0.932±0.05	0.676±0.05	0.894±0.03	0.742±0.02	0.86±0.05
	0.845-0.99	0.549-0.72	0.848-0.92	0.707-0.79	0.77-0.92
200µg/ml	0.865±0.03	0.568±0.04	0.606±0.01	0.719±0.04	0.83±0.11
	0.833-0.92	0.482-0.64	0.58-0.624	0.67-0.779	0.57-0.93
2mg/ml	0.875±0.06	0.451±0.03	0.48±0.026	0.74±0.027	0.77±0.08
	0.783-0.96	0.402-0.48	0.435-0.52	0.694-0.77	0.64-0.93
20mg/ml	0.877±0.03	0.398±0.02	0.294±0.05	0.643±0.07	0.78±0.13
	0.817-0.92	0.375-0.43	0.198-0.35	0.525-0.73	0.53-0.99

As the concentration used for treatment was increased to 20mg/ml, an effect on root growth was noticed as the R.E (s) of plant species decreased with respect to their Blanks. This is because at higher concentrations, the increased weight of the suspension (particles and Milli-Q water) improved the chances of more particles 0.025µm or smaller passing through the membrane pores, resulting in the increased presence of the toxic Al^{+3} species in the permeate at this high concentration, in contrast to that at lower concentrations. This in effect counteracted the effect of membrane fouling that occurred at high concentrations which led to the formation of a cake-like structure on the membranes surfaces thereby slowing the process by reducing flux and providing *enhanced* filtration. During experimentation, accumulation and formation of membrane fouling structures normally starts after a time interval depending on concentration, therefore, toxic particles must have passed through membrane pores before this formation.

A second membrane pore size of 0.05µm was also used in this study to make size effect comparisons, the results of which are displayed in Table 6.5. As a result of a larger pore size, the production of the cake-like structure, and hence membrane fouling was reduced, this meant that more particles 0.05µm or smaller were able to make it to the permeate than in the case of the 0.025µm pore size membrane. Although there was noticeable reduction in root growths among plant species with respect to their Blanks with the 0.05µm pore size membranes, there were differences when compared to the results obtained with the 0.025µm pore size membranes.

For *Z.mays*, it was discovered that the highest concentration of 20mg/ml, using the 0.025µm pore size membranes has the highest effect in plant root growth

inhibition (24.5 mm) compared to the Blank with an R.E of 32.3 mm or even with the least concentration of 20µg/ml with an R.E of 32.3 mm. While with the use of the 0.05µm pore size membrane with the same concentration of 20mg/ml, the root growth inhibitory effect was reduced to an R.E of 29.0 mm, thereby suggesting that the plant root growth inhibitory effect of alumina nanoparticles is size specific. This reduction in inhibitory effect from 24.5mm to 29.0 mm with 20mg/ml permeate is not withstanding of the fact that at the larger pore size of 0.05µm, there were more particles present in the permeate as to cause toxic effect but rather the particles were too large to exist as individual particles in the permeate, in addition to the amount present, but instead formed agglomerates that presented even lager particle sizes in the permeate thereby decreasing the chances of particles penetrating root cell walls where they are thought to interfere with cell division during growth. Agglomeration is a time dependent phenomenon that is occasioned by the formation of clusters of particles which are larger in size compared to the parent particles. This formation is controlled by the existence or lack thereof, of surface charges or zeta potential, which in turn is conditioned by the pH of the solution or in this case the suspension. Agglomerates begins to form at zero zeta potential or the isoelectric potential, iep, therefore, zeta potential above the isoelectric potential are positive and denote positive charges existing on the surfaces of the particles, thereby resulting in particles repelling each other and hence remaining dispersed in suspension or de-agglomerated. On the other hand, zeta potentials that are lower than the isoelectric potential are negative and also result in particles remaining dispersed in suspension. Isoelectric potential of macro-sized particles, especially oxides, as it relates to solution/suspension pH, are well discussed in literature

(www.colloidmeasurements.com/zeta.html) and are known to be influenced by impurity, crystal structure, among others. The study of nanosized particles is still in its infancy, hence is not yet clear if the above described phenomenon could be extended to the understanding of the agglomeration of nanoparticles in suspension, since the chemical and physical properties of nanoparticles are different and at times far removed from those of their macro cousins from the same material. Furthermore, with the increased presence of the toxic Al^{3+} species in the permeate with the use of 0.05µm pore size membrane and 20mg/ml alumina nanoparticles suspension feed, the possibilities of Aluminum resistance were increased for *Z.mays*, since the presence of aluminum was in the highest concentration of 20mg/ml was detected in chapter five and the larger pore size of 0.05µm suggests that more particles were able to make it to the permeate region as opposed to the use of the 0.025µm. These together led to the slightly higher RE obtained with this membrane. This further explains the R.R.G of 0.877 obtained with *Z.mays*, using 0.05µm pore size membrane and 20mg/ml alumina nanoparticles permeate as compared to 0.75 from 0.025µm pore size membrane with the same concentration.

For the 0.05µm pore size membrane, lower concentrations; 2mg/ml, 200µg/ml and 20µg/ml presented a reversal in R.Es for *Z.mays* when compared to the result obtained when permeate from 0.025µm pore size membrane was used, since the permeate from the 0.05µm pore size membrane showed inhibitory effect from these concentrations than when compared to the former as indicated in Tables 6.4 and 6.5 respectively, mainly due to decrease in resistance. Lower concentrations also means that there were smaller amounts of particles present in the permeate and reduced possibility

for the formation of agglomerates, hence greater chances of individual particles penetrating the cell wall, in addition to decreased phytotoxic resistance from *Z.mays*.

When the larger pore size of 0.05µm was used together with low concentrations, porous cake-like structure of diminished thickness was formed on the surfaces of the membranes; this led to the absence of enhanced (secondary) filtration effect which was guaranteed by this structure. The result was the introduction of greater amount of toxic species in the permeate from alumina nanoparticles suspension from low concentrations. This was in contrast to the use of the 0.025µm pore size membrane from the same low concentrations, which formed thicker cake-like structure because of the very fine pore size nature of the membrane compared to the 0.05µm membrane; except with the lowest concentration of 20µg/ml, this explains the reduced R.Es observed with this pore size. In fact, when the 0.025µm pore size membrane was used with the 20µg/ml alumina nanoparticles suspension, the filtration process was fast and efficient so that the resulting permeate produced an R.E similar to that of the Blank (Table 6.4).

From Tables 6.4 and 6.5, considering the results obtained while using *Z.mays* as a test species, the lowest percentage error of 3.79% resulted when the 0.05µm pore size membrane and 20mg/ml were utilized, as against 5.88% from the use of 0.025µm pore size and 2mg/ml Alumina nanoparticles permeate. Therefore, the use of the larger pore size of 0.05µm and the highest concentration of 20mg/ml resulted in Root Elongation measurements that were close to the mean R.E.

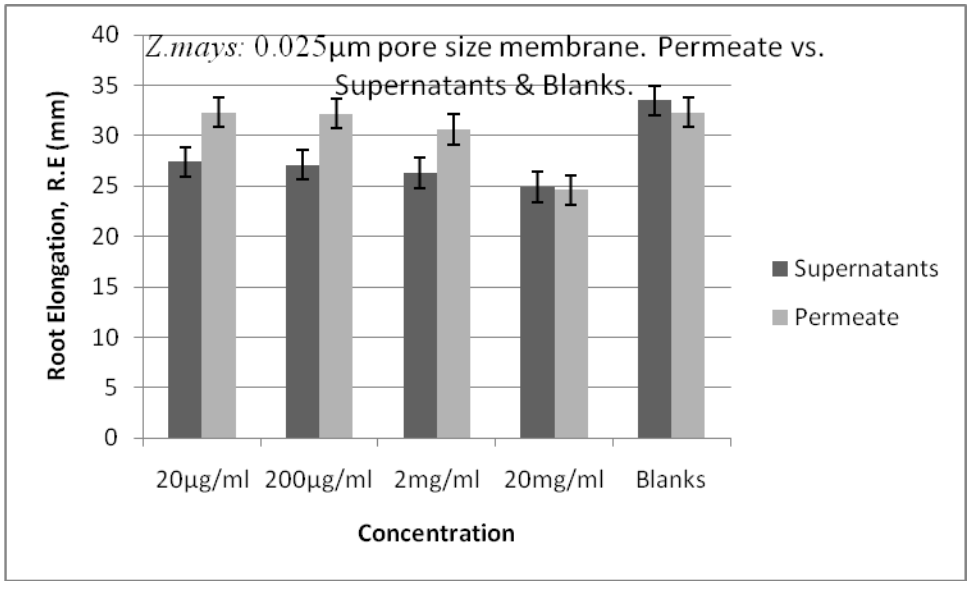

Figure 6.5 Effects of permeate and supernatants on the root growth of *Z.mays* using the 0.025µm pore size membrane at different concentrations, effects compared to Blank (control).

When plant root growth inhibitory effect on *Z.mays* from both supernatants and permeate of alumina nanoparticles were compared, it was observed that supernatants were more inhibitory to growth than permeate at lower concentrations. At the highest concentration of 20mg/ml, the reverse seems to be the case as the permeate from 0.025µm pore size membrane appeared to be more inhibitory to root growth as could be seen in Figure 6.5, Tables 6.8, 6.4 and 4.1. This, as explained earlier, was due to the existence of high amount of very small toxic particles that are 0.025µm or less in size in the permeate at this high concentration, that were able to penetrate root cell walls, a situation which was denied other concentrations, based on Figure 5.5, where traces of toxic soluble aluminum were found on the alumina nanoparticles when using the concentration of 20mg/ml. As the concentration decreased, the observed R.Es approaches that of the Blank due to almost complete filtration, assisted by the cake layer on the membranes.

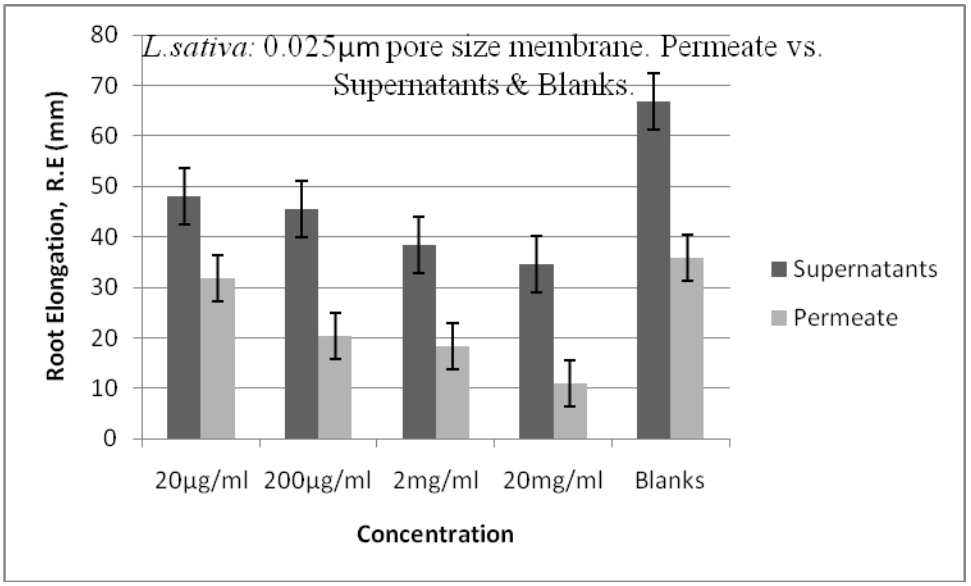

Figure 6.6 Effects of permeate and supernatants from Alumina nanoparticles on the root growth of *L.sativa* using the 0.025µm pore size membrane at different concentrations, effects compared to Blank (control).

A similar effect was noticed on *L.sativa* and *D.carota* using permeate from 0.025µm pore size membrane from Alumina nanoparticles permeate, as shown in Figures 6.6 and 6.7. From these Figures, it can be concluded that; the permeate was more detrimental to root growth from the 20mg/ml to the 200µg/ml concentrations, than the supernatants from the same concentrations.

The different growth rate recorded with the Blanks was the effect of storage, as the study with permeate took place months after that with the permeates.

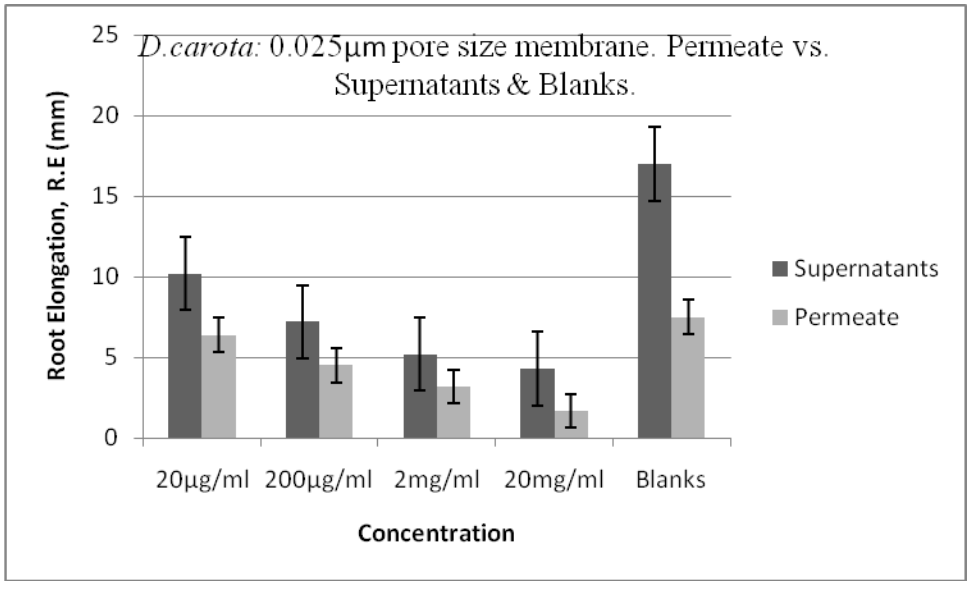

Figure 6.7 Effects of permeate and supernatants on the root growth of *D.carota* using the 0.025µm pore size membrane at different concentrations, effects compared to Blank (control).

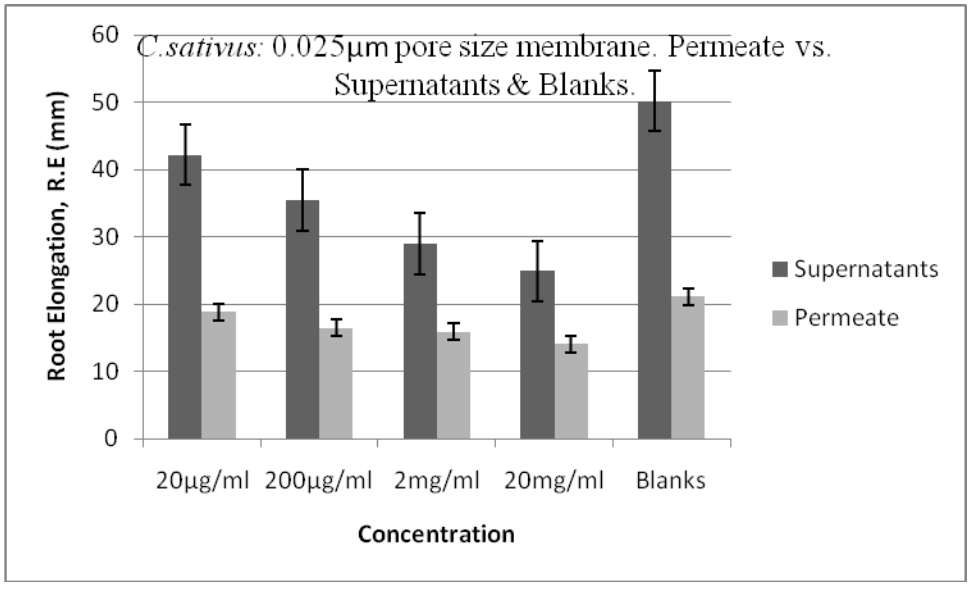

Figure 6.8 Effects of permeate and supernatants on the root growth of *C.sativus* using the 0.025µm pore size membrane at different concentrations of Alumina nanoparticles vs. Blank.

The results of the study using these two plant species are shown graphically in Figures 6.8 and 6.9 respectively.

With the use of a larger pore size membrane of 0.05µm, the resultant permeate contained particles that were too large to have significant inhibition to growth compared to the supernatants, even at highest concentration of 20mg/ml, except for *L.sativa* and *D.carota* (Figures 6.13 & 6.14). These particles, apart from their individual large sizes, form agglomerates with less impact on root growth as displayed in Figures 6.10, 6.11 and 6.12 for *Z.mays*, *C.sativus*, and *B.oleracea* respectively.

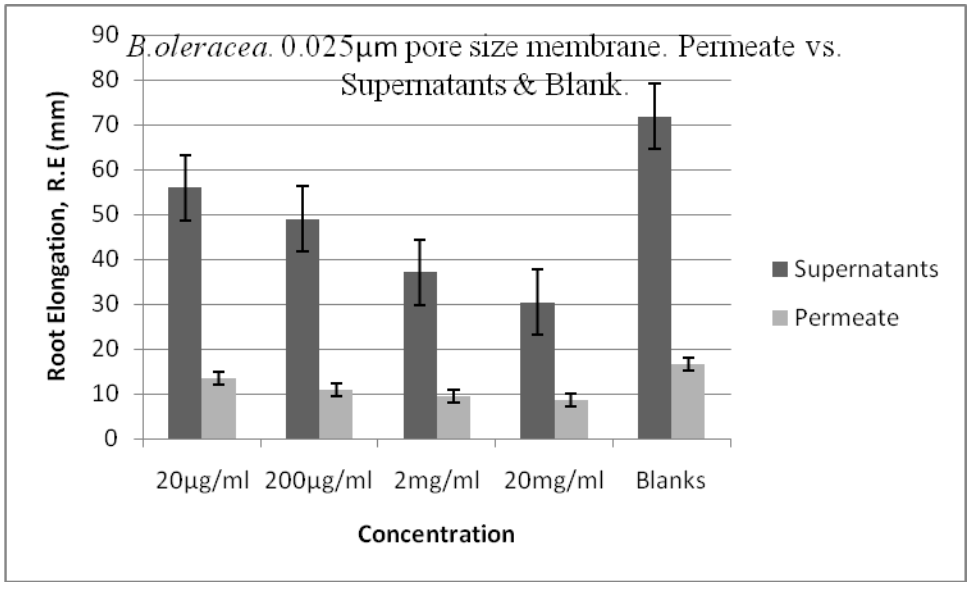

Figure 6.9 Effects of permeate and supernatants on the root growth of *B.oleracea* using the 0.025µm pore size membrane at different concentrations of Alumina nanoparticles, effects compared to Blank (control).

For the other two plant species; *D.carota* and *L.sativa*, there was less reduction in plant root growth using the 0.05µm pore size membrane as compared to the 0.025µm pore size

membrane, considering the reduction of their R.Es as displayed in Table 6.5 and Figures 6.13 and 6.14 respectively, but when compared to the supernatants with the same concentrations, the reductions become significant. No matter the specimen used, plant species react differently to the same treatment due to their unique chemical compositions and internal structures.

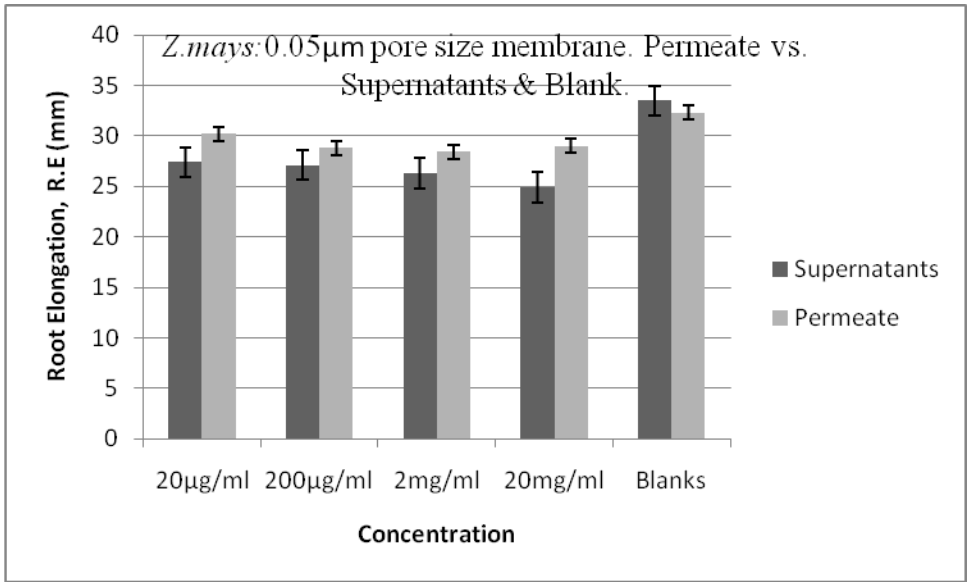

Figure 6.10 Effects of permeate and supernatants on the root growth of *Z.mays* using the 0.05µm pore size membrane at different concentrations of Alumina nanoparticles, effects compared to Blank (control).

To this end, and based on the result obtained, a comparison was made among the plant species used in this study to ascertain their response to various treatments using permeate from both the 0.025µm and 0.05µm respectively of Alumina nanoparticles at different concentrations.

Figure 6.15 shows the differences in mean root elongation of the five different plant species used in this investigation while using the highest concentration of 20mg/ml and the 0.025µm pore size membrane.

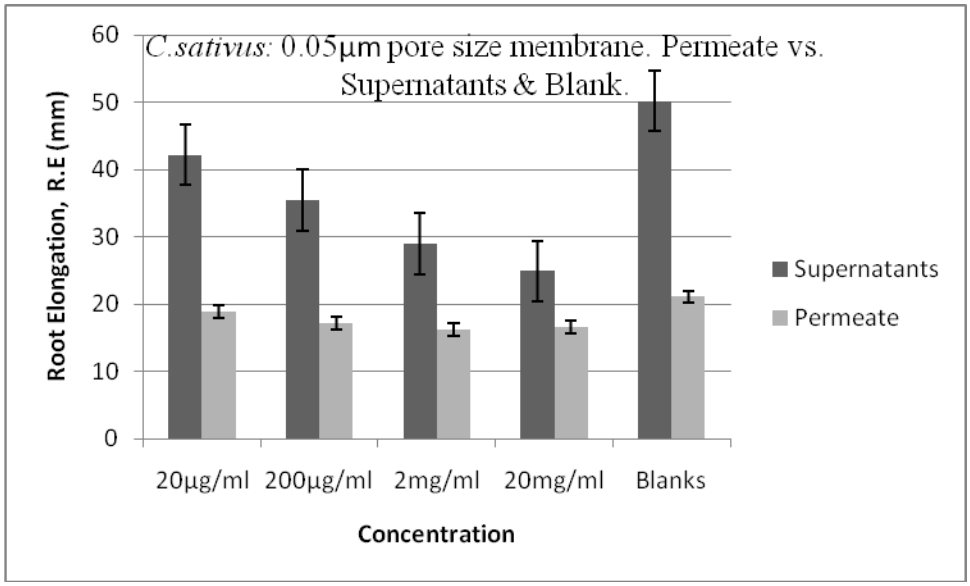

Figure 6.11 Effects of permeate and supernatants on the root growth of *C.sativus* using 0.05µm pore size membrane at different concentrations of Alumina nanoparticles, effects compared to Blank (control).

From Figure 6.15, it is obvious that all the plant species were affected by the exposure to the permeate, but in varying degree. When compared to its Blank, *L.sativa* was the most affected plant species when using the 0.025µm pore size membrane permeate of the 20mg/ml concentration of Alumina nanoparticles. All other plant species were comparatively affected by the permeate, considering their Blanks. This suggests that permeate from ultra filtration using the 0.025µm membrane contained particles so small

that they were able to cause inhibition to root growth by disrupting cell activities that lead to growth.

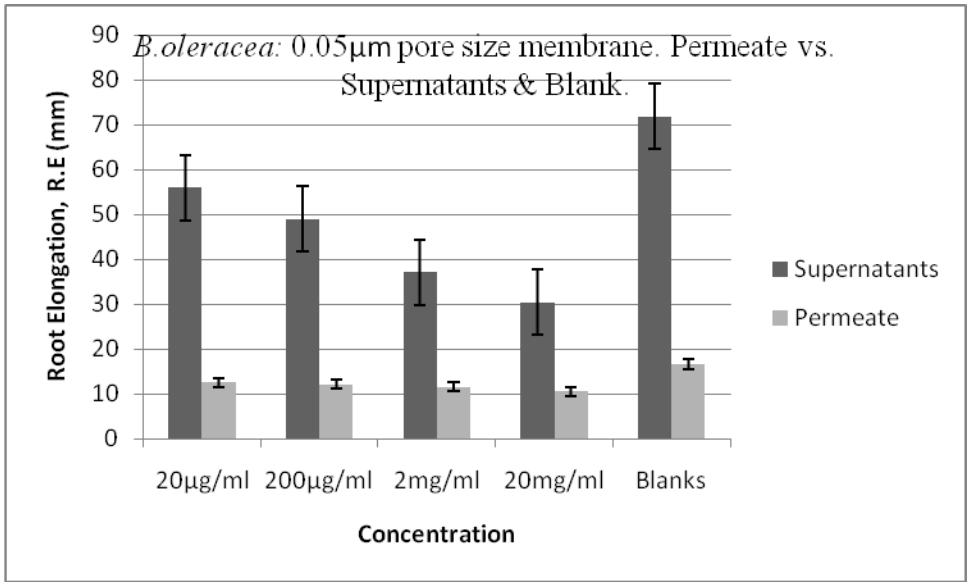

Figure 6.12 Effects of permeate and supernatants on the root growth of *B.oleracea* using 0.05µm pore size membrane at different concentrations of Alumina nanoparticles, effects compared to Blank (control).

When this result is compared to that obtained using permeate from 0.05µm pore size membrane from the same concentration of 20mg/ml of Alumina nanoparticles suspension, as is shown in Figure 6.16, a distinguishable size effect is established. Once again as it was in the case with the 0.025µm pore size membrane, *L.sativa* was the most affected, while the least affected was *Z.mays.*

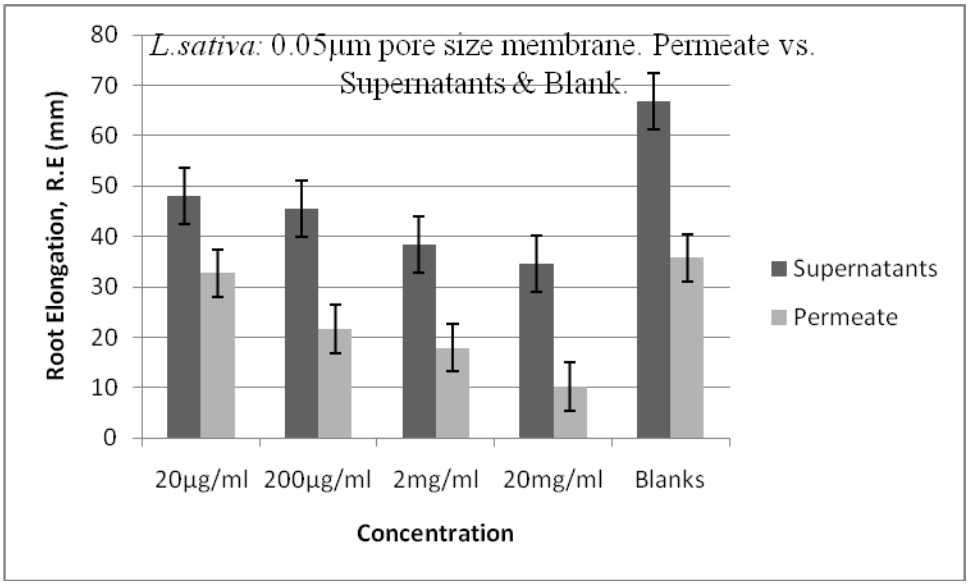

Figure 6.13 Effects of permeate and supernatants on the root growth of *L.sativa* using the 0.05µm pore size membrane at different concentrations of Alumina nanoparticles, effects compared to Blank (control).

Figures 6.17 and 6.18 display graphically the result obtained when the least concentration of 20µg/ml of Alumina nanoparticles permeate was used with either the 0.025µm or 0.05µm pore size membranes on the plant species used in this study. As can be gleaned from these charts, there was drastic reduction in inhibitory effect in root growth of the five plant species when compared with higher concentrations. When *Z. mays* was treated with the permeate from the 0.025µm pore size membrane, there was actually no difference between the treated specimen and the Blank as displayed in Figure 6.17. In the same respect, all other species showed significant reduction in differences between the R.E of their treated specimen and their Blanks.

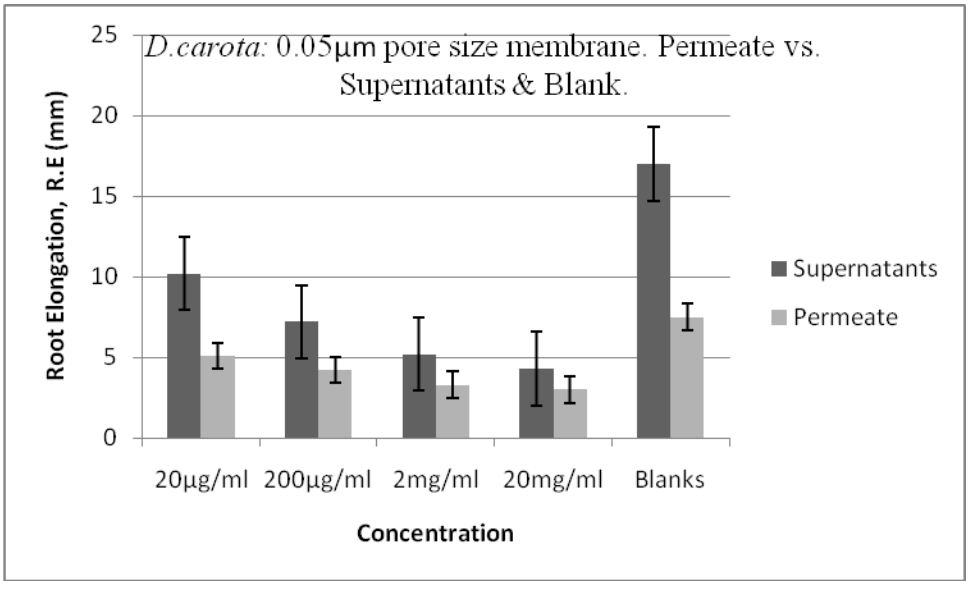

Figure 6.14 Effects of permeate and supernatants on the root growth of *D.carota* using the 0.05µm pore size membrane at different concentrations of Alumina nanoparticles, effects compared to Blank (control).

This is an indication that the lowest concentration of 20µg/ml permeate contained significantly less amount of particles since the feed (20µg/ml suspension) comparatively has lower concentration of Alumina particles, ultra filtration using the 0.025µm pore size membrane further reduced the amount of particles found in the permeate.

When a larger pore sized membrane of 0.05µm and the same concentration of 20µg/ml were used, increasingly noticeable differences between the R.E of the treated samples to the Blanks of the plant species began to emerge as could be seen in Figure 6.18.

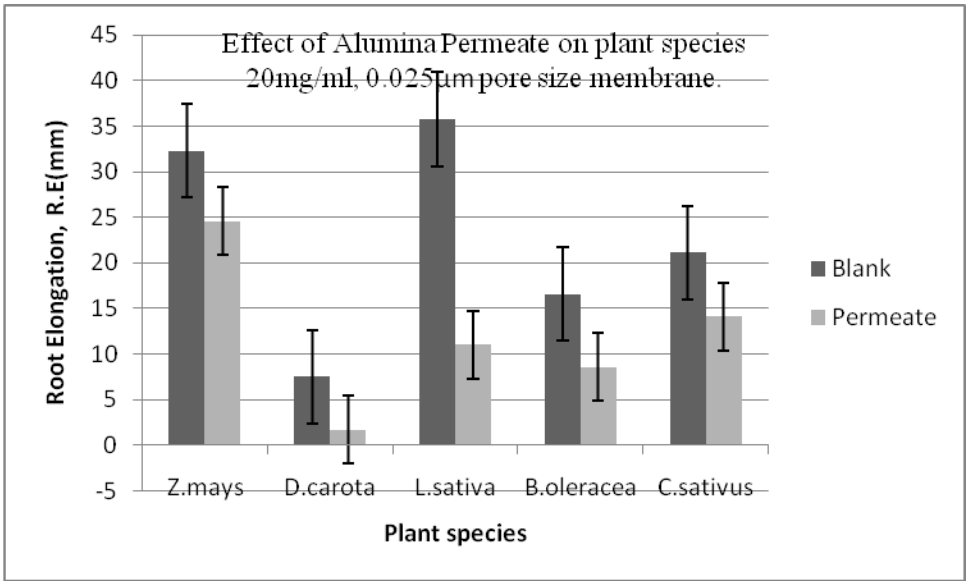

Figure 6.15 Effect of 20mg/ml Alumina nanoparticles permeate from 0.025µm pore size membrane on five plant species, mean root elongations compared to Blanks (control).

This reduction in the R.E of plant species was due to fact that larger pore size guaranteed that a larger amount of toxic Alumina nanoparticles was able to pass through the membrane, especially with the virtual absence of the cake-like structure as a result of the low concentration and larger pore size used. Since there were fewer particles in the permeate with this concentration as compared to the other concentrations used in this study, the chances for the formation of agglomerates were slim. Particle agglomeration is primarily governed by the size(s) of the particles, the amount of particles present and the existence of Van der Waals forces, among others (To D et al, 2009).

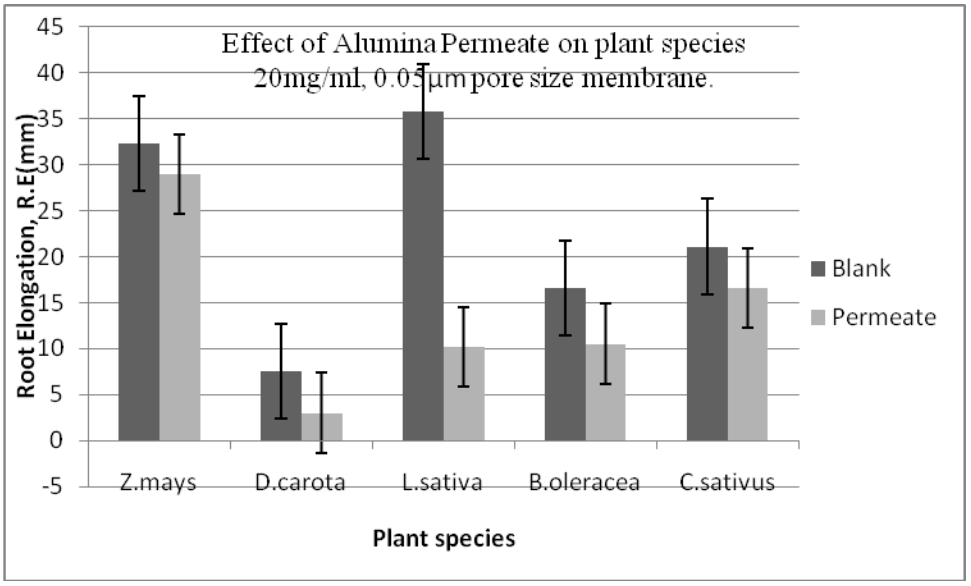

Figure 6.16 Effect of 20mg/ml permeate from Alumina nanoparticles suspension using 0.05µm pore size membrane on five plant species, mean root elongations compared to Blanks.

As mentioned earlier, these agglomerates, due to their relative larger sizes would have reduced the inhibitory effect of the permeate. During the study, attempts were made to reduce the effects of agglomeration by sonicating the permeate of each concentration for 60 minutes prior to their use to treat plant seedlings.

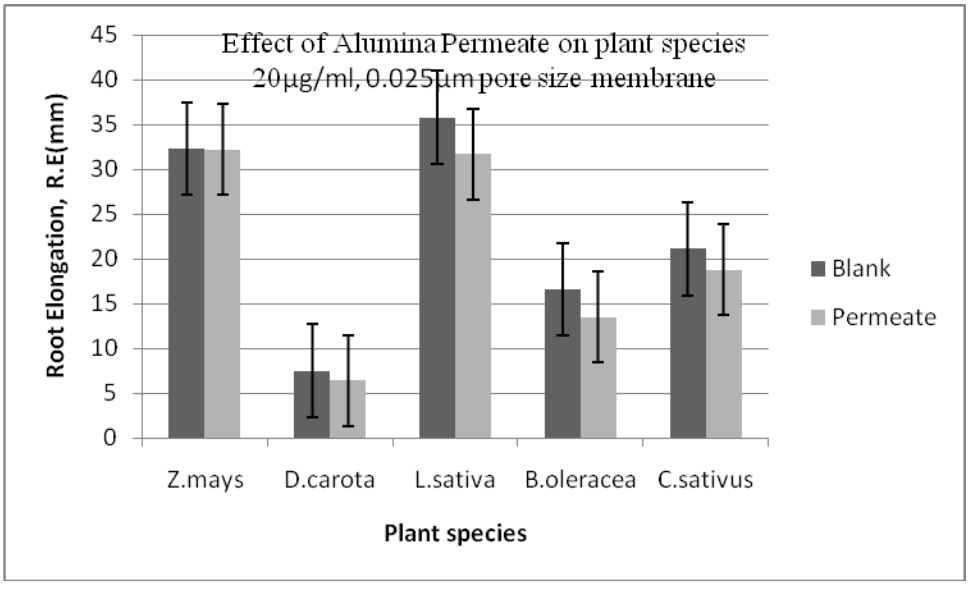

Figure 6.17 Effect of 20µg/ml permeate from 0.025µm pore size membrane on five plant species, mean root elongations compared to Blanks.

Tables 6.4 and 6.5 contain the result of statistical analysis of root elongation measurements of both plant species and their Blanks obtained by using *One-way Anova* as described in section 3.1.2 as well as in appendix A. These analyses were conducted to ascertain if there were significant differences between the root elongations of treated species, and their untreated counterparts; Blanks. Statistically significant difference exists when the calculated probability *p*, is less than the level of significance of 0.05.

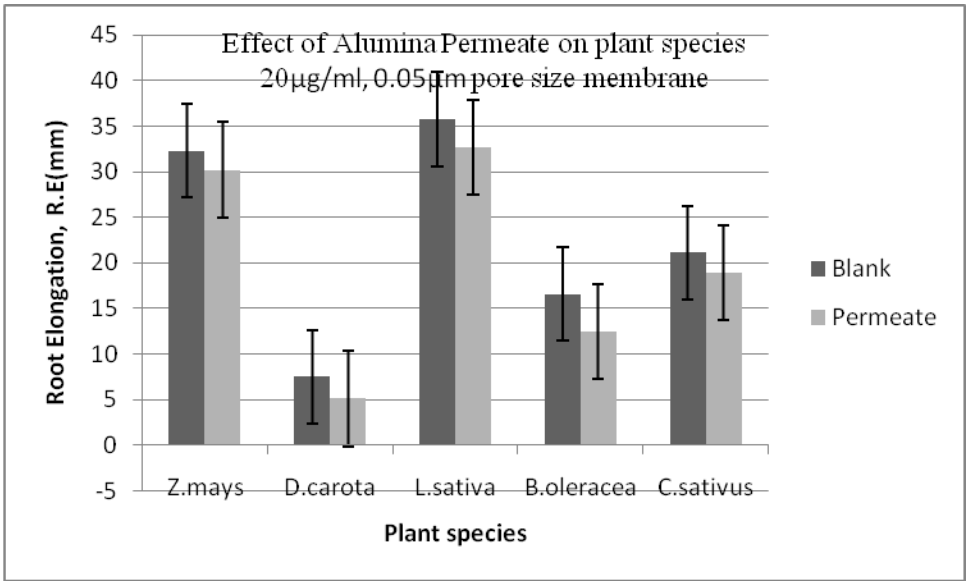

Figure 6.18 Effect of 20µg/ml permeate from 0.05µm pore size membrane on five plant species, mean root elongations compared to Blanks.

In addition to the probability, *p*, the tables also contains the coefficient of determination, R^2, as well as the *f* statistics. The R^2, evaluates the correlation between two samples, increasing R^2 suggests the root growth of the seedlings exposed to the permeate approaches that of the seedlings cultured in the blank. A perfect correlation exists when the coefficient of determination is unity. Therefore, values closer to unity suggest a strong correlation between the root elongations of treated and untreated specimen.

Table 6.6 Statistical Analysis Results of the Root Elongation (RE) of Plant Seedlings Exposed to Alumina Nanoparticles Permeate using **0.025µm** Pore Size Membrane for 72 hrs in the Dark at 25 ± 1ºC

Results from the *one-way ANOVA* procedure are reported as the value of *f*, *p*, and the coefficient of determination (R^2). Statistical difference is reported as *p* smaller than 0.05.

Conc.	*Z.mays*	*D.carota*	*L.sativa*	*B.oleracea*	*C.sativus*
20µg/ml	*p*=0.12 R^2= 0.941 *f=1.843*	p= 0.057 *R^2= 0.86* *f= 2.305*	p= 0.05 R^2= 0.91 *f= 2.386*	p= 0.062 *R^2= 0.895* *f= 2.254*	p=0.061 *R^2= 0.9561* *f=2.264*
200µg/ml	*p= 0.04* *R^2=0.8245* *f=2.523*	p= 0.000 R^2= 0.80 *f= 6.385*	p=0.024 R^2= 0.71 *f= 2.837*	p= 0.05 *R^2=0.8041* *f=2.386*	p= 0.006 *R^2= 0.8372* *f=3.695*
2mg/ml	*p=0.008* R^2= 0.754 *f=3.515*	p= 0.024 R^2= 0.73 *f= 2.837*	p= 0.01 R^2= 0.72 *f= 3.377*	p= 0.03 *R^2= 0.642* *f=2.7*	p= 0.001 *R^2= 0.8013* *f=4.836*
20mg/ml	*p= 0.001* R^2= 0.427 *f=4.836*	p= 0.036 R^2= 0.52 *f= 2.588*	p= 0.001 R^2= 0.62 *f= 4.836*	p= 0.01 *R^2=0.4156* *f=3.377*	p= 0.008 *R^2= 0.7215* *f= 3.515*

From Table 6.6, *p*, for *Z.mays* using the least concentration of 20µg/ml of Alumina nanoparticles permeate is 0.12 and an R^2 of 0.941 which indicates that there was no significant difference between the specimen exposed to the permeate and the Blank as well as a high degree of correlation between the two. This is evidenced by the root elongation result in Table 6.4 at this concentration.

Table 6.7 Statistical Analysis Results of the Root Elongation (RE) of Plant Seedlings Exposed to Alumina Nanoparticles Permeate using **0.05µm** Pore Size Membrane for 72 hrs in the Dark at 25 ± 1º C

Results from the *one-way ANOVA* procedure are reported as the value of *f*, *p*, and the coefficient of determination (R^2). Statistical difference is reported as *p* smaller than 0.05.

Conc.	*Z.mays*	*D.carota*	*L.sativa*	*B.oleracea*	*C.sativus*
20µg/ml	*p*=0.148 R^2= 0.86 *f=1.71*	p= 0.08 *R^2= 0.93* *f= 2.096*	p= 0.07 R^2= 0.78 *f= 2.179*	p= 0.071 *R^2= 0.91* *f= 2.170*	p=0.052 *R^2= 0.97* *f=2.362*
200µg/ml	*p= 0.04* *R^2=0.73* *f=2.523*	p= 0.01 R^2= 0.89 *f= 3.377*	p=0.034 R^2= 0.70 *f= 2.623*	p= 0.03 *R^2=0.90* *f=2.7*	p= 0.011 *R^2= 0.902* *f=3.318*
2mg/ml	*p=0.001* R^2= 0.67 *f=4.836*	p= 0.00 R^2= 0.78 *f= 4.836*	p= 0.01 R^2= 0.61 *f= 3.377*	p= 0.01 *R^2= 0.81* *f=3.377*	p= 0.009 *R^2= 0.884* *f=3.442*
20mg/ml	*p= 0.005* R^2= 0.74 *f=3.809*	p= 0.01 R^2= 0.40 *f= 3.377*	p= 0.01 R^2= 0.50 *f= 3.377*	p= 0.000 *R^2=0.701* *f=6.385*	p= 0.025 *R^2= 0.513* *f= 2.812*

This is in contrast to the result obtained when the highest concentration of 20 mg/ml was used, with *p* equal to 0.005 and R^2 of 0.74 respectively, a declaration of significant difference and comparatively less correlation between the treated specimen and the Blank. For *Z.mays*, as the concentration was increased from 20µg/ml to 20mg/ml, the values of both *p* and R^2 decreases.

A similar situation was recorded with the rest of the plant species used in this study, with *D.carota* having the least R^2 value of 0.40 and a p value of 0.01, at the

concentration of 20mg/ml, further departing from unity. This indicates a slight difference in effect from the treatment with high concentration of Alumina nanoparticles permeate had on the plant species, while using the larger pore size of 0.05µm, and also in contrast to the use of the least pore size of 0.025µm where the recorded R^2 was 0.521 at the same concentration of 20mg/ml.

Attempt was then made to statistically compare the phytotoxic effect of supernatants to that of the permeate from both pore sizes and the same concentrations using Alumina nanoparticles. To achieve this objective, the student t-test was utilized to test the mean root elongations of the two groups of samples (supernatants and permeate), once again using the 95% confidence interval and 0.05 level of significance, the degree of freedom, df, for all the calculations was 18, since n, was 20.

The result of this analysis is displayed in Tables 6.8 and 6.9 and contains the values of t statistics and probability, *p*.

As was the case with the *One way-ANOVA*, *p* values that were less than the level of significance were found to be significantly different and thus led to the rejection of the null hypothesis that; there was no difference between the supernatants and permeate; otherwise the null hypothesis was accepted.

Table 6.8 Statistical Analysis Results of the Root Elongation (RE) of Plant Seedlings Exposed to Alumina Nanoparticles S**upernatants** and P**ermeate** using the **0.025µm** Membrane for 72 hrs in the Dark at 25 ± 1ºC

Results from the *Student's t*-test are reported as the value of *t* and the value of probability of the result assuming the null hypothesis (*p*). Statistical significance is reported when p is less than 0.05.

Conc.	*Z.mays*	*D.carota*	*L.sativa*	*B.oleracea*	*C.sativus*
20µg/ml	*t=3.13*	t= 0.68	t=2.76	t= 1.65	t= 0.63
	p= 0.01	p= 0.51	p= 0.01	p=*0.12*	p= 0.54
200µg/ml	*t=3.09*	t= 1.85	t= 2.03	t= 3.73	t= 2.70
	p= 0.01	p= 0.08	p= 0.06	p =0.001	p= 0.04
2mg/ml	*t= 2.07*	t= 2.81	t= 2.51	t= 4.24	t= 2.75
	p= 0.05	p= 0.01	p= 0.02	p=0.009	p= 0.014
20mg/ml	*t=3.92*	t= 5.30	t= 3.22	t= 2.5	t= 2.05
	p= 0.00	p= 0.00	p= 0.01	p=0.022	p= 0.055

Additionally, t values that were higher than the critical t (tabular) value also had associated p values that were less than the level of significance and subsequently led to the rejection of the null hypothesis, otherwise the null hypothesis was accepted. In comparing the difference in toxicity between the supernatants and permeate of Alumina nanoparticles using the 0.025µm pore size membrane, as displayed in Table 6.8, it was found that in most cases there was no statistical difference between the two groups of samples when using the least concentration of 20µg/ml, except for *Z.mays* and *L.sativa* with p values of 0.01. Those were in contrast to *D.carota, B.oleracea* and *C.sativus* with p values of 0.51, 0.31 and 0.54 respectively, when the least concentration of 20µg/ml was used, thereby suggesting that; there was no significant difference between the phytotoxic

effects of supernatants and permeate at this concentration and pore size of 0.025µm for these three plant species.

Table 6.9 Statistical Analysis Results of the Root Elongation (RE) of Plant Seedlings Exposed to Alumina Nanoparticles **Supernatants** and **Permeate** using the **0.05µm** Membrane for 72 hrs in the Dark at 25 ± 1ºC

Results from the *Student's t*-test are reported as the value of *t* and the value of probability of the result assuming the null hypothesis (*p*). Statistical significance is reported when p is less than 0.05.

Conc.	*Z.mays*	*D.carota*	*L.sativa*	*B.oleracea*	*C.sativus*
20µg/ml	*t=0.95*	t= 1.13	t=1.95	t= 4.13	t= 0.04
	p= 0.35	p= 0.273	p= 0.07	p=*0.001*	p= 0.969
200µg/ml	*t=0.204*	t= 3.66	t= 0.810	t= 2.74	t= 1.67
	p= 0.84	p=0.002	p= 0.43	p =0.01	p= 0.112
2mg/ml	*t= 0.701*	t= 3.56	t= 2.43	t= 12.6	t= 1.50
	p= 0.49	p= 0.002	p= 0.03	p=0.000	p= 0.151
20mg/ml	*t=0.81*	t= 1.79	t= 4.26	t= 13.0	t= 1.96
	p= 0.43	p= 0.09	p= 0.00	p=0.000	p= 0.066

With the use of the larger pore size of 0.05µm, as shown in Table 6.9, *B.oleracea* seemed to be the only plant species that displayed statistical difference between supernatants and permeate at all concentrations, while *D.carota* and *L.sativa* showed significant difference at higher concentrations.

Table 6.10 Statistical Analysis Results of the Root Elongation (RE) of Plant Seedlings Exposed to Alumina Nanoparticles **Permeate** using both the **0.025µm** and **0.05µm** Membrane for 72 hrs in the Dark at 25 ± 1ºC (Student t test of 0.025µm vs. 0.05µm)

Results from the *Student's t*-test are reported as the value of *t* and the value of probability of the result assuming the null hypothesis (*p*). Statistical significance is reported when p is less than 0.05.

Conc.	*Z.mays*	*D.carota*	*L.sativa*	*B.oleracea*	*C.sativus*
20µg/ml	*t=0.99*	t= 1.49	t=1.90	t= 0.979	t= 0.53
	p= 0.34	p= 0.154	p= 0.07	p=*0.341*	p= 0.603
200µg/ml	*t=3.33*	t= 0.676	t= 1.46	t= 2.28	t= 1.63
	p= 0.00	p=0.508	p= 0.16	p =0.04	p= 0.121
2mg/ml	*t= 0.48*	t= 3.73	t= 1.27	t= 4.56	t= 0.18
	p= 0.64	p= 0.00	p= 0.22	p=0.000	p= 0.869
20mg/ml	*t=3.27*	t= 7.96	t= 0.46	t= 2.49	t= 2.63
	p= 0.00	p= 0.00	p= 0.65	p=0.023	p= 0.017

The high level of statistical difference recorded with the use of a larger pore size of 0.05µm, was as a result of the introduction of more toxic particles into the permeate from Alumina nanoparticles suspension as opposed to the supernatants and the use of the 0.025µm pore size membrane.

Table 6.9 compares statistically, the results of mean root growth obtained using both membranes of pore sizes; 0.025µm and 0.05µm respectively. This comparison was done using the student's t- test and displays the t and *p* values. These results indicate that statistical difference does exist between the two pore sizes, especially at high concentrations. Except for *L.sativa,* with p values of 0.07, 0.16, 0.22 and 0.65, when

exposed to permeate of the following concentrations; 20µg/ml, 200µg/ml, 2mg/ml and 20mg/ml, respectively.

Other plant species; *Z.mays, D.carota, B.oleracea* and *C.sativus* have *p* values of 0.00, 0.00, 0.023 and 0.017 respectively at the highest concentration of 20mg/ml. This means that there was a significant difference between the permeate from 0.025µm and 0.05µm pore size membranes. This difference may be connected to the formation of a thicker "cake-like" structure on the surface of the 0.025µm pore size membrane at the highest concentration of 20mg/ml during filtration, in addition to the "unique benefit" gained from enhanced *filtration* as a result of this structure, smaller particles of 0.025µm or less, interacted more with plant cells due to decreased chances of the formation of agglomerates due to singular existence. While the use of the larger pore size of 0.05µm yielded a thinner "cake-like" structure on the surfaces of membranes used, additionally, larger pore size allowed not only more particles into the permeate but larger particles as well (that is, more than 0.025µm, but 0.05µm or less, in sizes). While in the permeate, because of their relative larger sizes, particles found it difficult to exist as individual single particles but rather form agglomerates which posses an even larger size(s) to plant cell walls, and thence found it difficult to penetrate plant cell walls, thereby leading to decreased inhibitory effect to root growth.

Conclusion

For Alumina nanoparticles permeate, phytotoxic effect on the five plant species used in this study was determined first by the concentrations involved, then by the pore sizes

used for ultrafiltration. Using 0.025μm pore size membrane for ultra filtration of Alumina nanoparticles suspension of low concentration; 20μg/ml, resulted in a permeate that was less toxic and hence less inhibitory to plant root growth, since almost all the particles were virtually filtered off. But as the concentration was increased there was a subsequent increase in the amount of particles less than or equal to 0.025μm that were able to pass through the membrane and into the permeate section of the filtration system as a result of increased weight of nanoparticles suspension, which comes with increased concentration. Hence, permeates from higher concentrations were found to be more inhibitory to plant root growth as evidenced by a reduction in plant roots' mean root elongation as compared to their Blank counterparts.

With the use of a larger pore size of 0.05μm pore size membrane, there was a decrease in phytotoxic effect from the resultant permeate on plant species at high concentrations, because there was an increased amount of particles 0.05μm or less that were able to pass through the membrane because of the larger pore size. These particles, because of their large sizes, could not exist individually easily as single particles but rather quickly formed agglomerates that presented even larger sizes, and hence were less likely to penetrate plant cell walls, therefore leading to a reduction in inhibitory effect, as mentioned before.

6.2 Plant roots Exposure to Ultra Filtered hydrophilic Silica Nanoparticles Permeate

As mentioned earlier, in addition to Alumina nanoparticles, hydrophilic silica nanoparticles were also used to investigate particle size effect on plant root growth and to compare this inhibitory effect on plant root growth to that from Alumina nanoparticles.

Hydrophilic silica, as suspensions of different concentrations, was extensively investigated by the previous researchers in this area of research but were not studied further in this series of studies, except in this experiment where it is thought that particles sizes could play a role in inhibitory effect on plant root growth.

Table 6.11 contains the results of the mean root elongation measurements, R.E and the relative root growth, R.R.G, which is the ratio of the root elongation measurement of the specimen to that of the Blank, using hydrophilic silica nanoparticles permeate from 0.025μm pore size membrane. From these results, it could be gleaned that exposure of plant seedlings to this permeate leads to a decrease in plant root growth with increasing concentration of hydrophilic silica nanoparticles in the suspension (feed). This also is irrespective of the plant species, for *Z.mays*, when treated with the least concentration of 20μg/ml, the root elongation was 29.9 mm, this value decreased to 27.5 mm with the highest concentration of 20mg/ml.

Table 6.11 Root Elongation (RE) and Relative Root Growth (RRG) of Plant Seedlings Exposed to Different Concentrations of Silica Nanoparticles Permeate using **0.025µm** Membrane for 72 hrs in the Dark at 25 ± 1ºC

RE expressed in mm, plus and minus the standard deviation, Range expressed as Min~Max

Conc.	*Z.mays*	*D.carota*	*L.sativa*	*B.oleracea*	*C.sativus*
R.E					
Blank	32.3±4.1	7.5±0.5	35.8±2.7	16.6±1.6	21.1±2.3
	30.5~38.4	6.8~8.4	32.1~40.7	13.5~19.0	17.0~24.4
20µg/ml	29.9±1.2	6.3±0.2	32.4±1.6	14.5±0.8	18.4±0.6
	28.4~31.6	5.9~6.6	30.2~34.8	13.3~15.5	17.5~19.3
200µg/ml	29.0±1.3	5.1±0.3	22.2±1.0	13.0±0.9	16.7±0.6
	26.7~30.7	4.6~5.4	20.7~23.5	11.8~14.3	15.8~17.5
2mg/ml	28.9±1.7	3.0±0.3	18.8±0.9	10.9±0.9	15.4±0.8
	25.6~31.2	2.6~3.4	17.7~20.5	9.4~12.3	14.0~16.4
20mg/ml	27.5±0.7	2.2±0.3	11.1±0.8	9.4±0.9	14.7±0.7
	26.3~28.5	1.8~2.6	9.9~12.4	8.1~10.5	13.4~15.8
R.R.G					
20µg/ml	0.925±0.03	0.843±0.03	0.898±0.04	0.873±0.04	0.89±0.03
	0.88-0.98	0.776-0.88	0.84-0.95	0.81-0.04	0.85-0.93
200µg/ml	0.90±0.05	0.698±0.04	0.634±0.03	0.805±0.05	0.80±0.02
	0.78-0.96	0.629-0.75	0.58-0.67	0.74-0.88	0.76-0.83
2mg/ml	0.90±0.04	0.434±0.03	0.528±0.03	0.665±0.05	0.73±0.04
	0.84-0.97	0.388-0.47	0.49-0.59	0.59-0.74	0.65-0.77
20mg/ml	0.853±0.02	0.308±0.03	0.315±0.02	0.557±0.05	0.70±0.03
	0.82-0.87	0.241-0.34	0.28-0.34	0.48-0.62	0.64-0.75

The R.R.G, when compared to the Blank (Table 6.4), also reduced to 0.85046 from 0.92642 when concentration was increased from the least concentration of 20µg/ml to the highest concentration of 20mg/ml. The same can be said of other species used in this study, *D.carota, L.sativa, B.oleracea* and *C.sativus* all had their root elongation reduced to 2.2, 11.1, 9.4 and 14.7 (mm), respectively from 6.3, 32.4, 14.5 and 18.4 (mm) when concentration was increased from 20µg to 20 mg/ml, so was also the case with the R.R.G (Table 6.11).

Table 6.12 Root Elongation (RE) and Relative Root Growth (RRG) of Plant Seedlings Exposed to Different Concentrations of Silica Nanoparticles Permeate using **0.05µm** Membrane for 72 hrs in the Dark at 25 ± 1ºC

RE expressed in mm, plus and minus the standard deviation, Range expressed as Min~Max

Conc.	*Z.mays*	*D.carota*	*L.sativa*	*B.oleracea*	*C.sativus*
R.E					
Blank	32.3±4.1	7.5±0.5	35.8±2.7	16.6±1.6	21.1±2.3
	30.5~38.4	6.8~8.4	32.1~40.7	13.5~19.0	17.0~24.4
20µg/ml	28.4±1.7	5.3±0.2	33.9±1.7	14.5±0.7	18.9±1.0
	25.8~30.9	5.3~5.6	30.8~36.1	13.5~15.6	17.4~20.4
200µg/ml	27.9±1.4	4.4±0.2	23.8±1.0	13.6±0.6	17.7±0.7
	25.7~29.8	4.1~4.7	21.6~25.6	12.6~14.5	16.5~18.9
2mg/ml	27.3±1.5	3.4±0.2	18.4±0.8	12.1±0.9	17.4±0.8
	25.0~29.6	3.1~3.7	17.7~20.5	11.0~13.3	16.1~18.5
20mg/ml	27.3±1.3	3.1±0.2	11.7±0.9	11.4±0.7	18.1±0.9
	24.9~29.2	2.7~3.5	10.4~13.3	10.4~12.7	16.8~19.5
R.R.G					
20µg/ml	0.868±0.04	0.70±0.03	0.944±0.05	0.87±0.04	0.90±0.05
	0.805-0.932	0.64-0.75	0.86-1.01	0.81-0.94	0.812-1.0
200µg/ml	0.855±0.05	0.59±0.03	0.669±0.03	0.83±0.03	0.84±0.03
	0.777-0.94	0.549-0.62	0.615-0.71	0.79-0.86	0.798-0.9
2mg/ml	0.83±0.05	0.459±0.03	0.52±0.02	0.72±0.04	0.82±0.04
	0.752-0.91	0.42-0.48	0.49-0.55	0.66-0.78	0.76-0.88
20mg/ml	0.86±0.04	0.422±0.03	0.324±0.02	0.682±0.04	0.86±0.05
	0.77-0.92	0.375-0.48	0.295-0.36	0.63-0.75	0.78-0.93

When plant seedlings were treated with hydrophilic silica nanoparticles permeate from 0.05µm pore size membrane, a similar reduction in root elongation was observed, as displayed in Table 6.12, except for *C.sativus* and *Z.mays*. For *C.sativus*, the root elongation decreased from 18.9 to 17.4, (mm) when the concentrations of silica nanoparticles were increased from 20µg/ml to 2mg/ml, but rose slightly to 18.1 mm when the highest concentration of 20mg/ml was used. The R.R.G at this concentration for *C.sativus* remained much below unity; 0.86135, suggesting a reduction in root elongation compared to the Blank. For *Z.mays*, the inhibitory effects were evident but not to a considerable extent as the concentration was increased from 20µg/ml to 20mg/ml.

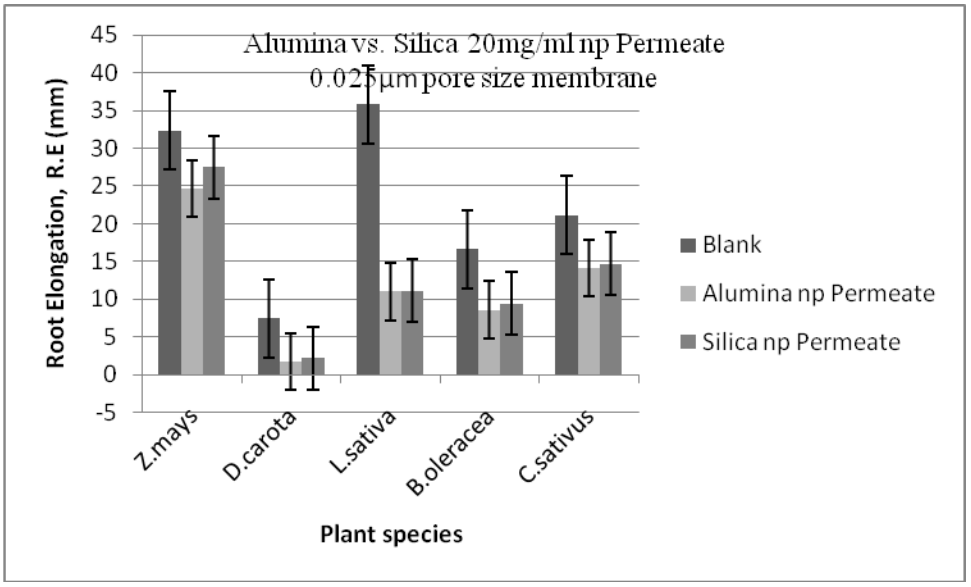

Figure 6.19 Plant species treated with Alumina nanoparticles permeate compared to those treated with hydrophilic Silica nanoparticles permeate using 0.025µm pore size membrane and 20mg/ml concentration of feed suspension.

The motivation for the use of Silica was primarily for comparison with Alumina nanoparticles; to this end a graphical representation of the phytotoxicity of both

nanoparticles together with their Blanks became obvious. Figures 6.19 and 6.20 compares both particles (Alumina and Silica) at their highest concentration of 20mg/ml, while using both the 0.025µm and 0.05µm pore size membranes. From these figures, it could be observed that Silica nanoparticles permeate from either membrane has less phytotoxic effect on plant roots than Alumina nanoparticles permeate as evidenced by a higher root elongation with respect to the later.

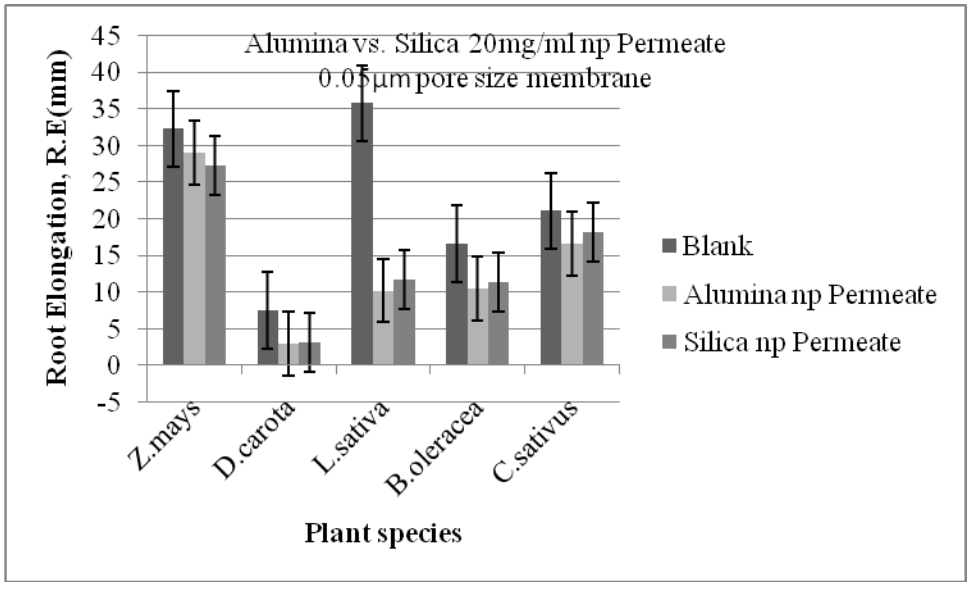

Figure 6.20 Plant species treated with Alumina nanoparticles permeate compared to those treated with hydrophilic Silica nanoparticles permeate using 0.05µm pore size membrane and 20mg/ml concentration of feed suspension.

An exclusion to this being *Z.mays* when the permeate from 0.05µm membrane was used, as displayed in Figure 6.20, where Alumina nanoparticles permeate seems to be less detrimental to root growth than Silica nanoparticles permeate. This may be because, for

Z.mays, there was the tendency to develop Aluminum resistance (from soluble Aluminum forms), since the 0.05µm pore size, in addition to thinner "cake-like" structure on the membrane surface gave room for more Alumina nanoparticles to pass through to the permeate region, and subsequently to the roots and hence the resistance.

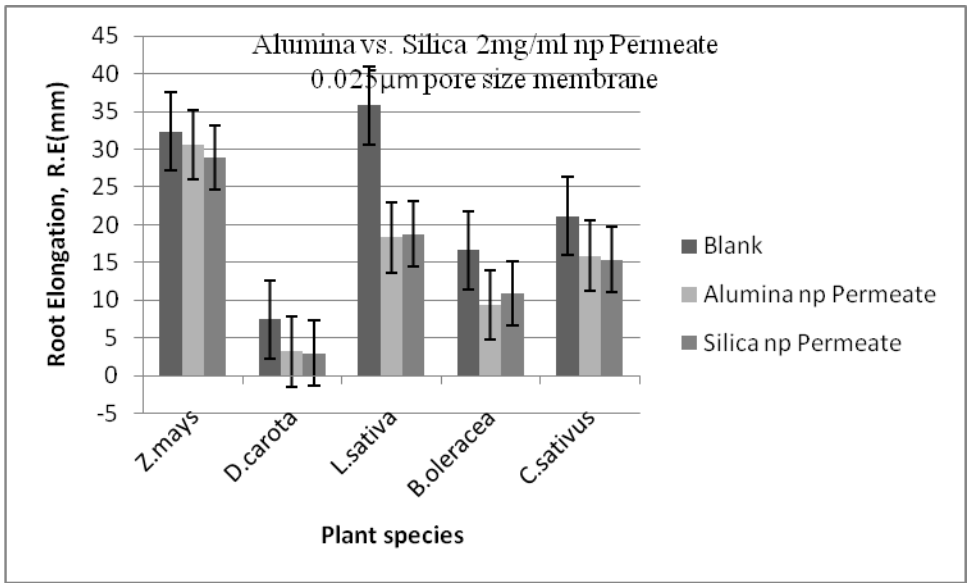

Figure 6.21 Plant species treated with Alumina nanoparticles permeate compared to those treated with hydrophilic Silica nanoparticles permeate using 0.025µm pore size membrane and 2mg/ml concentration of feed suspension.

The results also suggest that, apart from the size factor, the observed phytotoxic effect of Alumina nanoparticles permeate was associated with the very toxic nature of Al^{3+} species attached to Alumina nanoparticles in contrast to the hydrophilic Silica.

In Figure 6.23, the phytotoxic effect of hydrophilic Silica permeate on *Z.mays* seems to be similar to that of Alumina nanoparticles permeate at the concentration of 200µg/ml and the pore size of 0.025µm.

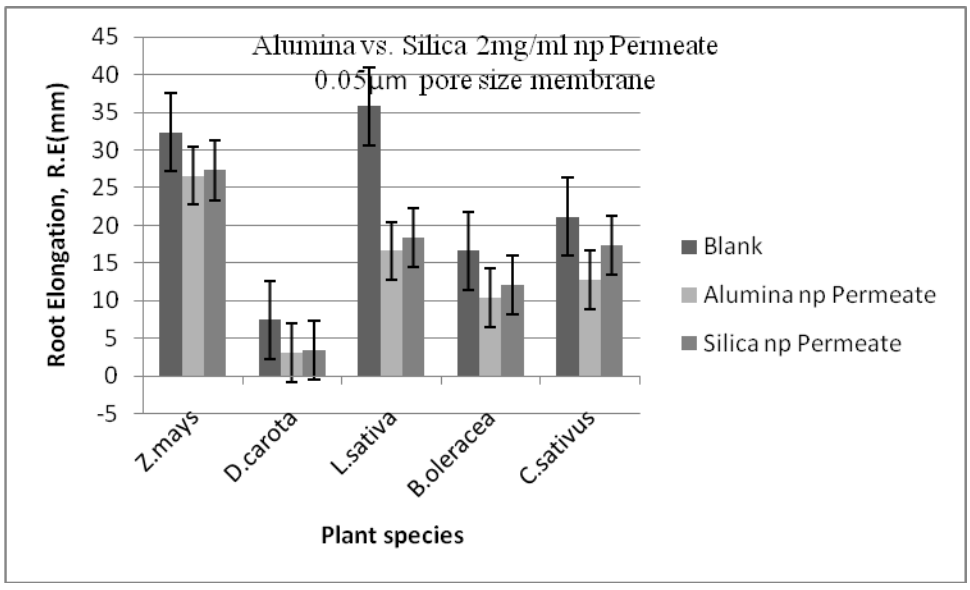

Figure 6.22 Plant species treated with Alumina nanoparticles permeate compared to those treated with hydrophilic Silica nanoparticles permeate using 0.05µm pore size membrane and 2mg/ml concentration of feed suspension.

Also at this critical concentration and pore size, *C.sativus* was at par in growth with both Alumina and hydrophilic Silica nanoparticles permeate, and *D.carota* experienced a noticeable root growth inhibitory effect by hydrophilic Silica nanoparticles permeate as shown in Figure 6.23. A similar effect was noticed at lower concentration of 20µg/ml, using both pore sizes, though to a lesser extent.

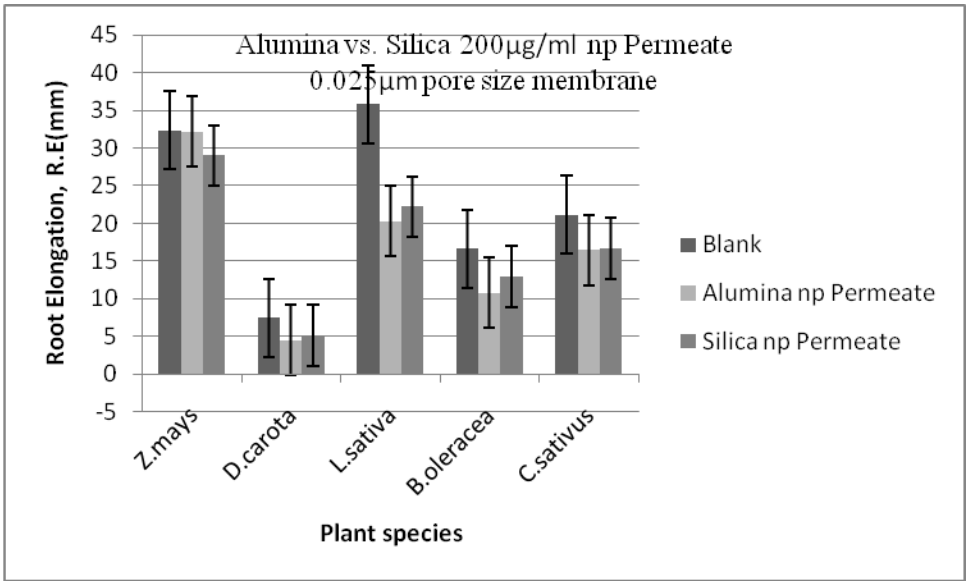

Figure 6.23 Plant species treated with Alumina nanoparticles permeate compared to those treated with hydrophilic Silica nanoparticles permeate using 0.025µm pore size membrane and 200µg/ml concentration of feed suspension.

Tables 6.13 and 6.14 contains the results of One-way ANOVA analysis of root elongation measurements from plant seedlings treated with hydrophilic Silica nanoparticles permeate using both the 0.025µm and 0.05µm pore sizes. From these results, the *p* values for root elongations obtained using the lowest concentration of 20µg/ml together with the 0.025µm and 0.05µm pore size membranes, are greater than 0.05, irrespective of the plant species. This suggests that at this concentration, there was no statistical difference between the root elongation from this concentration and that from the Blanks.

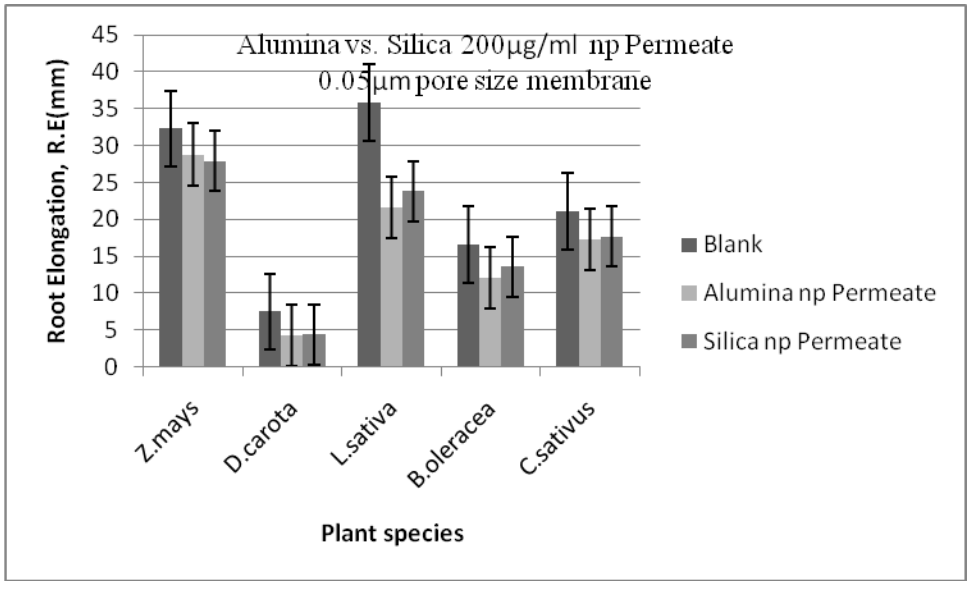

Figure 6.24 Plant species treated with Alumina nanoparticles permeate compared to those treated with hydrophilic Silica nanoparticles permeate using 0.05µm pore size membrane and 200µg/ml concentration of feed suspension.

In the same respect, the coefficient of determination, R^2, also approached unity at this concentration, with the highest recorded for *C.sativus* with a value of 0.97. When using the 0.05µm pore size membrane and the same least concentration of 20µg/ml, the p values for *C.sativus* and *D.carota* were 0.21 and 0.08, while their R^2 were 0.93 and 0.92 respectively, indicating a close correlation between the root elongations of treated specimen and Blanks, and further establishing the fact that ultra filtration was effective in removing the slight amount of particles contained in the 20µg/ml suspension without regard to the pore size.

As the concentration was increased from 20µg/ml to 20mg/ml, the *p* and R^2 decreases considerably with *p* values under 0.05 and reaching zero, while R^2 decreases to

0.39 for *C.*sativus at 20mg/ml and 0.025µm pore size. With the use of the larger pore size of 0.05µm and at the highest concentration of 20mg/ml, the p values for *C.sativus* and *D.carota* were 0.00 and 0.03 while their R^2 values were 0.52 and 0.36 respectively, thereby suggesting a statistical difference between the treated samples and the Blanks.

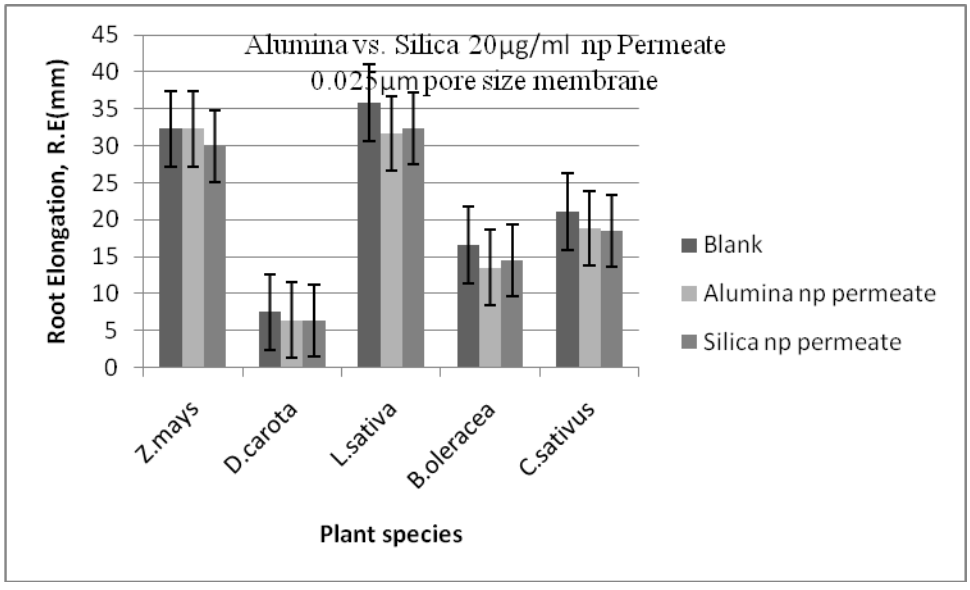

Figure 6.25 Plant species treated with Alumina nanoparticles permeate compared to those treated with hydrophilic Silica nanoparticles permeate using 0.025µm pore size membrane and 20µg/ml concentration of feed suspension.

This led to the rejection of the null hypothesis that there is no statistical difference between the R.Es of treated seedlings and their Blanks when the seedlings were exposed to hydrophilic Silica permeate of concentrations greater than 20µg/ml, without regard to the particle sizes used. In other words, hydrophilic Silica permeates are phytotoxic to plant root growth at high concentrations.

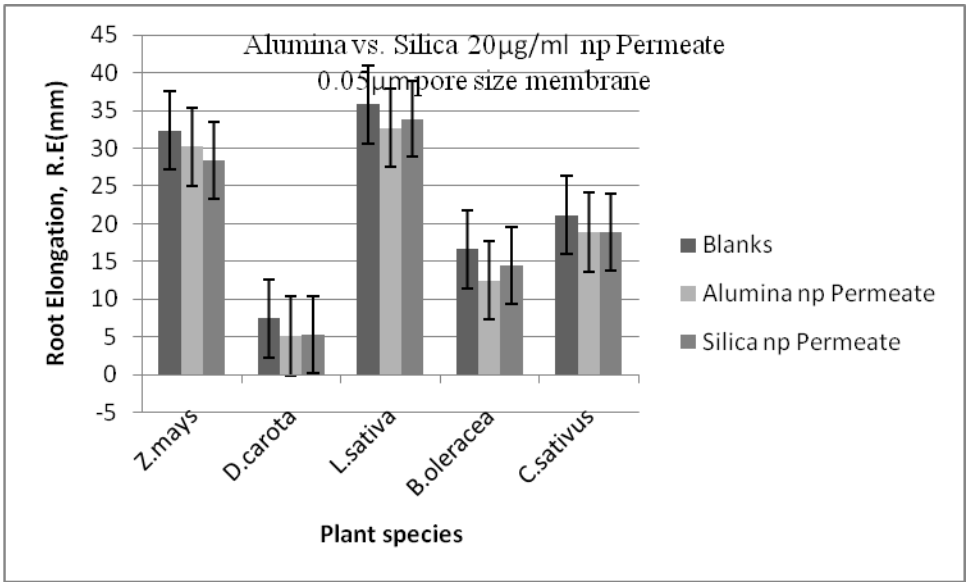

Figure 6.26 Plant species treated with Alumina nanoparticles permeate compared to those treated with hydrophilic Silica nanoparticles permeate using 0.05µm pore size membrane and 20µg/ml concentration of feed suspension.

Table 6.13 Statistical Analysis Results of the Root Elongation (RE) of Plant Seedlings Exposed to Silica Nanoparticles Permeate using **0.025µm** Pore Size Membrane for 72 hrs in the Dark at 25 ± 1ºC

Results from the *one-way ANOVA* procedure are reported as the value of *f*, *p*, and the coefficient of determination (R^2). Statistical difference is reported as *p* smaller than 0.05.

Conc.	*Z.mays*	*D.carota*	*L.sativa*	*B.oleracea*	*C.sativus*
20µg/ml	*p*=0.07 R^2= 0.83 *f=2.18*	p= 0.06 *R^2= 0.91* *f= 2.27*	p= 0.18 R^2= 0.89 *f= 1.59*	p= 0.09 *R^2= 0.90* *f= 2.02*	p=0.10 *R^2= 0.97* *f=1.96*
200µg/ml	*p= 0.01* *R^2=0.74* *f=3.77*	p= 0.01 R^2= 0.79 *f= 3.77*	p=0.04 R^2= 0.80 *f= 2.52*	p= 0.00 *R^2=0.73* *f=6.39*	p= 0.01 *R^2= 0.80* *f=3.77*
2mg/ml	*p=0.01* R^2= 0.74 *f=3.77*	p= 0.04 R^2= 0.70 *f= 2.52*	p= 0.03 R^2= 0.77 *f= 2.70*	p= 0.04 *R^2= 0.69* *f=2.52*	p= 0.03 *R^2= 0.70* *f=2.70*
20mg/ml	*p= 0.00* R^2= 0.57 *f=6.39*	p= 0.03 R^2= 0.62 *f= 2.70*	p= 0.00 R^2= 0.46 *f= 6.39*	p= 0.02 *R^2=0.51* *f=2.95*	p= 0.03 *R^2= 0.39* *f= 2.70*

Table 6.15 contains the statistical analysis results using the Student's t test that compares the phytotoxicity of Silica nanoparticles permeate from 0.025µm and 0.05µm pore size membranes, using all the four concentrations that had been used in this investigation. From this table, there seems to be a significant difference at low concentrations of 20µg/ml and 200µg/ml for *Z.mays,* with the p values of 0.01 and 0.00, but increased to 0.13 and 0.59 with increases in concentration to 2mg/ml and 20mg/ml respectively.

Table 6.14 Statistical Analysis Results of the Root Elongation (RE) of Plant Seedlings Exposed to Silica Nanoparticles Permeate using **0.05µm** Pore Size Membrane for 72 hrs in the Dark at 25 ± 1ºC

Results from the *one-way ANOVA* procedure are reported as the value of *f*, *p*, and the coefficient of determination (R^2). Statistical difference is reported as *p* smaller than 0.05.

Conc.	*Z.mays*	*D.carota*	*L.sativa*	*B.oleracea*	*C.sativus*
20µg/ml	*p*=0.06 R^2= 0.90 *f=2.27*	p= 0.05 *R^2= 0.87* *f= 2.39*	p= 0.08 R^2= 0.92 *f= 2.1*	p= 0.13 *R^2= 0.73* *f= 1.79*	p=0.21 *R^2= 0.93* *f=1.49*
200µg/ml	*p= 0.01* *R^2=0.79* *f=3.77*	p= 0.03 R^2= 0.81 *f= 2.70*	p=0.02 R^2= 0.90 *f= 2.95*	p= 0.02 *R^2=0.71* *f=2.95*	p= 0.01 *R^2= 0.81* *f=3.77*
2mg/ml	*p=0.01* R^2= 0.64 *f=3.77*	p= 0.04 R^2= 0.75 *f= 2.52*	p= 0.05 R^2= 0.88 *f= 2.39*	p= 0.00 *R^2= 0.61* *f=6.39*	p= 0.03 *R^2= 0.76* *f=2.70*
20mg/ml	*p= 0.00* R^2= 0.57 *f=6.39*	p= 0.03 R^2= 0.36 *f= 2.70*	p= 0.00 R^2= 0.6 *f= 6.39*	p= 0.02 *R^2=0.3* *f=2.95*	p= 0.00 *R^2= 0.52* *f= 6.39*

For *D.carota* and *C.sativus*, there was statistical difference between the two samples irrespective of the concentration used; their p values were less than 0.05. A slightly different set of results were obtained when Silica nanoparticles permeate from both pore sizes were used to treat *L.sativa* and *B.oleracea*, for these plant species, significant difference only occurs at high concentrations; 20mg/ml, for *L.sativa*, with a p value of 0.02, and 2mg/ml, 20mg/ml for *B.oleracea*, with p values of 0.004 and 0.00.

Table 6.15 Statistical Analysis Results of the Root Elongation (RE) of Plant Seedlings Exposed to Silica Nanoparticles Permeate using both 0.025µm and 0.05µm Membrane for 72 hrs in the Dark at 25 ± 1˚C (Student's t of 0.025µm vs. 0.05µm)

Results from the *Student's t*-test are reported as the value of *t* and the value of probability of the result assuming the null hypothesis (*p*). Statistical significance is reported when p is less than 0.05.

Conc.	*Z.mays*	*D.carota*	*L.sativa*	*B.oleracea*	*C.sativus*
20µg/ml	t= 3.04 p= 0.01	t= 14.1 p= 0.00	t= 0.69 p= 0.50	t= 0.32 p= 0.75	t= 2.36 p= 0.03
200µg/ml	t= 3.73 p = 0.00	t= 6.01 p= 0.00	t=1.86 p= 0.08	t= 1.26 p= 0.22	t= 3.42 p= 0.003
2mg/ml	t=1.57 p= 0.13	t=5.97 p= 0.00	t= 1.69 p= 0.11	t= 3.3 p= 0.004	t= 6.15 p= 0.00
20mg/ml	t= 0.55 p= 0.59	t= 9.75 p= 0.00	t= 2.45 p= 0.02	t= 5.30 p= 0.00	t=9.8 p= 0.00

These results suggest that particles size do play a major role in the phytotoxicity of Silica nanoparticles and could be the only source to inhibitory root growth for this nanomaterial.

Conclusion

Fumed hydrophilic silica nanoparticles permeate is more phytotoxic to plants species at concentrations higher than 20μg/ml, irrespective of the particle size. When silica nanoparticles permeate from the membranes of the two pore sizes and four concentrations were compared to those of alumina nanoparticles permeate from the same pore sizes and concentrations, the results suggested that alumina nanoparticles are more phytotoxic than silica nanoparticles. Furthermore, the phytotoxicity of alumina nanoparticles permeate is more size specific than that from hydrophilic silica nanoparticles permeate.

CHAPTER 7

SUMMARY AND CONCLUSIONS

In this dissertation, the phytotoxic effects of two types of nanoparticles; Alumina and fumed hydrophilic Silica, were studied, with primary emphasis on Alumina nanoparticles. During the course of investigation, it however became necessary to also study the phytotoxicity of Aluminum standard solution and its dilutions and make a comparison between it and that from Alumina nanoparticles suspension, using the highest concentration of 20mg/ml Alumina nanoparticles suspension.

The concentrations used in this work were; 20mg/ml, 2mg/ml, 200μg/ml and 20μg/ml, they were the same concentrations used by the previous researchers, who came up with the conclusion; that Alumina nanoparticles are phytotoxic to plant species. Similarly, plant species that were used; *Z.mays, D.carota, B.oleracea, C.sativus* and *L.sativa* were also the same utilized by the past investigators and represents those recommended by the EPA, for the study of phytotoxicity. Additionally, both nanoparticles were obtained from the same sources; Alumina nanoparticles from Degussa and Silica nanoparticles from Cabolt Inc. Though, the materials, and in some cases, the experimental methods were similar, no attempt was made to repeat, replicate or duplicate past investigations by this group but rather efforts were made to further investigate the phytotoxicity of Alumina nanoparticles and at some point, that of fumed hydrophilic Silica, as was reported by them, using different approaches.

These approaches included; the investigation of surface characteristics of Alumina nanoparticles through the use of its supernatants, comparing the phytotoxicity of the supernatants to that from the suspension, determining the soluble Aluminum content of the Alumina nanoparticles supernatants and hence the suspension through the use of Morin, particle size investigation with the aid of ultra filtration using hydrophilic membranes of two pore sizes; 0.025µm and 0.05µm, obtained from Millipore Inc., and finally, the particle size study being extended to fumed hydrophilic Silica for comparison purposes, while using the same pore sizes and concentrations as the Alumina nanoparticles.

Consequently, the aforementioned approaches led to the following conclusions;

1. Alumina nanoparticles supernatants are phytotoxic to plant species, especially at higher concentrations. *Z.mays* was less affected by Alumina nanoparticles supernatants due to phytotoxic resistance from root exudates apparently induced by the presence of soluble forms of aluminum.

2. Alumina nanoparticles suspension is also phytotoxic to plants and there is a statistical difference between the phytotoxicity from the suspension and that from the supernatants. This difference is diminished when the test species is *D.carota*.

3. There is a presence of one or more soluble forms of Aluminum in the supernatant liquid obtained from centrifuging Alumina nanoparticles which becomes obvious at higher concentrations.

4. Aluminum standard solution (0.0371M) and its dilutions are phytotoxic to plant species and there is no statistical difference between the level of toxic effects from 20mg/ml Alumina nanoparticles suspension and undiluted Aluminum standard solution, rather difference begins to appear at higher dilutions of the Aluminum standard solution. Such statistical difference does not exist when *Z.mays* is used as test species, irrespective of the dilution with the set of dilutions studied.

5. Permeate from the least concentration of 20µg/ml Alumina nanoparticles suspension and from 0.025µm pore size membrane is less phytotoxic compared to permeate(s) from higher concentrations but from the same pore size of 0.025µm. This appears to be as a result of increased presence of particles in the permeate with increased concentration.

6. Permeate from the larger pore size of 0.05µm is less phytotoxic when compared to 0.025µm pore size, especially as the concentration is increased. This is likely a result of aggloromeration of particles; 0.05µm or less in size, found in the permeate, and the inability of the formed agglomerates to penetrate plant cell walls due to their larger sizes. The agglomerates were formed as a result of greater presence of particles in the permeate due to increased concentration and the use of larger pore size ultrafilters. During this investigation, an attempt to reduce agglomeration was done through sonication immediately after filtration and application to plant seedlings. With the least concentration of 20µg/ml, there was no statistical difference in growth compared to when the plants were exposed only to the Blanks. Stated differently, there appears to be penetration of small alumina particles into plant root cells that as a result interfere with cell growth.

7. Fumed hydrophilic Silica permeates are more phytotoxic at higher concentrations than at the least concentration of 20µg/ml, irrespective of the particle size within the nanoparticle size range. Comparing Alumina nanoparticles permeate to fumed hydrophilic Silica permeate, results in the conclusion that the former is more phytotoxic than the later, regardless of the particle size. Furthermore, phytotoxicity from Alumina nanoparticles permeate is more size specific than Silica nanoparticles permeate.

Hence in answering the questions raised at the beginning of this dissertation;

Alumina nanoparticles were found to be phytotoxic in part because of the presence of soluble forms of aluminum on the surfaces or/ and in the nanoparticles matrix, especially at the highest concentration of 20mg/ml as discovered in chapter five. The sources of this phytotoxicity include; surface constituents containing aluminum, which was obtained by centrifugation, as was shown in chapters four and five. Additionally, particle size of

alumina was also found to be related to phytotoxicity; as established in chapter six, where permeate from 0.025μm was found to be more phytotoxic than those from the larger pore size of 0.05μm suggesting the movement of small alumina particles into plant root cells. The presence of soluble forms of aluminum is likely the reason why alumina nanoparticles are more phytotoxic than silica nanoparticles with same particle size.

The mechanism of phytotoxicity therefore involves the penetration of plant cell walls by nano-sized particles of alumina where they can either reside in the apoplast, thereby impeding activities that aid cell division, hence growth or within the cell which might result in DNA damage.

Based on the foregoing, it could be concluded that the observed phytotoxicity from Alumina nanoparticles is primarily from the nanometer sized particles of Alumina with a contribution from residual Aluminum, especially at high concentration, while that of Silica is attributed mainly to the particle size.

If these two factors are carefully controlled, the danger posed by these particulates to the survival and growth of plant species and to the environment at large could be minimized.

APPENDIX A

EXAMPLE OF THE PROCEDURE FOR THE CALCULATION OF ONE-WAY ANOVA

The following example illustrates the method used in *One-way Anova* calculations using R.E values obtained during phytotoxicity investigations.

The data used in this example are from the study of the 72-hr exposure of Aluminum solution (1|1000 dilution) on *L.sativa* seedlings, as reported in Table 5.1.

Blank. Group 1.

Before Exposure (mm)	After Exposure (mm)	R.E (mm)
15.2	50.8	35.6
14.1	63.3	49.2
12.7	62.8	50.1
17.4	70.0	52.6
10.1	65.4	55.3
14.8	75.1	60.3
11.2	72.5	61.3
16.0	79.1	63.1
10.0	76.2	66.2
13.0	63.9	50.9
		Average R.E = **54.5**

Blank Group 2

Before Exposure (mm)	After Exposure (mm)	R.E (mm)
20.7	68.0	47.3
16.3	68.1	51.8
15.2	69.8	54.6
18.8	74.9	56.1
13.3	76.5	63.2
22.0	91.1	69.1
16.3	87.9	71.6
18.1	92.3	74.2
14.8	89.3	75.2
16.0	89.3	81.6

Average R.E = **64.**

Blank Group 3

Before Exposure (mm)	After Exposure (mm)	R.E (mm)
13.0	62.7	49.7
12.5	65.5	53.0
23.6	79.7	56.1
20.5	81.8	61.3
17.4	80.2	62.8
10.7	74.6	63.9
18.3	85.2	66.9
14.8	89.7	74.9
21.6	99.2	77.6
19.1	107.2	88.1

Average R.E = **65.4**

Average of the three groups = 61.467. This value was used to calculate the Relative Root Growth, RRGs from the exposed samples.

Samples exposed to 1|1000 dilution of Aluminum solution:

Group 1

Before Exposure (mm)	After Exposure (mm)	R.E (mm)	R.R.G
18.0	58.2	40.2	0.6540094685
16.7	59.3	42.6	0.6930548099
18.1	64.4	46.3	0.7532497112
15.0	63.7	48.7	0.7922950526
24.0	73.1	49.1	0.7988026095
22.6	76.7	50.8	0.8264597264
20.6	76.7	56.1	0.9126848553
21.0	78.1	57.1	0.9289537475
20.3	79.9	59.6	0.9696259782
19.6	80.6	61.0	0.9924024273

Average R.E = **51.2** Average R.R.G = **0.8321538386**

Group 2.

Before Exposure (mm)	After Exposure (mm)	R.E (mm)	R.R.G
15.0	59.9	44.9	0.7304732621
20.3	68.9	48.6	0.7906681634
24.1	73.4	49.3	0.802056388
20.6	70.7	50.1	0.8150715018
19.1	70.3	51.2	0.8329672833
24.0	76.6	52.6	0.8557437324
16.6	70.7	54.1	0.8801470708
21.1	77.3	56.2	0.9143117445
18.0	80.1	62.1	1.010298209
23.7	73.9	50.2	0.816698391
	Average R.E = **51.9**	Average R.E = **0.7631737355**	

Group 3.

Before Exposure (mm)	After Exposure (mm)	R.E (mm)	R.R.G
20.4	53.0	32.6	0.5303658874
20.9	60.7	39.8	0.5986952348
14.0	60.3	46.3	0.7532497112
20.8	70.0	49.2	0.8004294988
15.6	65.7	50.1	0.8150715018
23.7	73.3	50.2	0.816698391
15.1	67.4	52.3	0.8508630647
24.3	77.1	52.8	0.8589975109
19.7	73.8	54.1	0.8801470708
21.5	81.7	60.2	0.9793873135
	Average R.E = **48.8**	Average R.R.G = **0.7883905185**	

Statistical analysis procedure using One-way Anova for treated samples (comparing samples within groups);

Sample exposed to 1|1000 Aluminum dilution;

$$SST = \sum_{i=1}^{3} n_i (\bar{y}_i - \bar{y})^2$$

$$SSE = \sum_{i=1}^{3} \sum_{j=1}^{n_i} (y_{ij} - \bar{y}_i)^2$$

$n_1 = n_2 = n_3 = 10$, $\bar{y}_1 = 51.2$, $\bar{y}_2 = 51.9$, $\bar{y}_3 = 48.8$, and $\bar{y} = 50.633$,

$SST = 52.866$, $SSE = 1196.14$.

Calculation of *MST* and *MSE*;

MST= *SST/DFT*, Where *DFT = k −1* *k being* the number of groups.

So, *MST* = 26.433, Since, *DFT*= 2

MSE = *SSE/DFE* *DFE*= $(n_{1+} n_{2+} n_3) - k$,

Therefore, MSE = 44.3014, with *DFE* = 27 (30−3).

Calculation of F;

F = *MST/MSE*

= 26.433/44.3014

F = 0.5967

For *DFT* of 2 and *DFE* of 27, the tabular(http://faculty.vassar.edu/lowry/PDF/Ftable.pdf, 2009.) critical F value is 3.354, since the calculated F value is much less than the critical F value, therefore the three groups are not statistically different.

The *P* value was then calculated using the *DFT, DFE* and the calculated F from the website;

(graphpad.com/quickcalcs/PValue1.cfm, 2009).

With *DFT* = 2, *DFE* = 27 and F = 0.5967, *P* = 0.558.

Since the calculated *P* is greater than 0.05, therefore, there is no difference between the three groups treated with 1|1000 Aluminum dilution.

Table A.1 Anova Summary for the Treated Samples;

Source	SS	DF	MS	F
Treatment	52.866	2	26.43	0.597
Error	1196.14	27	44.301	
Total	1249.01	29		

Anova procedure for all six groups of samples, comparing treated samples with the Blank;

$$SST = \sum_{i=1}^{6} n_i (\bar{y}_i - \bar{y})^2$$

$$SSE = \sum_{i=1}^{6} \sum_{j=1}^{n_i} (y_{ij} - \bar{y}_i)^2$$

$n_1 = n_2 = n_3 = n_4 = n_5 = n_6 = 10$, $\bar{y}_1 = 54.5$, $\bar{y}_2 = 64.5$, $\bar{y}_3 = 65.4$, and $\bar{y} = 56.05$
$\bar{y}_4 = 51.2$, $\bar{y}_5 = 51.9$, $\bar{y}_6 = 48.8$.

Therefore, $SST = 2545.35$ and $SSE = 4377.88$
$DFT = k - 1 = 6 - 1 = 5$ $DFE = (n_1 + n_2 + n_3 + n_4 + n_5 + n_6) - k = 54$

Calculating the MST and MSE;

$MST = 2545.35/5 = 509.07$ $MSE = 4377.88/54 = 81.07$

Calculating F;
$F = MST/MSE = 509.07/81.07 = 6.279.$

Again, from the website; http://faculty.vassar.edu/lowry/PDF/Ftable.pdf, 2009, using 5 as the *DFT* and 54 as *DFE* the tabular critical F was found to be 2.38. Since the calculated F is greater than the tabular critical F, the six groups are statistically different.

The *P* value was found by using the same DFT, DFE and the calculated F. From the website;

(graphpad.com/quickcalcs/PValue1.cfm, 2009), the *P* value is found to be 0.0001 but approximated to 0.000 as reported in Table 5.1.

Table A.2 Anova Summary for both Treated and Blank Samples.

Source	SS	DF	MS	F
Treatment	2545.35	5	509.07	6.279
Error	4377.88	54	81.07	
Total	6923.23	59		

APPENDIX B

PARTICLES COUNTING RESULTS

Tables and Figures B.1 to B.20 shows the results of particle count analysis done on Alumina nanoparticles supernatants and Alumina and Silica nanoparticles permeate.

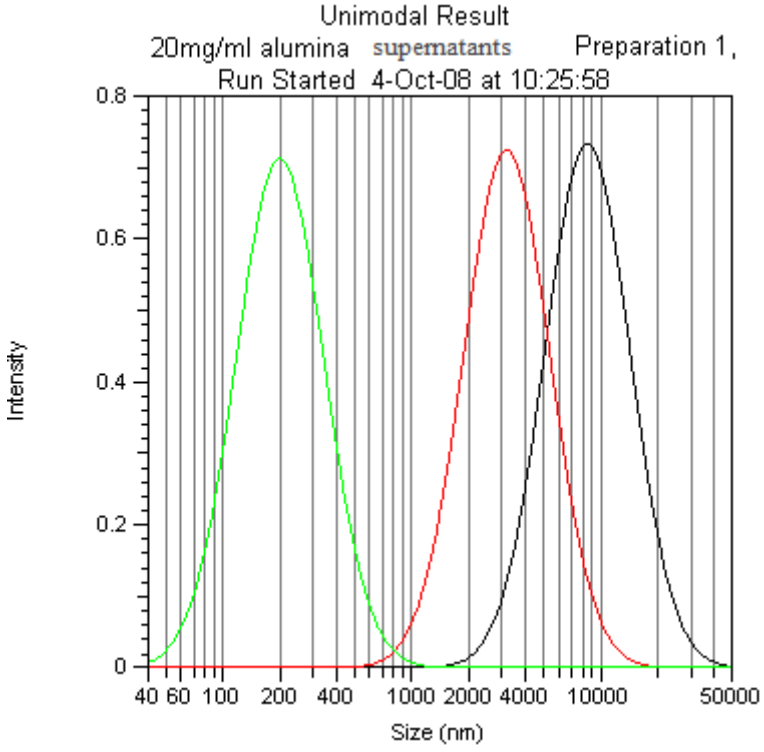

Black line is for 23 degrees
Red line is for 62.6 degrees
Green line is for 90 degrees.

Figure B.1 Particle count analysis result of 20mg/ml alumina nanoparticles supernatants.

Sample:	20mg/ml alumina supernatants	Preparation:	Preparation 1
Estimated Size:	Unknown	Diluent:	Water
Run Parameters:			
Temperature:	20.0°C	Refractive Index:	1.333
Date:	04-Oct-08	Viscosity:	1.002 centipoi
Time:	10:25:58 AM		

Angle	Mean Dia. (nm)	Std. Dev. (nm)	Polydispersity Index	Run Time (sec)
23.0°	9284.5	Not enough data	0.902	918
62.6°	3495.9	Broad	1.058	306
90.0°	221.9	Broad	1.370	180
Run Avg:	4334.1	1927.2	1.110	

Table B.1 Results of particle count analysis of 20mg/ml alumina nanoparticles supernatants.

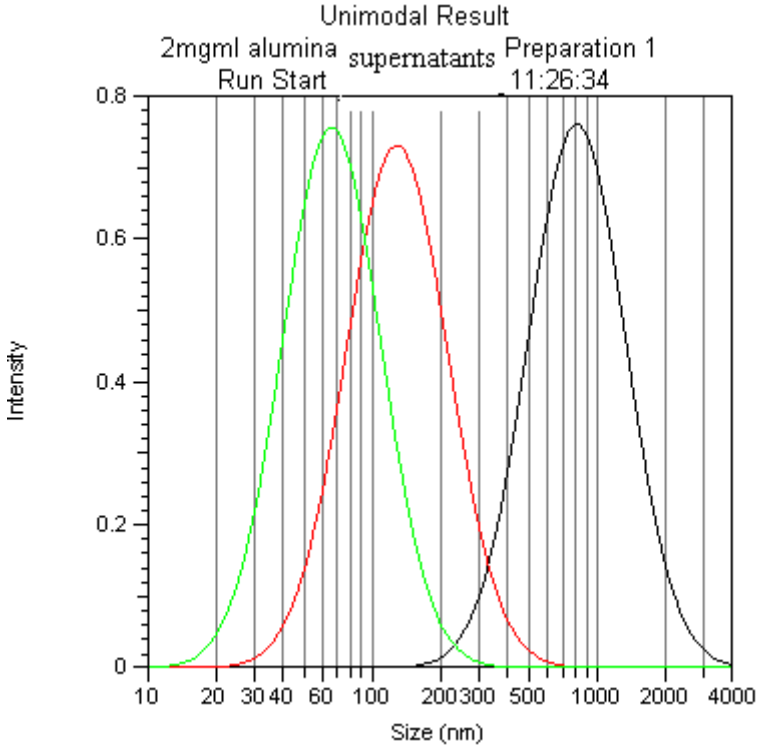

Black line is for 23 degrees
Red line is for 62.6 degrees
Green line is for 90 degrees.

Figure B.2 Particle count analysis result of 2mg/ml alumina nanoparticles supernatants.

Sample: 2mg/ml Alumina nanoparticles supernatants
Estimated Size:
Run Parameters
Temperature:
Date:
Time:

Preparation: Preparation 1
Diluent: Water

Refractive Index: 1.333
Viscosity: 1.002 centipoise

Angle	Mean Dia. (nm)	Std. Dev. (nm)	Polydispersity Index	Run Time (sec)
23.0°	874.4	Broad	0.620	918
62.6°	140.6	Broad	0.938	306
90.0°	71.1	Broad	0.656	180
Run Avg:	362.0	153.9	0.738	

Table B.2 Results of particle count analysis of 2mg/ml of alumina nanoparticles supernatants.

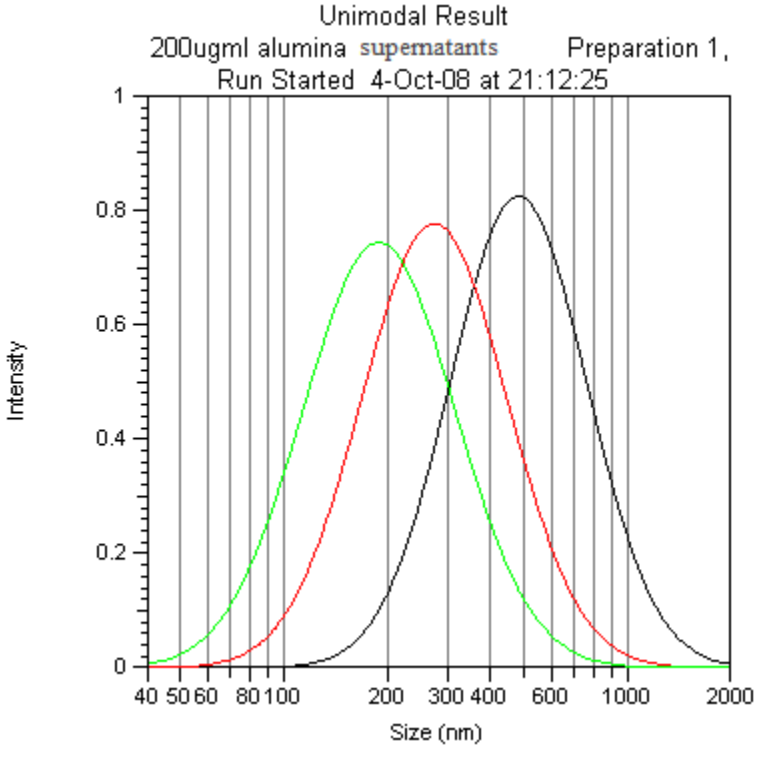

Black line is for 23 degrees
Red line is for 62.6 degrees
Green line is for 90 degrees.

Figure B.3 Particle count analysis result of 200µg/ml alumina nanoparticles supernatants.

Sample:	200ugml alumina supernatants	Preparation:	Preparation 1
Estimated Size:	Unknown	Diluent:	Water
Run Parameters:			
Temperature:	20.0°C	Refractive Index:	1.333
Date:	04-Oct-08	Viscosity:	1.002 centipoi
Time:	09:12:25 PM		

Angle	Mean Dia. (nm)	Std. Dev. (nm)	Polydispersity Index	Run Time (sec)
23.0°	506.0	Broad	0.348	918
62.6°	292.8	Broad	0.517	306
90.0°	205.2	Broad	0.763	180
Run Avg:	334.7	134.1	0.543	

Table B.3 Results of particle count analysis of 200µg/ml of alumina nanoparticles supernatants.

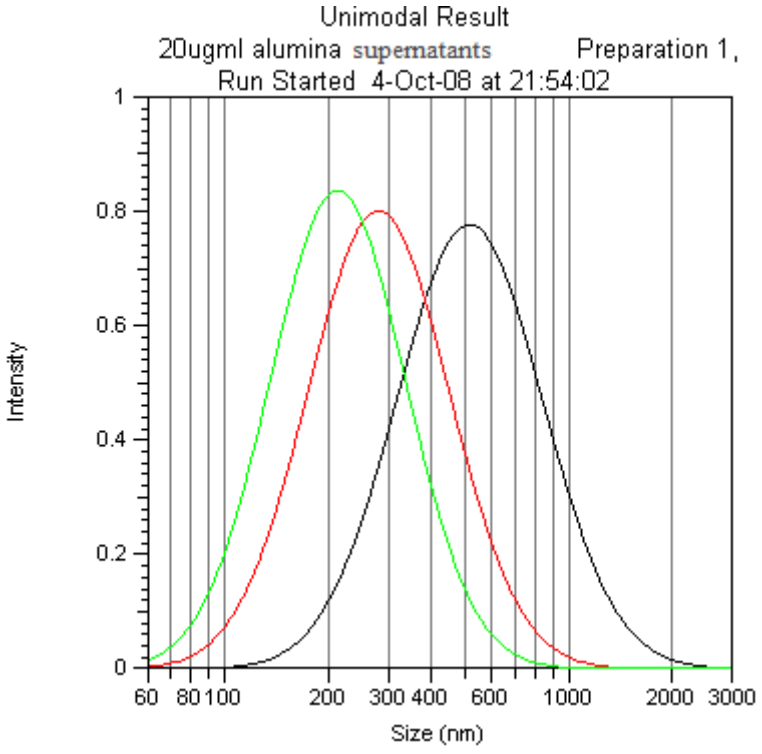

Black line is for 23 degrees
Red line is for 62.6 degrees
Green line is for 90 degrees.

Figure B.4 Particle count analysis result of 20µg/ml alumina nanoparticles supernatants.

Sample:	20ugml alumina supernatants	Preparation:	Preparation 1
Estimated Size:	Unknown	Diluent:	Water
Run Parameters:			
Temperature:	20.0°C	Refractive Index:	1.333
Date:	04-Oct-08	Viscosity:	1.002 centipois
Time:	09:54:02 PM		

Angle	Mean Dia. (nm)	Std. Dev. (nm)	Polydispersity Index	Run Time (sec)
23.0°	552.0	Broad	0.516	918
62.6°	297.6	Broad	0.414	306
90.0°	224.0	83.9	0.321	180
Run Avg:	357.9	142.6	0.417	

Table B.4 Results of particle count analysis of 20µg/ml of alumina nanoparticles supernatants.

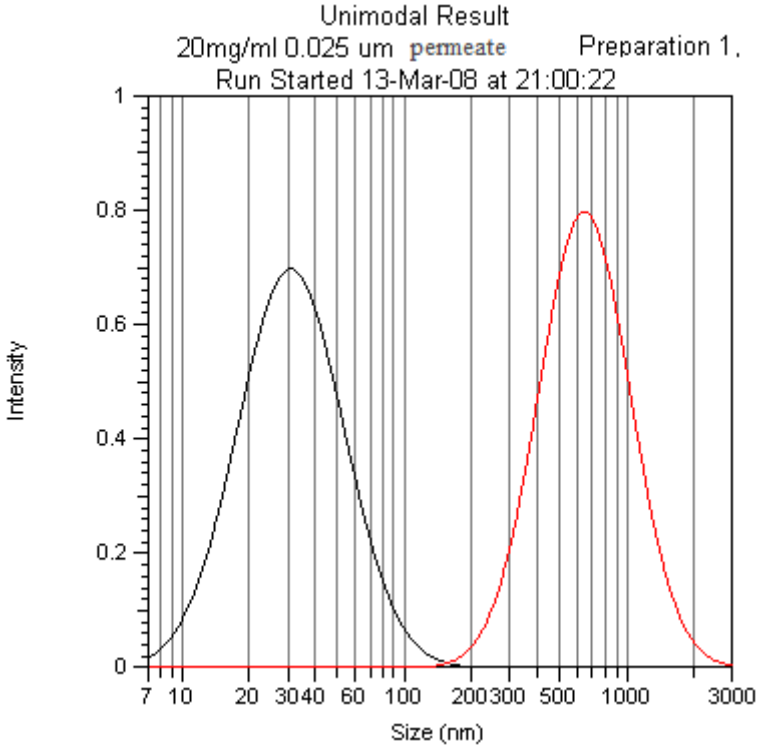

Black line is for 23 degrees
Red line is for 62.6 degrees

Figure B.5 Particle count analysis result of 20mg/ml, 0.025µm membrane alumina nanoparticles permeate.

Sample:	20mg/ml 0.025 um	Preparation:	Preparation 1
Estimated Size:	Unknown permeate	Diluent:	Water
Run Parameters:			
Temperature:	20.0°C	Refractive Index:	1.333
Date:	13-Mar-08	Viscosity:	1.002 centipoise
Time:	09:00:22 PM		

Angle	Mean Dia. (nm)	Std. Dev. (nm)	Polydispersity Index	Run Time (sec)
23.0°	34.4	Broad	2.058	918
62.6°	684.8	Broad	0.430	306
90.0°	-26.9	n/a	-1.132	180
Run Avg:	230.8	92.1	0.452	

Table B.5 Particle count analysis result of 20mg/ml, 0.025µm membrane alumina nanoparticles permeate.

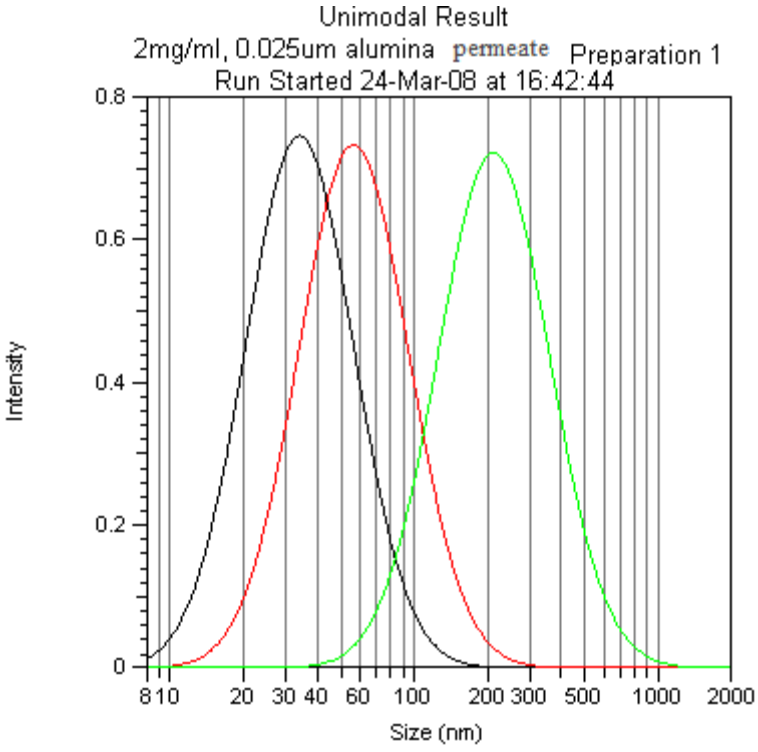

Black line is for 23 degrees
Red line is for 62.6 degrees
Green line is for 90 degrees.

Figure B.6 Particle count analysis result of 2mg/ml, 0.025µm membrane alumina nanoparticles permeate.

Sample: 2mg/ml, 0.025um alumina permeate
Estimated Size: Unknown
Preparation: Preparation
Diluent: Water
Run Parameters:
Temperature: 20.0°C
Refractive Index: 1.333
Date: 24-Mar-08
Viscosity: 1.002 centip
Time: 04:42:44 PM

Angle	Mean Dia. (nm)	Std. Dev. (nm)	Polydispersity Index	Run Time (sec)
23.0°	36.8	Broad	0.756	918
62.6°	61.6	Broad	0.904	306
90.0°	232.2	Broad	1.115	180
Run Avg:	110.2	49.4	0.925	

Table B.6 Particle count analysis result of 2mg/ml, 0.025µm membrane alumina nanoparticles permeate

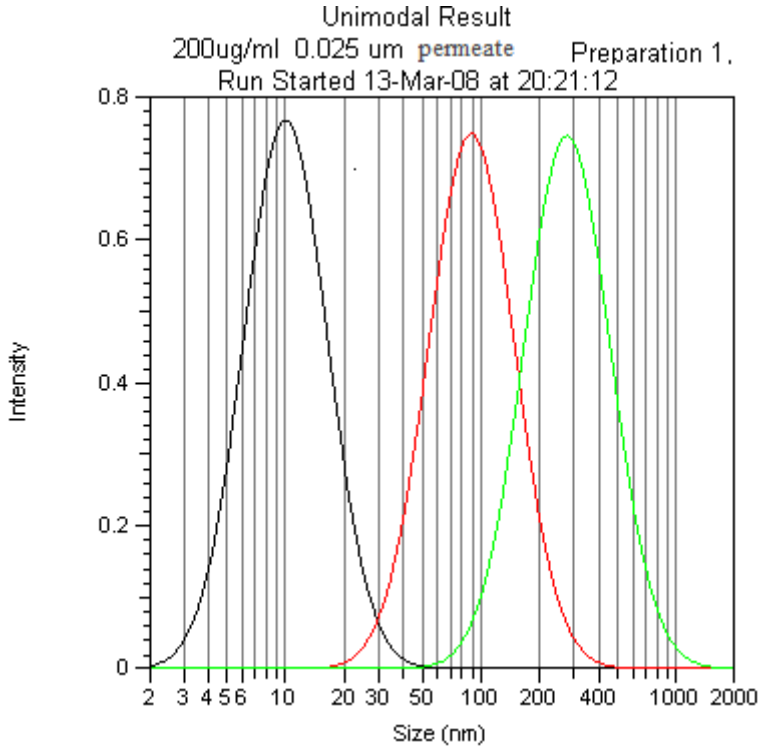

Black line is for 23 degrees
Red line is for 62.6 degrees
Green line is for 90 degrees.

Figure B.7 Particle count analysis result of 200µg/ml, 0.025µm membrane alumina nanoparticles permeate.

Sample:	200ug/ml 0.025 um	Preparation:	Preparation 1
Estimated Size:	Unknown permeate	Diluent:	Water
Run Parameters:			
Temperature:	20.0°C	Refractive Index:	1.333
Date:	13-Mar-08	Viscosity:	1.002 centipoise
Time:	08:21:12 PM		

Angle	Mean Dia. (nm)	Std. Dev. (nm)	Polydispersity Index	Run Time (sec)
23.0°	10.7	Broad	0.575	918
62.6°	96.9	Broad	0.720	306
90.0°	299.7	Broad	0.751	180
Run Avg:	135.8	58.7	0.682	

Table B.7 Particle count analysis result of 200µg/ml, 0.025µm membrane alumina nanoparticles permeate.

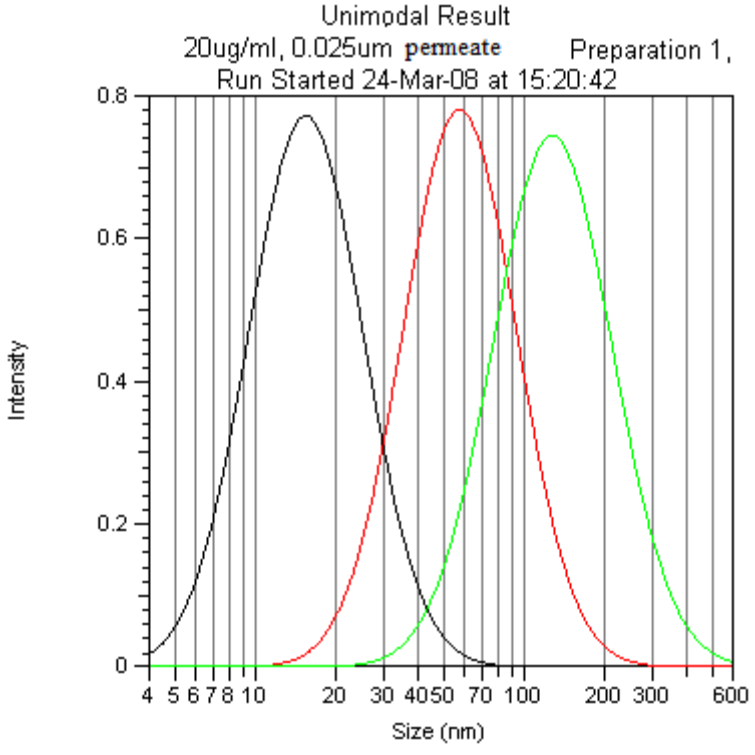

Black line is for 23 degrees
Red line is for 62.6 degrees
Green line is for 90 degrees.

Figure B.8 Particle count analysis result of 20µg/ml, 0.025µm membrane alumina nanoparticles permeate.

Sample:	20ug/ml, 0.025um	Preparation:	Preparation 1
Estimated Size:	Unknown permeate	Diluent:	Water
Run Parameters:			
Temperature:	20.0°C	Refractive Index:	1.333
Date:	24-Mar-08	Viscosity:	1.002 centipoise
Time:	03:20:42 PM		

Angle	Mean Dia. (nm)	Std. Dev. (nm)	Polydispersity Index	Run Time (sec)
23.0°	16.5	Broad	0.546	918
62.6°	61.3	Broad	0.500	306
90.0°	137.7	Broad	0.762	180
Run Avg:	71.8	30.5	0.603	

Table B.8 Particle count analysis result of 20µg/ml, 0.025µm membrane alumina nanoparticles permeate.

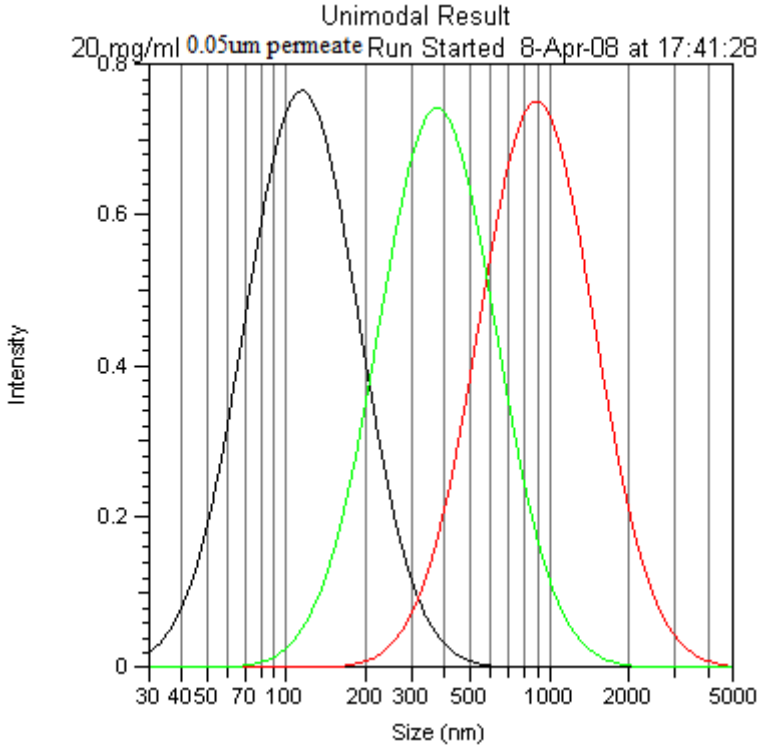

Black line is for 23 degrees
Red line is for 62.6 degrees
Green line is for 90 degrees.

Figure B.9 Particle count analysis result of 20mg/ml, 0.05µm membrane alumina nanoparticles permeate.

Sample:	20 mg/ml	Preparation:	Preparation 1
Estimated Size:	Unknown	Diluent:	Water
Run Parameters:	0.05um permeate		
Temperature:	20.0°C	Refractive Index:	1.333
Date:	08-Apr-08	Viscosity:	1.002 centipoise
Time:	05:41:28 PM		

Angle	Mean Dia. (nm)	Std. Dev. (nm)	Polydispersity Index	Run Time (sec)
23.0°	123.3	Broad	0.593	918
62.6°	966.0	Broad	0.703	306
90.0°	406.5	Broad	0.793	180
Run Avg:	498.6	214.6	0.696	

Table B.9 Particle count analysis result of 20mg/ml, 0.05µm membrane alumina nanoparticles permeate.

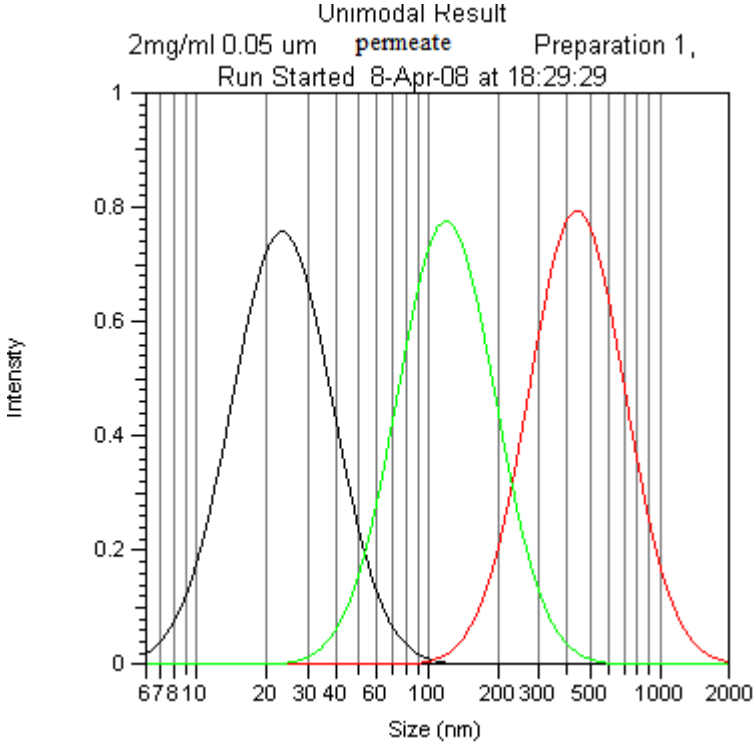

Black line is for 23 degrees
Red line is for 62.6 degrees
Green line is for 90 degrees.

Figure B.10 Particle count analysis result of 2mg/ml, 0.05µm membrane alumina nanoparticles permeate.

Sample:	2mg/ml 0.05 um permeate	Preparation:	Preparation
Estimated Size:	Unknown	Diluent:	Water
Run Parameters:			
Temperature:	20.0°C	Refractive Index:	1.333
Date:	08-Apr-08	Viscosity:	1.002 cent
Time:	06:29:29 PM		

Angle	Mean Dia. (nm)	Std. Dev. (nm)	Polydispersity Index	Run Time (sec)
23.0°	25.2	Broad	0.641	918
62.6°	464.8	Broad	0.441	306
90.0°	127.7	Broad	0.524	180
Run Avg:	205.9	83.0	0.535	

Table B.10 Particle count analysis result of 2mg/ml, 0.05µm membrane alumina nanoparticles permeate.

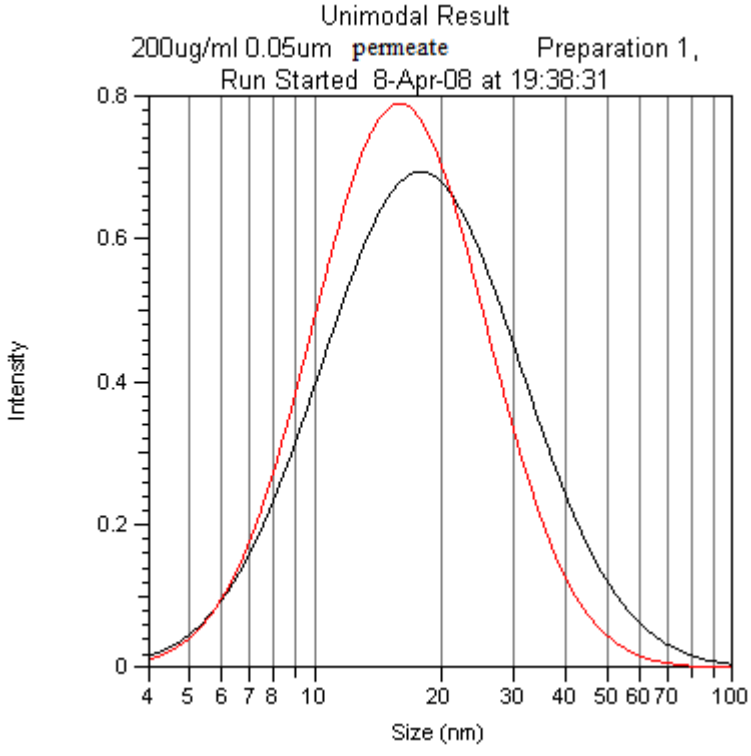

Black line-23 degrees
Red line - 90 degrees

Figure B.11 Particle count analysis result of 200µg/ml, 0.05µm membrane alumina nanoparticles permeate.

Sample:	200ug/ml 0.05um permeate	Preparation:	Preparatio
Estimated Size:	Unknown	Diluent:	Water
Run Parameters:			
Temperature:	20.0°C	Refractive Index:	1.333
Date:	08-Apr-08	Viscosity:	1.002 cent
Time:	07:38:31 PM		

Angle	Mean Dia. (nm)	Std. Dev. (nm)	Polydispersity Index	Run Time (sec)
23.0°	20.0	Narrow	-2.385	918
62.6°	-29.4	n/a	-1.612	306
90.0°	17.0	Broad	0.460	180
Run Avg:	2.5	0.9	-1.179	

Table B.11 Particle count analysis result of 200µg/ml, 0.05µm membrane alumina nanoparticles permeate.

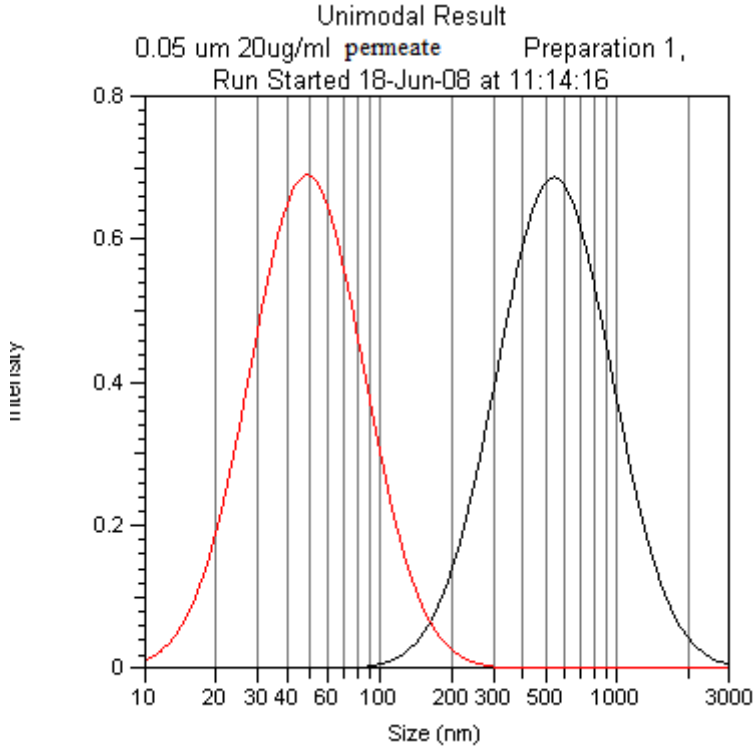

Black line-23 degrees
Red line-62.6 degrees

Figure B.12 Particle count analysis result of 20µg/ml, 0.05µm membrane alumina nanoparticles permeate.

Sample:	0.05 um 20ug/ml permeate	Preparation:	Preparation
Estimated Size:	Unknown	Diluent:	Water
Run Parameters:			
Temperature:	20.0°C	Refractive Index:	1.333
Date:	18-Jun-08	Viscosity:	1.002 centip
Time:	11:14:16 AM		

Angle	Mean Dia. (nm)	Std. Dev. (nm)	Polydispersity Index	Run Time (sec)
23.0°	608.3	Narrow	-3.456	425
62.6°	54.6	Broad	2.926	425
Run Avg:	331.5	160.0	-0.265	

Table B.12 Particle count analysis result of 20µg/ml, 0.05µm membrane alumina nanoparticles permeate.

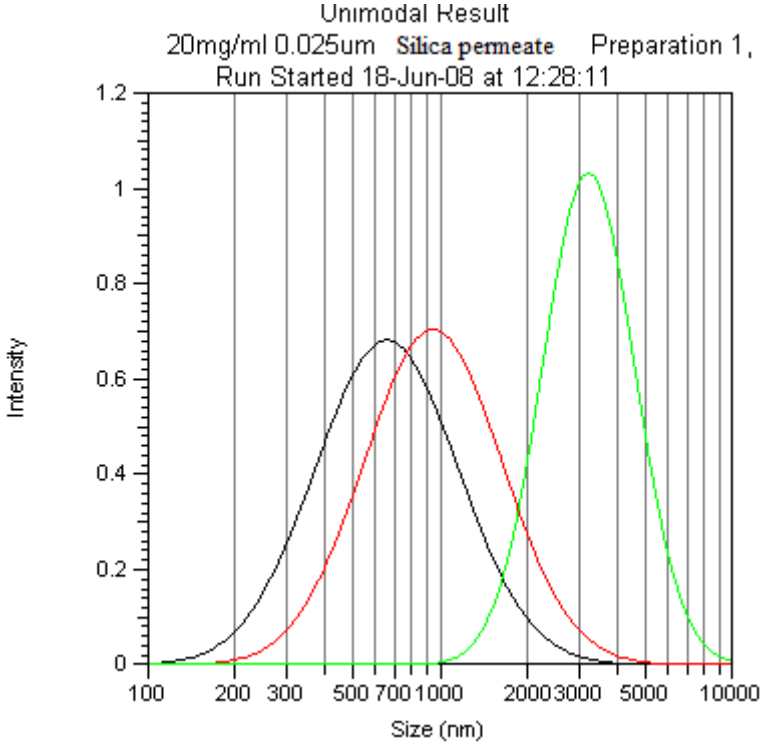

Black line is for 23 degrees
Red line is for 62.6 degrees
Green line is for 90 degrees.

Figure B.13 Particle count analysis results of 20mg/ml, 0.025µm membrane Silica nanoparticles permeate.

Sample:	20mg/ml 0.025um	Preparation:	Preparation 1
Estimated Size:	Unknown Silica permeate	Diluent:	Water
Run Parameters:			
Temperature:	20.0°C	Refractive Index:	1.333
Date:	18-Jun-08	Viscosity:	1.002 centipoise
Time:	12:28:11 PM		

Angle	Mean Dia. (nm)	Std. Dev. (nm)	Polydispersity Index	Run Time (sec)
23.0°	740.6	Narrow	-5.075	425
62.6°	1049.4	Broad	1.699	425
90.0°	3232.3	946.6	0.131	425
Run Avg:	1674.1	599.3	-1.082	

Table B.13 Particle count analysis results of 20mg/ml, 0.025µm membrane Silica nanoparticles permeate.

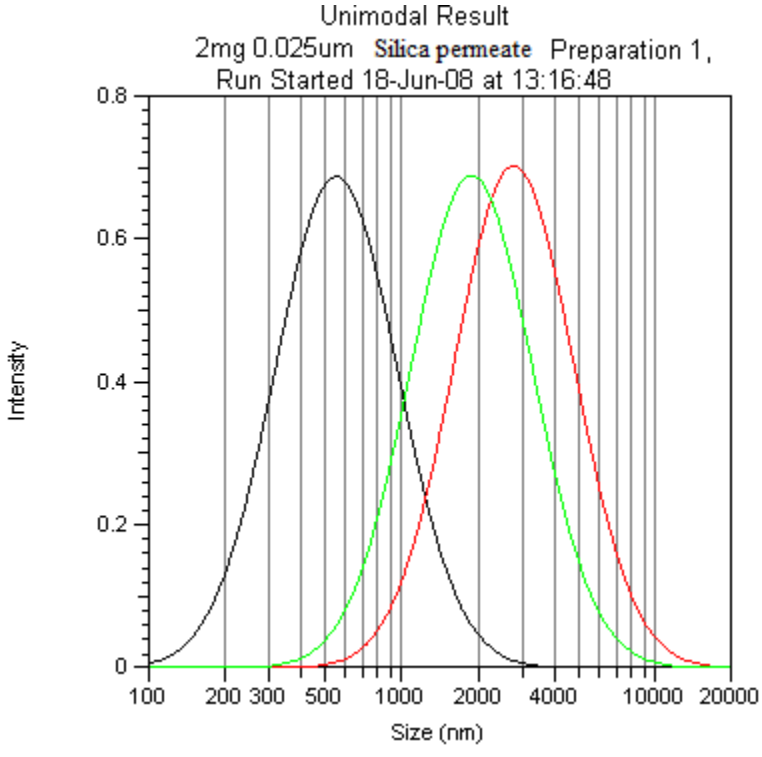

Black line is for 23 degrees
Red line is for 62.6 degrees
Green line is for 90 degrees.

Figure B.14 Particle count analysis results of 2mg/ml, 0.025µm membrane Silica nanoparticles permeate.

Sample:	2mg 0.025um	Preparation:	Preparation 1
Estimated Size:	Unknown	Diluent:	Water
Run Parameters:	Silica permeate		
Temperature:	20.0°C	Refractive Index:	1.333
Date:	18-Jun-08	Viscosity:	1.002 centipoise
Time:	01:16:48 PM		

Angle	Mean Dia. (nm)	Std. Dev. (nm)	Polydispersity Index	Run Time (sec)
23.0°	619.2	Narrow	-3.344	425
62.6°	3071.1	Narrow	-1.796	425
90.0°	2113.2	Broad	3.029	425
Run Avg:	1934.5	917.6	-0.704	

Table B.14 Particle count analysis results of 2mg/ml, 0.025µm membrane Silica nanoparticles permeate.

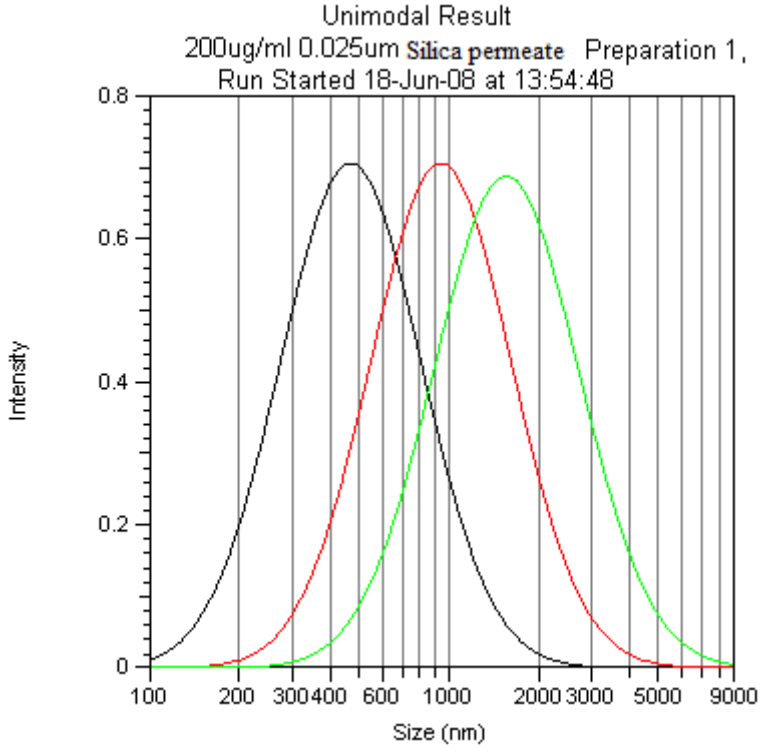

Black line is for 23 degrees
Red line is for 62.6 degrees
Green line is for 90 degrees.

Figure B.15 Particle count analysis results of 200µg/ml, 0.025µm membrane Silica nanoparticles permeate.

Sample:	200ug/ml 0.025um	Preparation:	Preparation 1
Estimated Size:	Unknown	Diluent:	Water
Run Parameters:	Silica permeate		
Temperature:	20.0°C	Refractive Index:	1.333
Date:	18-Jun-08	Viscosity:	1.002 centipoise
Time:	01:54:48 PM		

Angle	Mean Dia. (nm)	Std. Dev. (nm)	Polydispersity Index	Run Time (sec)
23.0°	521.0	Narrow	-1.620	425
62.6°	1042.2	Broad	1.603	425
90.0°	1739.6	Broad	3.178	425
Run Avg:	1100.9	521.5	1.054	

Table B.15 Particle count analysis results of 200µg/ml, 0.025µm membrane Silica nanoparticles permeate.

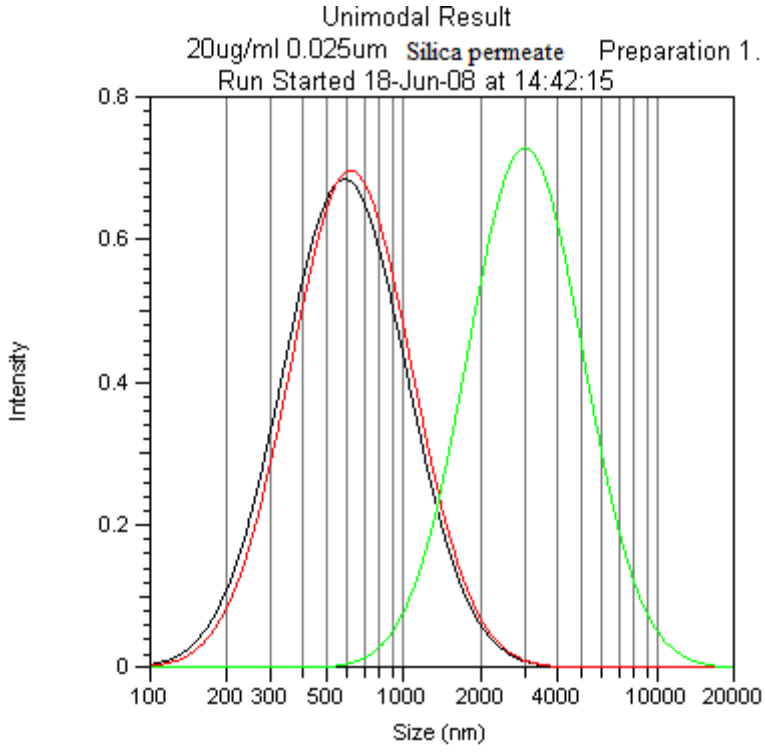

Black line is for 23 degrees
Red line is for 62.6 degrees
Green line is for 90 degrees.

Figure B.16 Particle count analysis results of 20µg/ml, 0.025µm membrane Silica nanoparticles permeate.

Sample:	20ug/ml 0.025um	Preparation:	Preparation 1
Estimated Size:	Unknown	Diluent:	Water
Run Parameters:	Silica permeate		
Temperature:	20.0°C	Refractive Index:	1.333
Date:	18-Jun-08	Viscosity:	1.002 centipoise
Time:	02:42:15 PM		

Angle	Mean Dia. (nm)	Std. Dev. (nm)	Polydispersity Index	Run Time (sec)
23.0°	659.0	Narrow	-3.912	425
62.6°	691.0	Broad	2.134	425
90.0°	3281.6	Broad	0.971	425
Run Avg:	1543.9	703.2	-0.269	

Table B.16 Particle count analysis results of 20µg/ml, 0.025µm membrane Silica nanoparticles permeate.

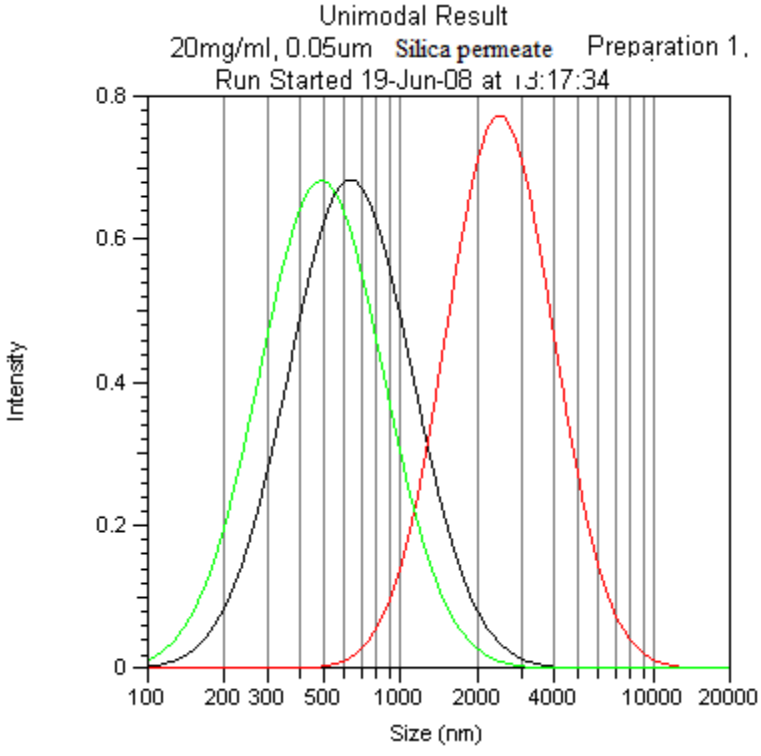

Black line is for 23 degrees
Red line is for 62.6 degrees
Green line is for 90 degrees.

Figure B.17 Particle count analysis results of 20mg/ml, 0.05µm membrane Silica nanoparticles permeate.

Sample:	20mg/ml, 0.05um	Preparation:	Preparation 1
Estimated Size:	Unknown	Diluent:	Water
Run Parameters:	Silica permeate		
Temperature:	20.0°C	Refractive Index:	1.333
Date:	19-Jun-08	Viscosity:	1.002 centipoise
Time:	01:17:34 PM		

Angle	Mean Dia. (nm)	Std. Dev. (nm)	Polydispersity Index	Run Time (sec)
23.0°	711.7	Narrow	-4.310	425
62.6°	2630.1	Narrow	-0.543	425
90.0°	548.6	Broad	4.961	425
Run Avg:	1296.8	567.3	0.036	

Table B.17 Particle count analysis results of 20mg/ml, 0.05µm membrane Silica nanoparticles permeate.

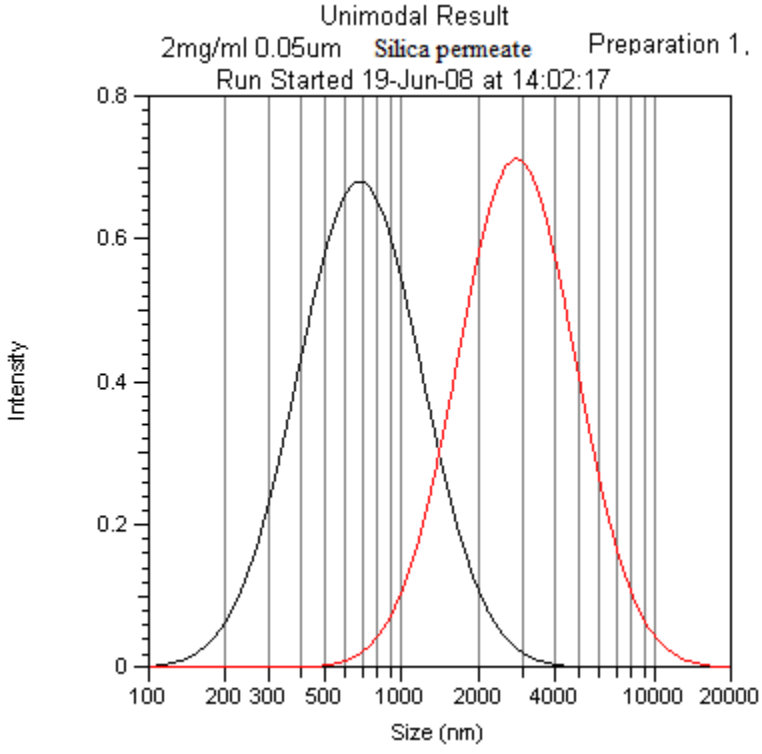

Black line-23 Degrees
Red line-62.6 Degrees

Figure B.18 Particle count analysis results of 2mg/ml, 0.05µm membrane Silica nanoparticles permeate.

Sample:	2mg/ml 0.05um	Preparation:	Preparation 1
Estimated Size:	Unknown	Diluent:	Water
Run Parameters:	Silica permeate		
Temperature:	20.0°C	Refractive Index:	1.333
Date:	19-Jun-08	Viscosity:	1.002 centipoise
Time:	02:02:17 PM		

Angle	Mean Dia. (nm)	Std. Dev. (nm)	Polydispersity Index	Run Time (sec)
23.0°	771.2	Narrow	-5.581	425
62.6°	3128.0	Narrow	-1.364	425
Run Avg:	1949.6	907.5	-3.472	

Table B.18 Particle count analysis results of 2mg/ml, 0.05µm membrane Silica nanoparticles permeate.

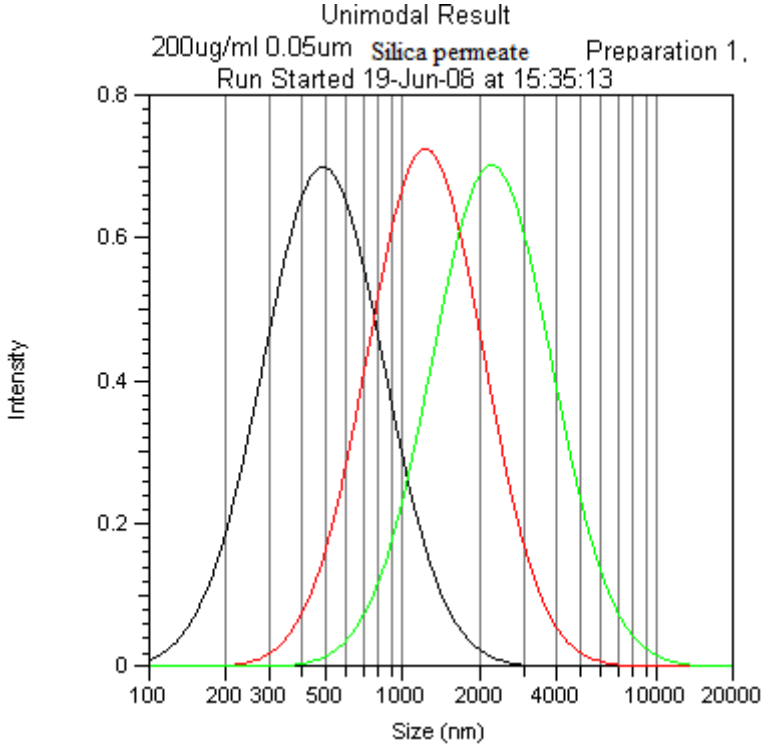

Black line is for 23 degrees
Red line is for 62.6 degrees
Green line is for 90 degrees.

Figure B.19 Particle count analysis results of 200µg/ml, 0.05µm membrane Silica nanoparticles permeate.

Sample:	200ug/ml 0.05um	Preparation:	Preparation 1
Estimated Size:	Unknown	Diluent:	Water
Run Parameters:	Silica permeate		
Temperature:	20.0°C	Refractive Index:	1.333
Date:	19-Jun-08	Viscosity:	1.002 centipoi
Time:	03:35:13 PM		

Angle	Mean Dia. (nm)	Std. Dev. (nm)	Polydispersity Index	Run Time (sec)
23.0°	542.0	Narrow	-1.971	425
62.6°	1345.7	Broad	1.052	425
90.0°	2483.3	Broad	1.844	425
Run Avg:	1457.0	675.1	0.308	

Table B.19 Particle count analysis results of 200µg/ml, 0.05µm membrane Silica nanoparticles permeate.

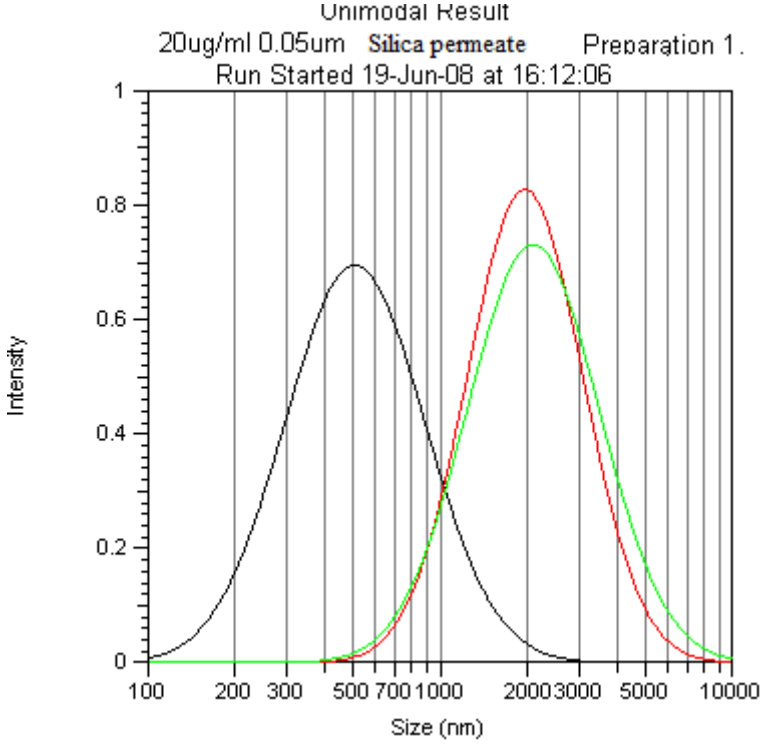

Black line is for 23 degrees
Red line is for 62.6 degrees
Green line is for 90 degrees.

Figure B.20 Particle count analysis results of 20µg/ml, 0.05µm membrane Silica nanoparticles permeate.

Sample:	20ug/ml 0.05um	Preparation:	Preparation 1
Estimated Size:	Unknown	Diluent:	Water
Run Parameters:	Silica permeate		
Temperature:	20.0°C	Refractive Index:	1.333
Date:	19-Jun-08	Viscosity:	1.002 centipoise
Time:	04:12:06 PM		

Angle	Mean Dia. (nm)	Std. Dev. (nm)	Polydispersity Index	Run Time (sec)
23.0°	570.7	Narrow	-2.260	425
62.6°	2046.2	Broad	0.340	425
90.0°	2270.6	Broad	0.929	425
Run Avg:	1629.2	685.1	-0.330	

Table B.20 Particle count analysis results of 20µg/ml, 0.05µm membrane Silica nanoparticles permeate.

APPENDIX C

EFFECT OF ALUMINUM ON PLANT GROWTH

The following are a graphical depiction of the effect of Aluminum on plant growth, based on studies using Aluminum standard solution and the five plant species.

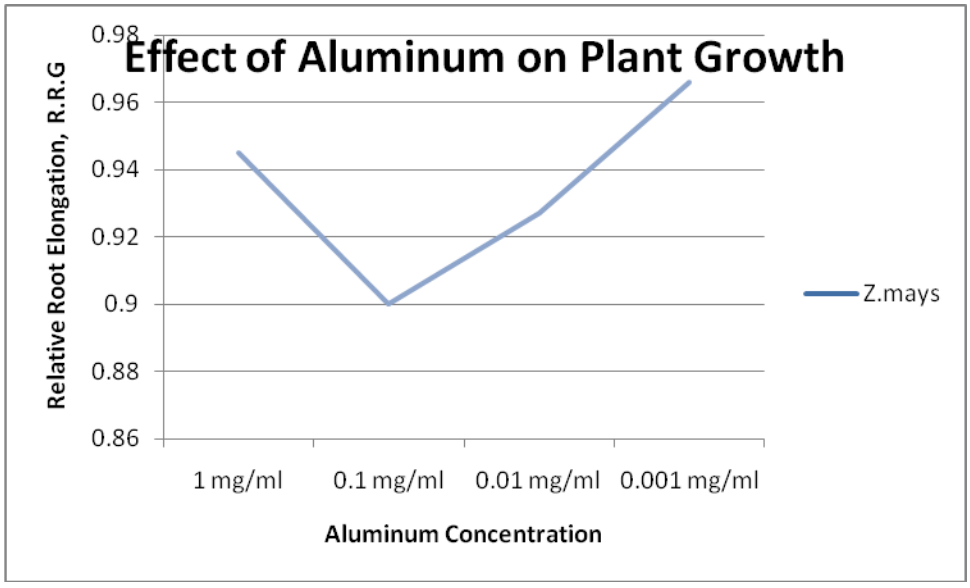

Figure C.1 Effect of Aluminum from Aluminum standard solution of different concentrations on the root growth of *Z.mays*.

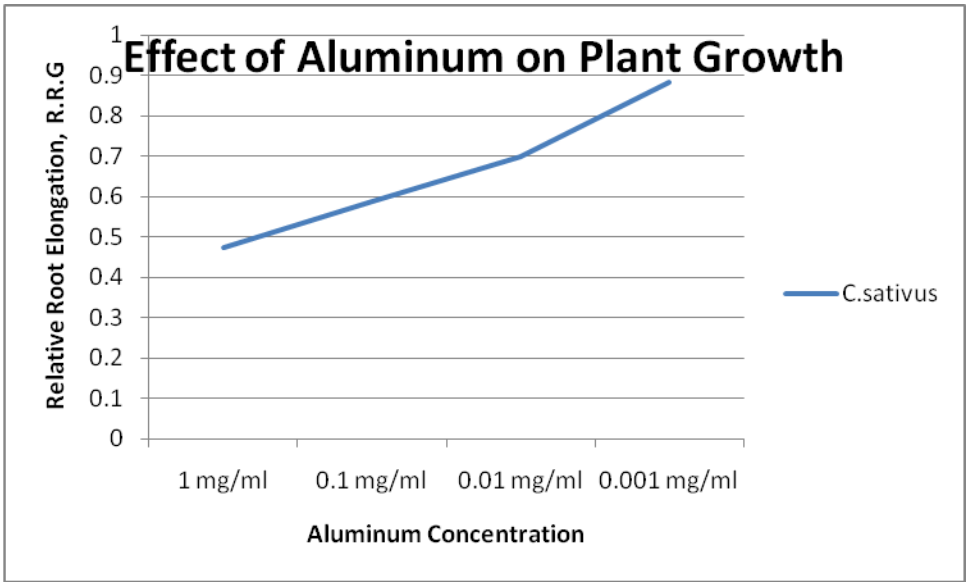

Figure C.2 Effect of Aluminum from Aluminum standard solution of different concentrations on the root growth of *C.sativus*.

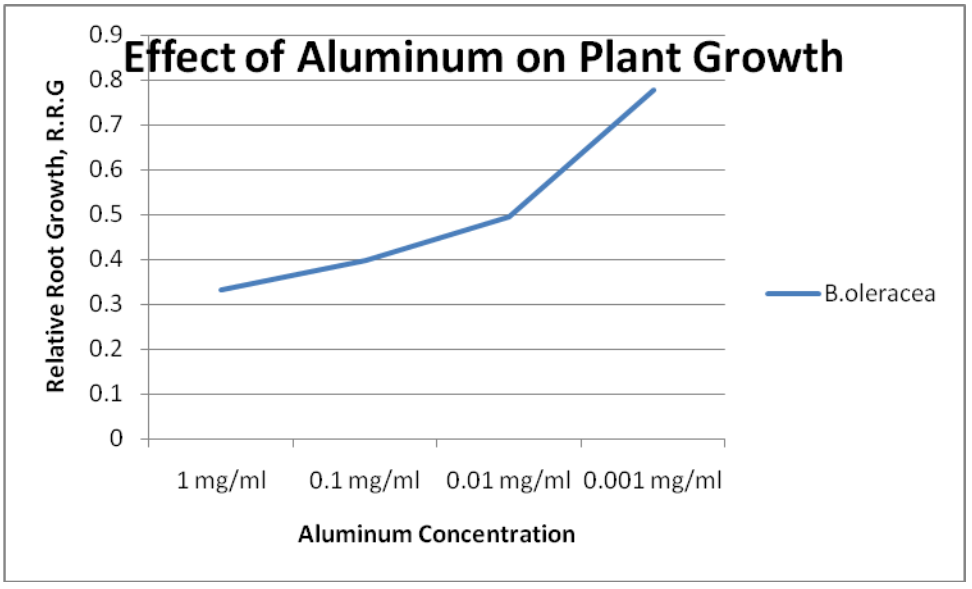

Figure C.3 Effect of Aluminum from Aluminum standard solution of different concentrations on the root growth of *B.oleracea*.

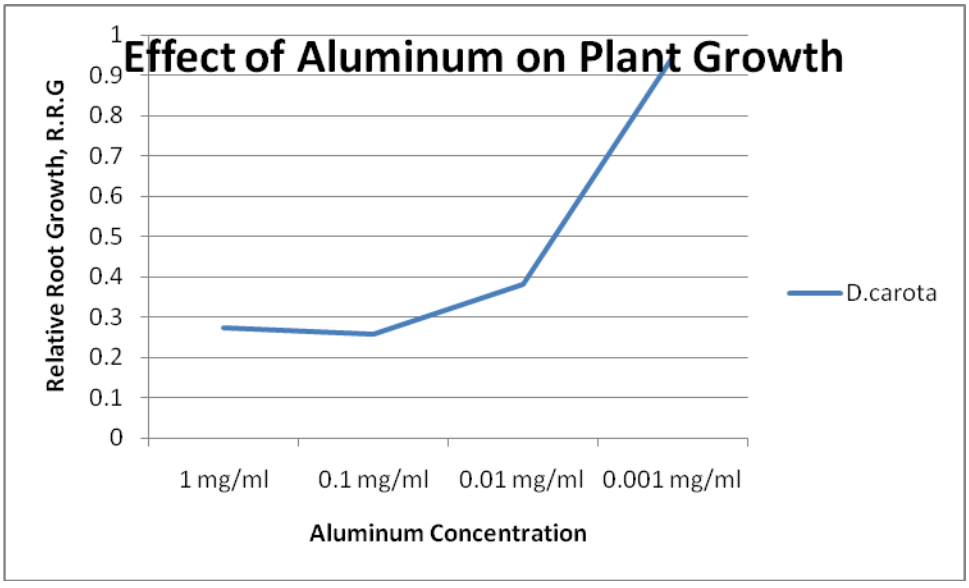

Figure C.4 Effect of Aluminum from Aluminum standard solution of different concentrations on the root growth of *D.carota*.

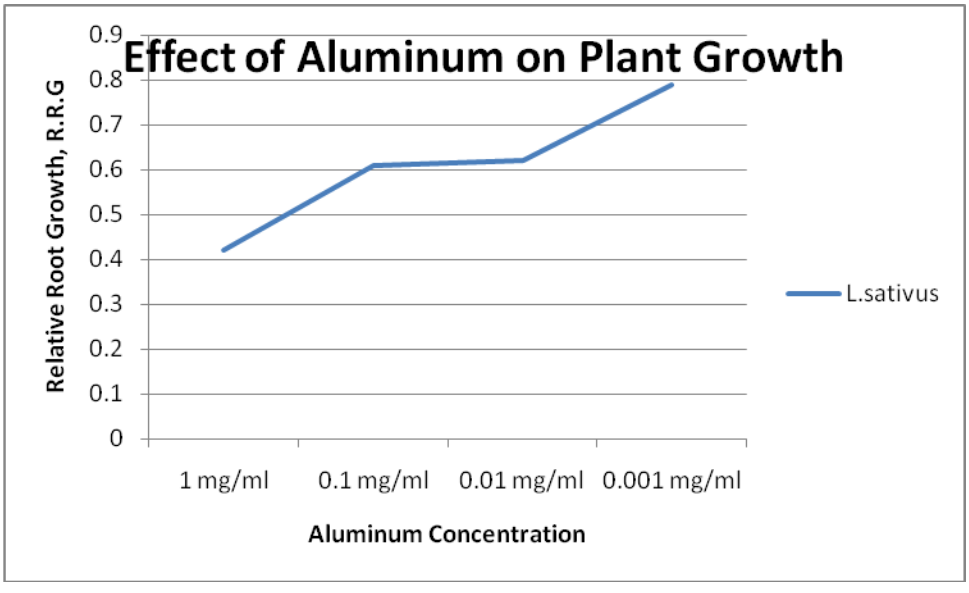

Figure C.5 Effect of Aluminum from Aluminum standard solution of different concentrations on the root growth of *L.sativus*.

REFERENCES

Ahmed M J, Hossan J. (1995). *Talanta* (42), p. 1135.

Akila R, Stollery B T and Riihimaki V. (1999). Decrements in cognitive performance in metal inert gas welders exposed to aluminum. Occupational Environmental Medicine. 56 (9), p.632-639.

Akerman M E, Chan W C, Laakkonen P, Bhatia S N, Ruoslahti E. (2002). Nanocrystal targeting in vivo. Proceedings of the National Academy of Science. 1:99(20), p.12617-21.

Araujo L, Lobenberg R, Kreuter J. (1999). Influence of the surfactant concentration on the body distribution of nanoparticles. J. Drug Target, (6) p.373-385.

Bais H P, Weir T, Perry L G, Gilroy S, Vivanco J M (2006) The role of root exudates in rhizosphere interactions with plants and other organisms. Annual Review. Plant Biology. (57), p.233-66.

Bais H P, Park S W, Weir T L, Callaway R M and Vivanco J M. (2004). How plants communicate using the underground information superhighway. Trend Plant Science. (9), p.26-3.

Bais H P, Vepachedu R, Gilroy S, Callaway R M and Vivanco J M. (2003). Allelopathy and exotic plant invasion: from molecules and genes to species interactions.

Bast-Pettersen R, Skaug V, Ellingsen D et al. (2000). Neurobehavioral performance of aluminum welders. American Journal of Industrial Medicine, 37(2), p.184-192.

Barceló J and Poschenrieder C. (1999). Structure and Ultrastructural changes in heavy metals exposed plants. Heavy metals stress in plants, from molecules to ecosystems, Springer, Berlin, p.183-205.

Barceló J, Poschenrieder C and Gunse B. (1997). Water transport properties of roots and root cortical cells in proton and aluminum stressed maize varieties. Plant Physiology. (113), p.595-602.

Barceló J, Poschenrieder C and Tolver P R. (2005). A role for cyclic hydroxamates in aluminum resistance in maize. Journal of inorganic Biochemistry.vol. 99, (9), p.1830-1836.

Barceló J, Poschenrieder C. (2002). Fast root growth responses, root exudates, and internal detoxification as clues to the mechanisms of aluminum toxicity and resistance: a review. Environmental and Experimental Botany (48), p.75–92.

Bradley D C, Mehrotra R C and Gaur D P. (1978). Metal Alkoxides (Lond.Acad.)

Brenner H and Gaydos L J. (1977). Journal of colloid and interface science, (58), p.312.

Buchta M, Kiesswetter E, Otto A, et al. **(**2003) Longitudinal study examining the neurotoxicity of occupational exposure to aluminum containing welder fumes. Institute of Arch Occupational Environmental Health, 76 (7), p.539-548.

Bhattacharjee S and Bhattacharya P K. (1992). Flux decline behaviour with low molecular weight solutes during ultra filtration in an unstirred batch cell. *Journal of Membrane Science,* (*72*), p.149-161.

Bodmeier R, Maincent P, Lieberman H, Rieger M M and Banker G S.(1998). Pharmaceutical dosage forms: disperse systems, volume 1, Marcel Dekker, Inc. New York.

Caruthers S D, Wickline S A, Lanza G M. (2007). Nanotechnological applications in medicine. Curr Opin Biotech, (18), p.26-30.

Catron D H, Schlatter L K, Thornton G L. (1998). Determination of peroxides from lipids. Journal of science (258), p.1022-48.

Chen F, Gerion D. (2004). Fluorescent CdSe/ZnS nanocrystal-peptide conjugates for long-term, nontoxic imaging and nuclear targeting in living cells. Nano Lett. (4), p.1827-1832.

Chen Z, Meng H, Xing G, Yuan H, Zhao F, Liu R, Chang X, Gao X, Wang T, Jia, G, Ye C, Chai Z F and Zhao Y. (2008). Age-related differences in pulmonary and cardiovascular responses to SiO_2 nanoparticles inhalation: Nanotoxicity has susceptible population. Environ. Sci. Technol., 42(23), p.8985-8992.

Chithrani B D, Ghazani A A, Chan W C W. (2006). Determining the size and shape dependence of gold nanoparticles uptake into mammalian cells. Nano Lett. (6), p.662-668.

Clarkson D T. (1965). The effect of aluminum and some other trivalent metal cations on cell division in the root apices of *Allium cepa*. Ann Bot., **(**29), p.310–315.

Colvin V L. (2003). The potential environmental impact of engineered Nanomaterials. Nat. Biotechnol, (21), p.1166-1170.

Cruz-Ortega R, Ayala-Cordero G and Anaya A L. (2002). Allelochemical stress produced by the aqueous leachate of callicarpa acuminate: effects on roots of beans, maize and tomato. Journal of Plant Physiology (116), p.20-27.

Dakora F D and Phillips D A. (2002). Root exudates as mediators of mineral acquisition in Low nutrient environments. Journal of Plant Soil (245), p.35-47.

Deng H, Van Bekel G J. (1998). J. *Mass Spectrom.* (33), p.1080.

Di Silvestre M, Guizzardi S, Bettini N, Gargiulo N, Savini R. (1991). "Powdered alumina implants in the experimental animal: a histological study conducted in the rat," Chir. degli Organi. di Mov (76), p.167-172.

Dion I, Bordenave L, Lefebre F, et al**.** (1994). "Physicochemistry and Cytotoxicity of ceramics Part II: Cytotoxicity of ceramics," J. Mater. Sci.: Materials in Medicine (5), p.18-24.

Draft Toxicological Profile for Aluminum. (2006).US Department of Health and Human Services, Public Health Services, agency for toxic substances and diseases.

Drew R T, Gupta B N, Bend J R et al. (1974). Inhalation studies with a glycol complex of aluminum-chloride-hydroxide., Arch. Environmental Health 28 (6), p.321-326.

Edelstein A S and Cammarata R C. (2002). Nanomaterials: synthesis, properties and applications, 2nd Edition, p.149-153.

Einhellig F A. (1995). Mechanisms of action of allelochemicals in allelopathy: organisms, process and applications. (96). American Chemical Society.

Edwards J D and Tosterud M.(1933). J.Physical Chemistry. 37(4), p.483-488.

Gao X, Cui Y, Levenson R M, Chung L W K and Nie S. (2004). In vivo cancer targeting and imaging with semiconductor quantum dots. Nat Biotechnol (22), p.969-976.

Georgia M, Friends of the Earth, Australia Nanotechnology Project, 2006, p.5-7.

Geiser M, Rothen-Rutlshauser B, Knapp N, Schurch S, Kreyling W, Schulz H, Semmler M, Im H, Heyder J and Gehr P. (2005). Ultrafine particles cross cellular Membranes by non-phagocytic mechanisms in lungs and in cultured cells. Journal of Environmental Health Perspectives 113 (11), p.1555-1560.

Golub M S and Germann S L. (2001). Long-term consequences of developmental exposure to aluminum in a suboptimal diet for growth and behavior of Swiss webster mice. Neurological Teratol, 23 (4): p.365-372.

Golub M S, Han B and Keen C L et al. (1992). Effects of dietary aluminum excess and manganese deficiency on neurobehavioral end points in adult mice. Toxical Application Pharmacol 112 (1), p.154-160.

Guharay J, Chaudhuri R, Chakrabarti A and Sengupta P K. (1997). *Spectrochim. Acta Part A* (53), p. 457.

Guharay J, Sengupta P K. (1997). Spectrochim. *Acta Part A* (53), p. 905.

Guilbault G G, Markham K R. (1973). *Practical Fluorescence, Theory, Methods and Techniques*. Marcel Dekker, New York, p. 221.

Gunse B, Poschenrieder C, Barceló J C. (1997).Water transport properties of roots and root cortical cells in proton and Al stressed maize varieties. Plant Physiol. (113), p.595-602.

Hanninen H, Matikainen E, Kovala T et al. Internal load of aluminum and the central nervous system functions of aluminum welders. (1994).Science and Journal works Environmental Health. 20 (4), p.279-285.

Hawes M C, Gunawardena U, Miyasaka S and Zhao X. (2000). The role of root border cells Plant defense, Trends Plant Science (5), p.128-33.

Holsapple M, Farland W, Landry T, Monteiro-Riviere N, Carter J, Walker N and Thomas K. (2005). Research strategies for safety evaluation of nanomaterials, Part 2. Toxicology and safety evaluation of nanomaterials, current challenges and data needs. Toxicological sciences 88 (1), p.1

Hollman P C H, van Trijp, J M P and Buysman M N C P. (1996). *Anal. Chem.* (68), p.3511.

Institute of occupational medicine for the Health and Safety Executive. Nanoparticles. (2004). An occupational hygiene review. Available at http: www.hse.gov, accessed July 2007.

Keyes W J, O' Malley D and Kim D G. (1998). On becoming a parasite: evaluating the role of wall oxidases in parasitic plant development, Chem. Biol. (5), p.103-17.

Khosla S N, Nand N and Khosla P. (1988). Aluminum Phosphide poisoning. Journal Tropical Medical Hygiene (91), p.196-198.

Kidd P S, Llugany M. Poschenrieder C, Gunse B and Barceló J**. (**2001). The role of roots exudates in aluminum resistance and silicon-induced amelioration of aluminum toxicity in three varieties of maize (*Zea mays*). Journal of Experimental Botany, (52), p.1339-1352.

King E J, Harrison C V, Mohanty G P, Nagelschmidt G. (1955). "The Effect of Various Forms of Alumina on the Lungs of Rats," J. Path. Bact. (69), p.81-93.

Kim E J, Kwak J M, Uozumi N and Schroeder J I. (1998). Atkup1: An arabidopsis gene encoding high-affinity potassium transport activity. Plant cell, (10), p.51-62.

Klimashevsky E and Dedov C. (1975). Toxicity of aluminum. Journal of Science and Botany, (35), p.56-70.

Klosterkotter W. (1960). Effects of ultramicroscopic gamma-aluminum oxide on rats and Mice. AMA Ach. Industrial Health (21), p.458-472.

Kochian LV, Hoekenga A O, Piñeros M A. (2004). How do plants tolerate acid soils? Mechanisms of aluminum tolerance and phosphorous efficiency. Annu Rev Plant Physiol Plant Mol Biol (55), p.459–493.

Kumar C. (2007). Nanomaterials for medical diagnosis and therapy Weinheim: Wiley-VCH.

Labhasetwar V, Song C, Humphrey W, Shebusky R and Levy R. (1998). Artery uptake of biodegradable nanoparticles; effect of surface modifications. J. Pharm Sci, (87), p.1229-12.

Lang H, Mertens T H. (1990). "The use of cultures of human osteoblastlike cells as an in vitro test system for dental materials," J. Oral Maxillofac. Surg. (48), p.606-611.

Lawrence K S, Douglas H C and Gregory L T. (1998). "Test kit for the qualitative determination of peroxide". US Patent 5770150, p.1-14.

Lei R, Wu C, Yang B, Ma H, Shi C, Wang Qu, Wang Qi, Yuan Y, and Liao M. (2008). Toxicology and applied pharmacology volume 232, (2), p.292-301.

Li N, Sioutes C, Cho A, Schmitz D, Misra C, Sempf J, Wang M, Oberley T, Froines J and Nel A. (2003). "Ultrafine particulate pollutants induce oxidative stress and mitochondrial damage". Environmental Health Perspectives, 111 (4): p.455-460.

Li J, Liu Y, Hermansson L, Soremark R. (1993). "Evaluation of biocompatibility of various ceramic powders with human fibroblasts in vitro," Clin. Mater. (12), p.197- 201.

Ling Y and Watts D. (2004). Toxicity of manufactured particulate materials on plant root growth. PhD Thesis, p.1-120.

Litaor M I. (1987). Aluminum Chemistry; Fraction, speciation and equilibria of soil interstitial waters of an alpine watershed, Front Range, Colorado. Geochim Cosmochim Acta (51), p.1285-1295.

Luo L, Savic R, Eisenberg A and Maysinger D. (2003). "Micellar nanocontainers distribute to defined cytoplasmic organelles".J. Science, (300), p. 615-618.

Ma J F. (2000). Role of organic acids in detoxification of aluminum in higher plants. Plant Cell Physiol (41), p.383–390.

Ma J F, Ryan P R, Delhaize E. (2001). Aluminum tolerance in plants and the complexing role of organic acids. Trends Plant Sci (6), p. 273–278.

McMorrow D, Kasha M J. (1984). *Phys. Chem.* (88), p. 2235.

Medintz I L, Uyeda H T, Goldman E R, Mattoussi H. (2005).Quantum dot bioconjugates for imaging, labeling and sensing. Nat Mater, (4), p.435-446.

Meiklejohn A. (1963). "The successful prevention of silicosis among China biscuit workers in the north Staffordshire potteries." Br. J. Ind. Med. (20), p.255-263.

Mukherjee S P. (1980). Journal of Non-Crystal Solids. (42), p.477.

Nel A, Xia T and Li N. (2006). "Toxic potential of materials at the nanolevels". Science vol. (311), p.622-627.

Neupert G, Ziller R, Glien W. (1984) "Behavior of cultured cells on the surface of Al_2O_3 ceramics of different consistencies." Exp. Chir. Transplant. Kunstliche. Organe. (17), p.109-115. In German.

Nishio K, Neo M, Akiyama H, Okada Y, Kokubo T, Nakamura T. (2001). "Effects of apatite and wollastonite containing glass-ceramic powder and two types of alumina powder in composites on osteoblastic differentiation of bone marrow cells." J. Biomed. Mater. Res. (55), p.164-176.

Nkamgueu E M, Adnet J J, Bernard J, Zierold K, Kilian L, Jallot E, Benhayoune .H, Bonhomme .P. (2000). "In vitro effects of zirconia and alumina particles on human blood monocyte-derived macrophages: X- ray microanalysis and flow cytometric studies." J. Biomed. Mater. Res. (52), p.587-594.

Oberdorster G, Maynard A, Donaldson K, Castranova V, Fitzpatrick J, Ausman K, Carter J, Karn B, Kreyling W, Lai D. Olin S, Monteiro-Riviere N, Warhelt D and Yang H.(2005). Principles for characterizing the potential human health effects from exposure to nanomaterials; elements of a screening strategy". Particles and Fiber Toxicology. (2), p.8.

Oberdoster G, Oberdoster E and Oberdoster J. (2005). "Nanotoxicology: an emerging discipline from studies of ultrafine particles". Environmental Health Perspective. 113 (7), p.823-839.

Olson P D, Varner J E. (1993). Hydrogen peroxide and lignifications. The Plant Journal, vol. 4, (5), p.887-892.

Pigot G H, Gaskell B A and Ishmael J. (1981). Effects of long term inhalation of alumina fibers in rats. British Journal of experimental Pathology. 62 (93), p.323-331.

Politycka I. (1996). Peroxidase activity and lipid peroxidation in roots of cucumber seedlings influenced by derivatives of cinnamic and benzoic acids. Acta Physiol. Plant (18), p.365-70.

Porter L J, Markham K R, J. (1970). Chem. Soc. (9), p.1309.

Psaro R, Guidotti M and Sgobba M. **(**2004). Inorganic and bio-inorganic chemistry. *Nanosystems*. p.1-51.

Pusz J, Kopacz M. (1992). Polish *J. Chem.* (66), p. 1935.

Pusz J, Nitka B. (1997). Microchem. *J.* (56), p.373.

Robards K, Antolovich M. (1997). Analyst (122), p. 11R.

Roh J, Sim S J, Yi J, Park K, Chung K H, Ryu D, Choi J. (2009). Ecotoxicity of Silver Nanoparticles on the soil nematode *Caenorhabditis elegans* using functional Ecotoxicogenomics. Environ.Sci.Technol., 43(100), p. 3933-3940.

Royal Society and the Royal Academy of Engineering, UK (2004). Nanoscience and Nanotechnologies. Available at http:// www. Royalsoc.ac.uk. Accessed April 2007.

Royal Society and the Royal Academy of Engineering, UK. (2004). Nanoscience and Nanotechnology: Opportunities and Uncertainties. p.14.

Ryan P R, Delhaize E, Jones D L. (2001). Function and mechanism of organic anion exudation from plant roots. Annual Review Plant Physiol Plant Mol Biol (52), p.527– 560.

Ryan P R, Ditomaso J M, Kochian LV. (1993). Aluminum toxicity in roots: an investigation of spatial sensitivity and the role of the root cap. J Exp Bot (44), p.437-446.

Sarkar M, Guharay J and Sengupta P K. (1996). *Spectrochim. Acta Part A* (52), p. 275.

Schildknecht P H P A and DeCampos V B. (2002). A role for the cell wall in Al^{3+} resistance and toxicity: crystallinity and availability of negative charges. International Archives of Bioscience. p.1087-1095.

Sengupta P K, Kasha M. (1979). *Chem. Phys. Lett.* (68), p. 382.

Singh H P, Batish D R and Kohl R K. **(**1999).Autotoxicity: concept, organisms and ecological significance. Critical Review. Plant Science. (18), p.757-72.

Singh R P and Heldman D R. (1993). Introduction to food engineering, 2nd edition. Academic Press Inc. San Diego, California.

Sivaguru M and Horst W J. (1998). "The distal part of the transition zones is the most aluminum-sensitive apical root zone of maize." J.Plant Physiology. (116), p.155-163.

Snyder J W, Serroni A, Savory J, Farber J L. (1995). The absence of extracellular calcium potentiates the killing of cultured hepatocytes by aluminum maltolate. Arch.Biochem.Biophysics.10; 316(1).

Smith G J, Markham K R J. (1998). *Photochem. Photobiol. A: Chem.* (118), p. 99.

Stacy B D, King E J, Harrison C V, Nagelschmidt G, Nelson S. (1959). "Tissue Changes in Rats' Lungs Caused by Hydroxides, Oxides, and Phosphates of Aluminum and Iron." J. Path. Bact. (77), p.417-426.

Stanley K J, Coleman G J, Weiss Jr. A C, Steevens A J. (2010). Sediment toxicity and

Bioaccumulation of nano and micro-sized aluminum oxide. Environ.Toxical. Chem.422-429.

Steinhagen W H, Cavender F L and Cockrell B Y. (1979). Six months inhalation exposures of rats and guinea pigs to aluminum chlorohydrate. J. Environ. Pathol. Toxicology. (1), p.267-277.

Stone C J, McLaurin D A, Steinhagen W H et al. (1979).Tissue deposition patterns after chronic inhalation exposures of rats and guinea pigs to aluminum chlorohydrate. Toxicol Appl. Pharmacol., (49), p.71-76.

Strandjord A J G, Barbara P F J. (1985). *Phys. Chem.* (89). p.2355.

Swiss Review (2004): Nanotechnology; small matter, many unknowns. Available at http:// www. Swissre.com, accessed April 2007.

Townsend M C, Enterline P E, Sussman N B, Bonney T B, Rippey L L.(1985). "Pulmonary function in relation to total dust exposure at a bauxite refinery and alumina-based chemical products plant," Am. Respir. Dis. (132), p.1174-1180.

To D, Rajesh D, Yin X and Sundaresan S. (2009). Deagglomeration of nanoparticles aggregates via rapid expansion of supercritical or high-pressure suspensions. Wiley InterScience. D01.1002/aic.11887.

Tran C, Donaldson K, Stone V, Fernandez T, Ford A, Christofi N, Ayres J, Steiner M, Hurley J, Aitken R and Seaton A. (2005). A scoping study to identify hazard data needs for addressing the risks presented by nanoparticles and nanotubes. Institute of occupational medicine, research report. p.675-680.

UK Department for Environment FaRA: Characterizing the potential risks posed by engineered nanoparticles, a first UK government research report. 2005.

United States environmental protection agency, USEPA. (1996). Ecological effects test guidelines, OPPTS 850.4200, seed germination / root elongation toxicity test. EPA 712-C-96-154, Prevention, Pesticides and Toxic substances (7170).

Uren N C. (2000). Types, amount and possible functions of compounds released into the rhizosphere by soil grown plants. New York: Marcel Dekker., p.19-40.

Verma D P S. (2001). Cytokinesis and building of the cell plate in plants. Annual Review of plant physiology and plant molecular Biology. (52), p.751-784.

Vicre M, Santaella C, Blanchet S, Gateau A and Driouich A. **(**2005). Root border-like cells of Arabidopsis. Microscopical characterization and role in the interaction with rhizobacteria. Plant Physiol. (138), p.998-1008.

Vivanco J M, Bais H P, Stermitz F R, Thelen G C and Callaway R M. (2004). Biographical variation in community response to roots allelochemistry: novel weapons and exotic invasion. Ecol. Lett., (7), p. 285-92.

Ward N I. (1989). Environmental contamination of aluminum and other elements in North Cornwall as a result of the Lowermoor water treatment works incident.CEP consultants. p.118-121.

Weir T L, Bais H P, Vivanco J M. (2003). Intraspecific and interspecific interactions mediated by a phytotoxin, (-) - catechin, secreted by the roots of centaurea maculosa (spotted knapweed). J. Chem. Ecol., (29), p. 2397-412.

Weir T L, Park S.W and Vivanco J M. (2004). Biochemical and physiological mechanism mediated by allelochemicals. Current Opinion. Plant Biology. (7), p.472-79.

Williamson G B. (1990). Allelopathy, Koch's postulates and neck riddles. In perspectives in Plant competition. London: Academic. p.143-62.

Wolfbeis O.S and Begum M. *Z.* (1983). *Naturforsch.* (39b), p. 231.

Wolfbeis, O S, Knierzinger A and Schipfer R. (1983). J. *Photochem.* 21 (1983), p. 67.

Xing B and Lin D. (2008). Root uptake and phytotoxicity of ZnO nanoparticles. Environ. Sci. Technol., 42(15), p. 5580-5585.

Yoldas B E. (1975). Journal of material science. (10), p.1856.

Zong-Yi Y. (1985). Three-dimensional hydrodynamic and osmotic pore entrance Phenomena. PhD dissertation. The City University of New York. p. 9, 14, 95.

http://www.ndwc.wvu.edu, accessed May 2009.

http://www.lenntech.com/membrane-technology.htm, accessed May 2009.

http://www.gewater.com, accessed May 2009.

http://faculty.vassar.edu/lowry/PDF/Ftable.pdf, accessed June 2009.

http://www.physics.csbju.edu, accessed June 2009.

http://www.weforum.org/pdf/TechPioneers/apax04.pdf, accessed December 2006.

http://www.chemlink.com.au/alumina.htm, accessed July 2010.

http://science.yourdictionary.com/haustorium accessed July 2010.

(http://www.beckmancoulter.com/coultercounter/product multisizer.jsp). accessed July 2010.

http:// www.colloidmeasurements.com/zeta.html, accessed July 2010.

http:// www.scielo.br/img/revistas/sa/v63n3/29836f1.gif, accessed July 2010.

http:// www.sparknotes.com/.../section2.rhtml, accessed July 2010.

http:// www.chemguide.co.uk, accessed November 2010.

http://www.nlm.nih.gov/medlineplus/ency/article/000376.htm

http:// www.Graphpad.com, accessed 2008.